DESIGN OF TUNNEL ROBOT FOR INSPECTION OF LARGE-DIA. SEWER L. W. C. 2017

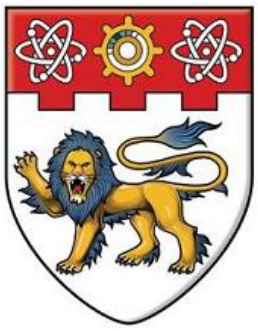

NANYANG TECHNOLOGICAL UNIVERSITY

DESIGN OF TUNNEL ROBOT FOR INSPECTION OF LARGE-DIAMETER SEWERAGE TUNNEL

LAW WEI CHUAN

SCHOOL OF MECHANICAL AND AEROSPACE ENGINEERING

NANYANG TECHNOLOGICAL UNIVERSITY

2017

DESIGN OF TUNNEL ROBOT FOR INSPECTION OF LARGE-DIAMETER SEWERAGE TUNNEL

LAW WEI CHUAN

Submitted

by

LAW WEI CHUAN

Robotics Research Centre

School of Mechanical and Aerospace Engineering

A thesis submitted to the Nanyang Technological University in partial fulfilment of the requirement for the degree of Master of Engineering (Mechanical Engineering)

2017

ABSTRACT

The used water superhighway is designed for used water collection, treatment, reclamation and disposal for the next 100 years of Singapore. It consists of trunk sewer, link sewer network and deep tunnel sewerage system. Tunnel maintenance is important to ensure the tunnel is in good working order to prolong its operating life. In-pipe robot is one of the important concepts to achieve automated tunnel maintenance such as inspection, cleaning and repairing because it can eliminate the risks that human always encounter in the tunnel. In order to identify available technologies that can be adopted in the design of the tunnel maintenance system, a study aimed to review existing pipeline and tunnel robots as well as hoisting system is then carried out. The robots can be classified into nine types of robotic system, namely PIG, Wheels, Crawler, Cylindrical, Legs, Inchworm, Helical, Snake and VVPIG type. The study implies that the research on pipeline and tunnel robot has been focusing on the maintenance of small diameter pipelines and it is seen that most of them just aim for short distance inspection. The scope of this works is to design a tunnel robot with a complete inspection system for large diameter tunnel inspections and a hoisting system for robot deployment. The robot must be water-proof, able to avoid sediment in the tunnel and has enough traction force for locomotion in the slippery condition. In this report, a preliminary design of the platform based on two types of locomotion, i.e. tracked and wheeled robot is carried out. Both track-based and wheel-based robots are simulated in CAD model to evaluate the functionality and feasibility of the design concept. The conceptual and detailed design of the robot chassis and the actuation mechanism to control the angle of the wheel frames will be covered in the subsequent chapters. The wheel frames are able to unfold to a certain angle to avoid the possible presence of soft debris along the bottom of the sewers. The robot will be designed as modules and assembled at the bottom of the access shaft. An overview of the configuration of the hoisting system for the deployment of the robotic platform has been presented. The whole system is composed of a number of subsystems, namely robotic platform, hoisting and winch system, ground control station and auxiliary system.

ACKNOWLEDGEMENTS

First of all, I would like to extend my greatest appreciation to my MEng supervisor, Professor Chen I-Ming, as well as principal investigators of this project, Associate Professor Yeo Song Huat and Associate Professor Gerald Seet Gim Lee, for their patient guidance and advice throughout my MEng Program. The accomplishment of this thesis would not have been possible without their guidance, valuable knowledge and dedication.

My gratitude also goes out to Mr. Burhan, Mr. Ang Yu Bin, Mr. Yuan Qilong, Mrs. Agnes Tan, Mr. Lim Eng Cheng, and Mr. You Kim San who spent their time on sharing their invaluable suggestions and ideas to the project. They have provided great support and assistance throughout the course of project.

In addition, I would like to express my heartfelt thanks for fellow research students and staffs from Robotics Research Centre who have helped me through the period of research and experiments.

Last but not least, I would like to thank my family for their encouragement and support.

TABLE OF CONTENTS

PAGE

LIST OF FIGURES

LIST OF TABLES

CHAPTER 1: INTRODUCTION

1.1 Motivation

The used water superhighway based in Singapore consists of three sewage systems, namely trunk sewer, link sewer network and Deep Tunnel Sewerage System (DTSS), as shown in Figure 1.1. It is a solution to meet Singapore's long term needs for used water collection, treatment, reclamation and disposal. The used water firstly flows into trunk sewer followed by link sewer network, and then converges to the DTSS. Eventually the used water in the deep tunnel sewer is transferred by gravity to the centralized water reclamation plants at the coastal areas [1].

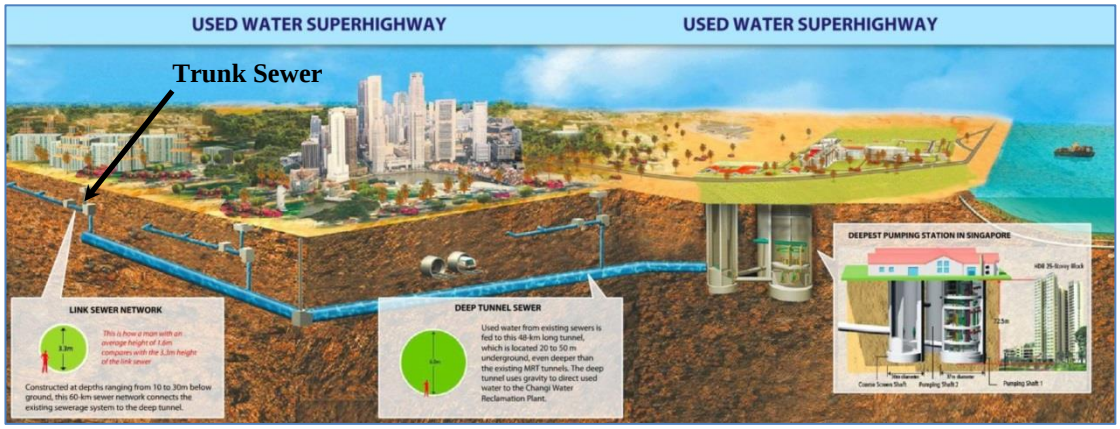

Figure 1.1: Used water superhighway in Singapore [1]

The trunk sewer with a height of 3-meter is constructed at depths ranging from 10 to 20m below ground, and its manhole entrance is 60cm x 60cm on the ground, as shown in Figure 1.2. The link sewer network is 60km long and 3.3 meters wide, constructed at the depths ranging from 10 to 30m underground connecting the trunk sewer to the DTSS. The DTSS comprises of two phases: The Phase 1 deep tunnels are now fully operational since 2009 while the target completion period of Phase 2 will be in 2024.

Phase 1 of the DTSS consists of a 48km long sewer tunnel from Kranji to Changi up to 6m diameter laid at a depth up to 50m deep across the island. The manhole opening of DTSS is 1.8m. This project will focus on the environment of the trunk sewer because it has severer condition compared to the DTSS. If the challenges of trunk sewer inspection can be satisfied, the inspection task of DTSS will be relatively easier.

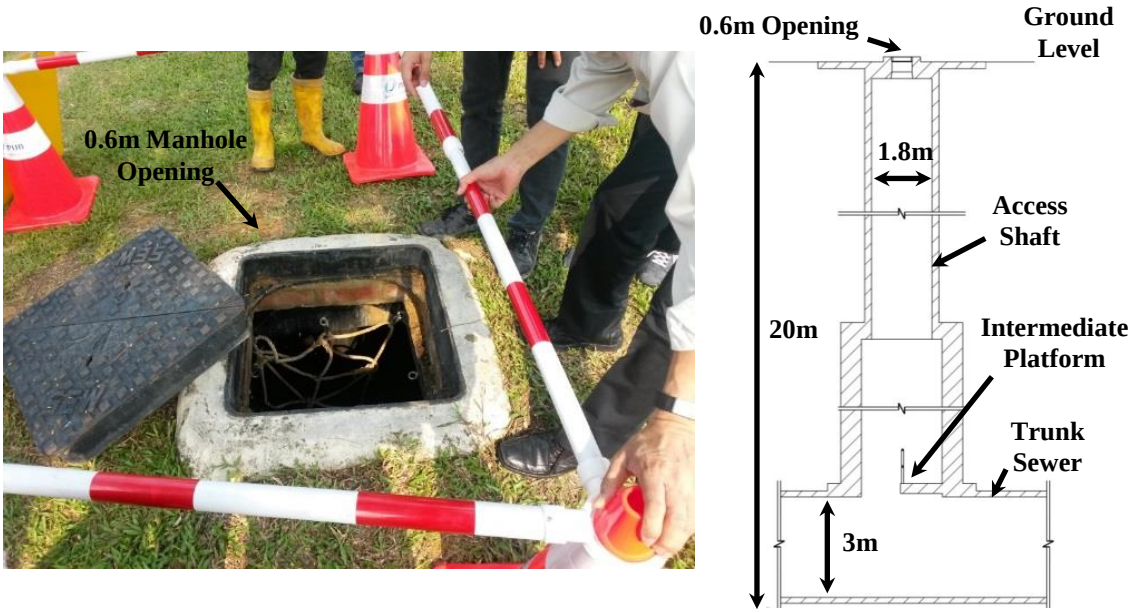

Figure 1.2: The Structure of Trunk Sewer

Due to a consequence of corrosion and climate change that can lead to wetting and drying cycles of soil, the sewage tunnels are vulnerable to crack, dislocated joints or even collapsed sections in the course of time which may cause wastewater leakage. Leaks from sewer tunnels may contaminate the surrounding land and can cause public health nuisance. In order to prolong the service life of the sewers and protect environment from contamination, inspecting the structural integrity of the tunnel such as cracked or damaged surfaces has to be carried out.

Significant research has been done on pipeline and tunnel robot due to its ability to access underground spaces and to achieve easier and better maintenance for large diameter sewerage tunnel. Bischoff & Guhl et al [2] have specifically addressed that there will be large demand on the robots for maintenance in dangerous environment or enclosed space in the future. Robotics solutions are advantageous from human because the former can eliminate the risks that humans always encounter [3], for instance, the

presence of contagions or biohazardous materials, explosive gases (hydrogen sulfide, methane), possible high concentrations of carbon dioxide or carbon monoxide, oxygen deprivation, absence of lighting and slippery walking conditions. Getting robots and machineries involved in this area not only greatly reduce potential dangers that human workers faced, it also maximizes the efficiencies and effectiveness of the performance by eliminating human errors. Although building robots for the purposes of sewages maintenance may incur costs such as robot maintenance and operator's training cost, the amount of money spent may prove to be a long term investment.

Historically, pipeline robots have been developed for maintenance of small or medium pipelines but have not been widely used in observation and maintenance of large-diameter sewer tunnels that are more than 3 meters. This is because the challenges of maintaining a large-diameter tunnel are different from those of the conventional small pipes. Large diameter tunnels are normally in partially or completely filled condition during normal operation, robot's dynamic adaption to external disturbances like water and gases flow is necessary. Moreover, robot in the underground can hardly be driven via wireless communication and navigation, a very long tether is required for data transmission and power supply. Uncertainties in the deep large diameter tunnel may also lead to the problem of abnormal operation in the robot systems. Therefore, there is a need for in-depth studies in order to develop a robotic technology that can effectively perform maintenance task and counter challenging situations in large-diameter tunnel.

The work for implementing robotics for maintenance of underground tunnel comprises of inspecting, cleaning and repairing the inner surface of the tunnel. The focus of this project is to design and develop a sewage inspection robotic platform to inspect 3-meter concrete sewage tunnels or larger. The robotic platform will be built to certain specifications to be noted, such as the robot being functional when partially submerged in wastewater, being resistant to corrosion because of varying pH values in wastewater, compact overall size that is easy and convenient to transport and allows it to go through the 60cm x 60cm manhole entrance without too much adjustment, and yet move stably within the sewage system.

1.2 Objective and Scopes

The objective of this project is to review existing tunnel robot and hoisting system, as well as to design and develop a generic locomotion mechanism for mobile platform that can cope with various tunnel conditions from dry, muddy, and partially filled water. The ability of the robotic platform to maneuver successfully in the trunk sewer under flow conveyance condition should be realized without stalling or being trapped. The platform should be able to access 60 x 60cm manhole entrance of trunk sewer, travel for a distance of up to 400m under normal operating conditions of the sewer, and capture seamless video image back to the control station on the ground suitable for real-time visual inspection of the tunnel bore. To achieve these functionalities, the size of the robotic platform needs to be small enough to fit into the manhole and yet large enough to obtain stability in the sewer. The robotic platform can be folded up for the ease of transportation and opened up to a certain width when it is inside the sewer. The robot should be integrated with various components such as cameras, LED spot lights, 8-inch hub motors, sonar profiler, laser profiler and ballast module. Besides, the design aspect of launching, deploying and retrieving of the robotic platform need to be considered.

A series of design steps has to be carried out to simulate the concept and functionality of the proposed design. The design concept of tunnel robot and hoisting system will be simulated in 3D model and further built up for testing in an actual 3-meter sewer tunnel.

The project scope is to address the potential gaps of the existing tunnel robot for the maintenance of large diameter tunnel so as to establish a research basis in this area and thereafter based on the defined gaps which assist in the design and development of a robotic platform, the design of the robotic platform and the hoisting system can be achieved. This report will be emphasizing on the concept of the structural design rather than the control and communication architecture.

A summary of the project scope is as follows:

- Literature Review
- Structural design of the robotic platform

- Structural design of the inspection and hoisting system
- Further improvement and recommendation
- Conclusion

1.3 Organization

This thesis is structured as follows. Chapter 1 has identified the need of an inspection robot for the inspection of large diameter tunnel. In Chapter 2, a critical review of existing work on in-pipe robot is provided. The review is based on the survey of major research thrusts and technologies related to pipeline and tunnel robots in the current literature of robotics. The structural differences and implementation among the nine types of robotic systems have been summarized. The review supports the research problem raised in Chapter 1, which is that a development of tunnel robot for long distance inspection in large-diameter tunnel with small entrance is missing and hence reaffirms the need to design such a robot.

Chapter 3 and Chapter 4 depict the design process for prototyping a tunnel robot. Chapter 3 describes the design requirements of the robotic platform and finalizes the design concept through designs evaluation. A preliminary design of robotic platform has been proposed in this chapter. In Chapter 4, the detailed design of the robotic platform and the structural analysis of the components are provided. Thereafter, in Chapter 5, we built up a simple prototype with the same design concept and a pulling test was carried out to evaluate the performance of the prototype. Various electronic systems will be installed, such as 8-inch hub motors to drive the robotic platform, cameras for visual inspection above water, sonar profiler for underwater inspection, pressure sensor to detect leakage in enclosures and LED spot lights are for illumination.

Chapter 6 provides the literature review of the hoisting and inspection system. The advantages and disadvantages of the systems are described. The water flow analysis for different shapes of TMS has been discussed in this chapter. A tripod winch will be implemented for robot deployment. Finally, Chapter 7 concludes the thesis by discussing the essential contribution and proposed future work of this project.

CHAPTER 2: PIPELINE AND TUNNEL ROBOTS

2.1 Literature Review

The purpose of this chapter is to present a review of the existing work of tunnel robot in order to affirm the identified research problem. While the review shows that there are many works applying on the maintenance of pipelines, small amount of related researches can be found to fulfill the task of maintenance of large-diameter tunnel. This review is important as it therefore points out the possible gaps that there is a need to develop a tunnel robot for the maintenance of large-diameter tunnel.

2.1.1 Design of Pipeline and Tunnel Robots

The pipeline robots can be able to perform a wide variety of tasks ranging from inspection to maintenance and construction. The information gathered from the patents of the pipeline robot has been analyzed and a few broad categories can be classified into nine robotic systems [4] as shown in the figure below:

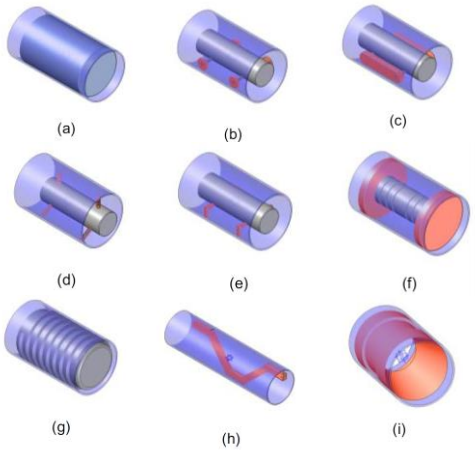

Figure 2.1: Classification of robotic systems for internal inspection of pipelines. [4, 5]

2.1.1.1 Conventional PIG (Pipeline Inspection Gauge) type

[5, 6] [7]

Figure 2.2: Conventional PIG Robots

The PIG is a self-drive pipeline robot which obtains its locomotion from the kinetic energy of fluid flow. It is pushed through a pipeline by the product transported in the pipe [7], therefore no power supply is required. During the journey, a number of tasks can be done by PIGs, including: cleaning the pipeline, removal of liquid, and inspection. One of the drawbacks is that this robot needs to be inserted at a specific point in pipeline during the application as it can only move in the direction of the fluid flow.

2.1.1.2 Wheels type

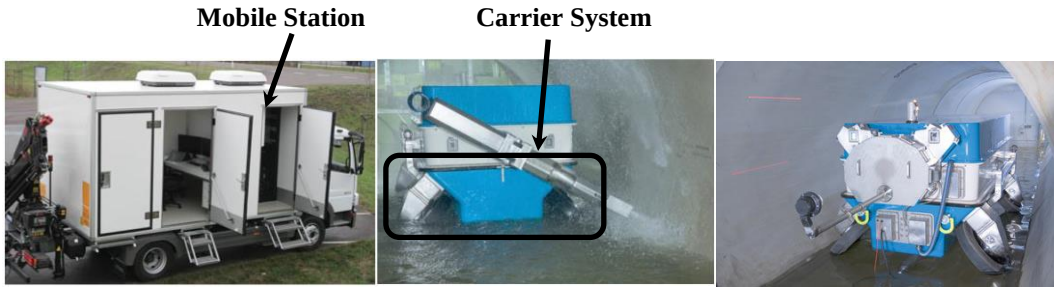

Figure 2.3: The SVM-RS, a wheel type robot [8]

The SVM-RS is designed to clean and measure damage of a public wastewater utility based in Essen, Germany which will commence operation in 2017. The sewer pipes will range in diameter between 1.6 to 2.8 m with a length of more than 51 km before ending in a large sewage treatment plant. The pipeline will be laid at a depth of 5 to 40 m underground and the maximum distance between entrances of sewer will be around 1.2km.

This robot consists of the main components listed below:

- Carrier system (robot motion kinematics) for positioning in the sewer
  - The carrier system is equipped with individual-wheel drive
  - The cleaning and inspection tools are joined with the carrier system into one system
- Cleaning tools for cleaning the walls above water as well as the sediment underwater
  - A robotic arm with 3 DOF is equipped with a nozzle bank and a Venturi nozzle. The Venturi nozzle provides the function of underwater cleaning during the forward trip in the sewer while the nozzle bank is used to clean the walls above water during the return trip to the pipe entrance
- Sensor system for above and below water inspection
  - Multiple-camera system for crack and pipe corrosion detection above water
  - Ultrasonic scanner for mechanical wear and sediments detection underwater
  - Video cameras for infiltrating water detection
  - Position measuring sensors including inclinometer
  - Combination sensor for detailed underwater inspection including underwater camera system, infiltration sensor and crack detection system
- A customized positively buoyant cable is tethered to the robot
  - Providing high-pressure water for cleaning
  - Electrical wires are used for power supply
  - Fiber optics are used to provide long distance media communications
  - The entire system able to be pulled out in case of a malfunction
- Control system and user interface
  - A mobile station with computer rack is used during the inspection. The operator is able to monitor the inspection and cleaning task at all times, includes a 2D high resolution layout views of the walls above water and a color coded mapping of sediments under water.

Figure 2.4: A KURT type robot platform [9]

KURT (**K**anal-**U**ntersuchungs-**R**oboter-**T**estplattform) [9] robot is a six-wheeled autonomous untethered robot with a dimension of 30×45×30cm. It has been successfully tested in a dry sewer at the premises of the Fraunhofer campus in Sankt Augustin. When performing the testing, a map provided beforehand to the robot represents the topology of the sewer pipes with a length of 80m, the position of the nine manholes in between, a start and a goal position. It is able to determine the sequence of junction types and manholes that it should pass on its path from starting point to goal. With the used of ultrasound sensor, this robot is able to classify the type of the pipe junction (Y-shaped, X-shaped or L-shaped) in front so as to determine its subsequent turning motion. For the control system, a notebook computer is used as CPU.

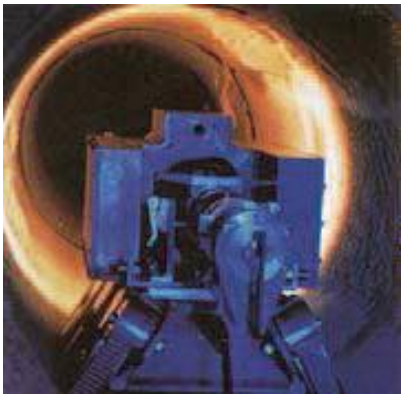

Figure 2.5: PIRAT, an automated video inspection platform [9]

PIRAT (**P**ipe **I**nspection **R**eal-Time **A**ssessment **T**echnique) [9] is a semi-autonomous tethered robot for the assessment of sewer condition which has been developed since 1993 in Australia. It is operated in 600mm sewer pipes from a surveillance unit by a human operator via a cable with a maximum length of 250m. This robot contains a

laser scanner/sonar scanner and a video camera. The sonar scanner is used when accessing the flooded sewers. In order to perform the in-pipe inspection, a 3D model of the scanned sewer pipe section is generated from both laser and sonar scanner data. After that, techniques from artificial intelligence are used to detect and classify damages on the inner wall of the pipe base on the generated 3D model data.

Figure 2.6: MAKRO robot [9]

MAKRO (**M**ehrsegmentiger Autonomer KanalROboter/multi-segmented autonomous sewer robot) [9], developed by a German group since 1997, is a self-steering articulated, fully autonomous, un-tethered robot platform. It is designed for autonomous inspection in sewer pipes with a diameter range of 300 to 600mm at dry weather condition. This robot consists of six segments and each segment is connected by a motor driven active joints. Totally five motor driven active joints are used in this design. This segmental design allows robot to simultaneously turn direction and climb a step. This robot carries all the needed resources onboard, includes industry standard PC104 computer system, standard NiCd batteries, etc.

Figure 2.7: A modular pipe cleaning mobile equipment [10]

Figure 2.8: ATRVJr with 3D sensors [11]

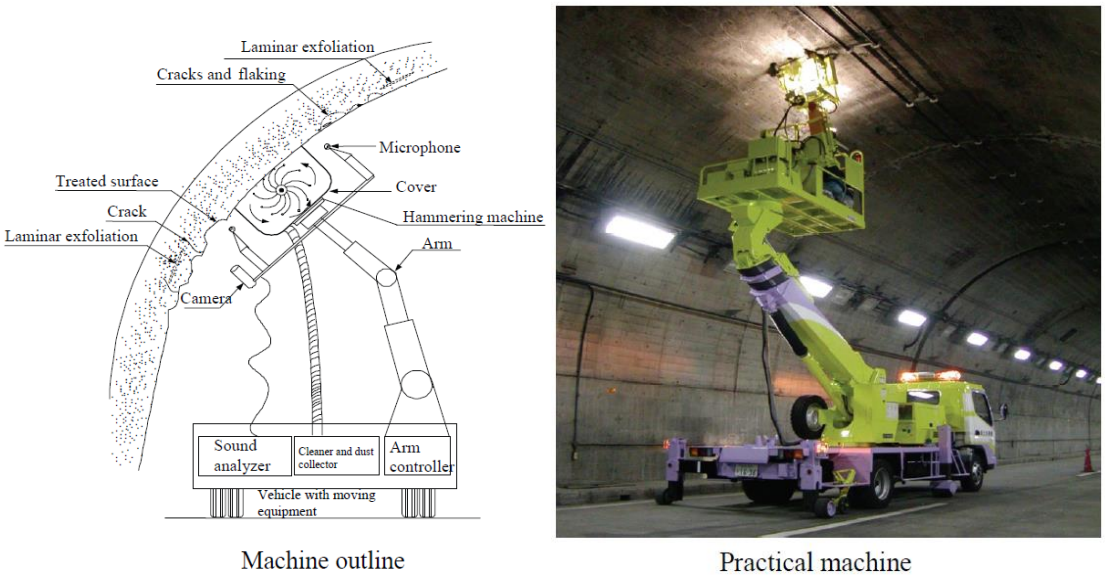

Figure 2.9: A vehicle is designed for road tunnel inspection [12]

Normally, the road tunnels are visually inspected for cracks, loosening and exfoliation of lining concrete by using a boom lift. However, this conventional method requires closing a lane for the maintenance. It is time consuming as well as by which cracks on arches cannot be detected easily. Therefore, Hideto et al [12] have designed a vehicle equipped with CCD cameras and laser beam to overcome these problems encountered in Japan road tunnel. The images of tunnel surface are captured and then processed by a system which can automatically prepare enlarged diagrams that contain cracks. Besides, the loosening and exfoliation of lining concrete will also be detected by hammering tests performed by the mechanism on the robotic arm.

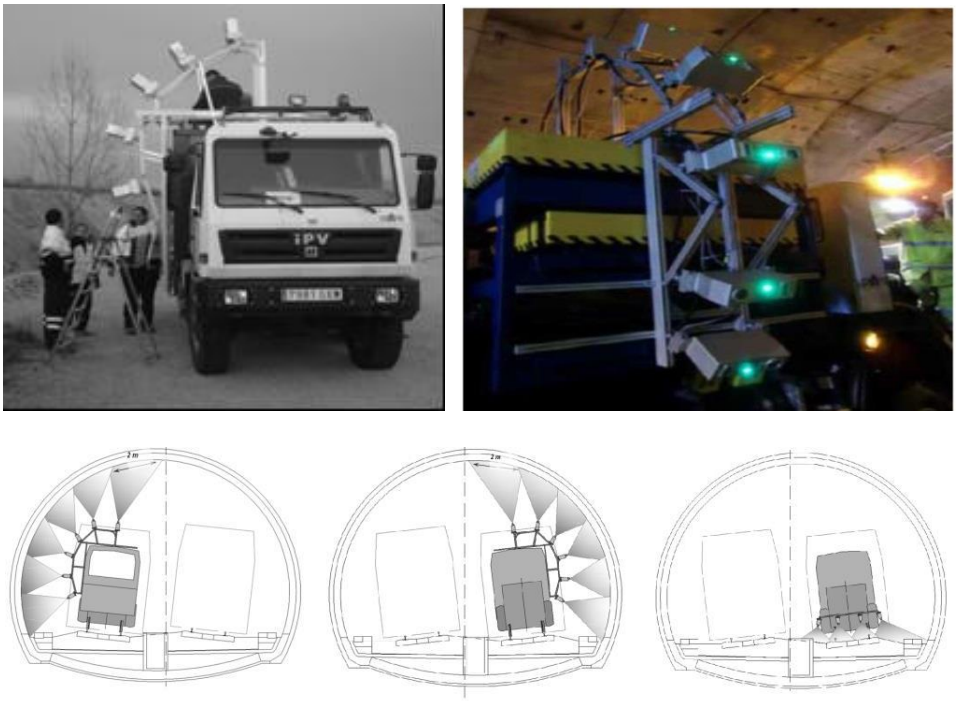

Figure 2.10: The Tunneling sensor structure [13, 14]

M. Gavilan et al [14] have developed the Tunneling, a high-performance tunnel lining inspection system which is able to carry out the long tunnel evaluations at travelling speeds up to 30km/h. It analyses the wall linings and railways, allowing for the detection of cracks, areas with running water and poorly assembled segments, etc. Six laser cameras are mounted on an all-terrain truck which provides flexibility to cope with different types of tunnels and infrastructures. Each laser-camera unit inspects a 2-meter wide section with a 1mm resolution. During the inspection, only one half of the tunnel section is covered each time so that the traffic on the free lanes will not be blocked. By using six laser cameras, a tunnel with 9m diameter can be inspected at system's maximum resolution.

2.1.1.3 Crawler type

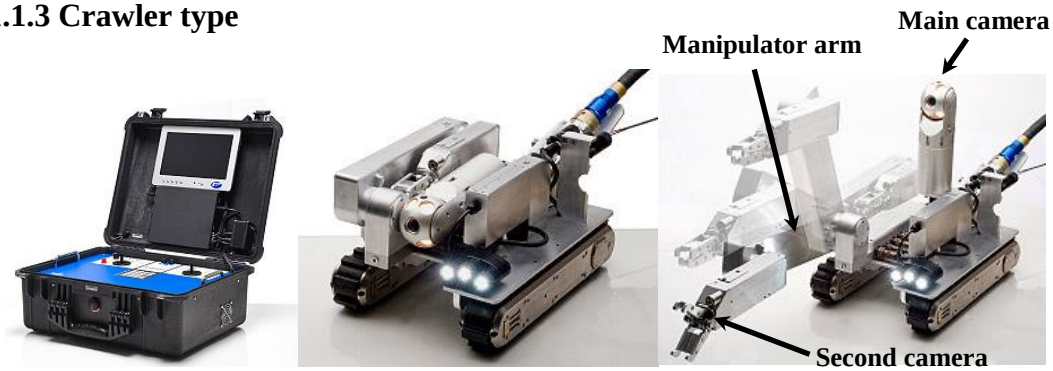

Figure 2.11: Crawler type robot from the Versatrax robot [15]

The Versatrax series robot can be directly purchased off-the-shelves on the website. It provides wide range of applications, including inspecting many miles of a sewer pipe, searching for survivors after a natural disaster, removing dangerous materials safely, completing assigned task in hazardous environments, etc. The Versatrax robot is applicable either in various diameters of round pipe or flat surface operation. The main camera can be lowered to carry out the navigation in tight spaces or can be raised upright to gain a 360 degree viewing. The manipulator arm integrated with a second camera can be unfolds from the crawler for remote handling of articles while the second camera enables user to monitor the handling operations closely. High output LED lights are mounted on both front and rear of the robot to provide high visibility in low light environments.

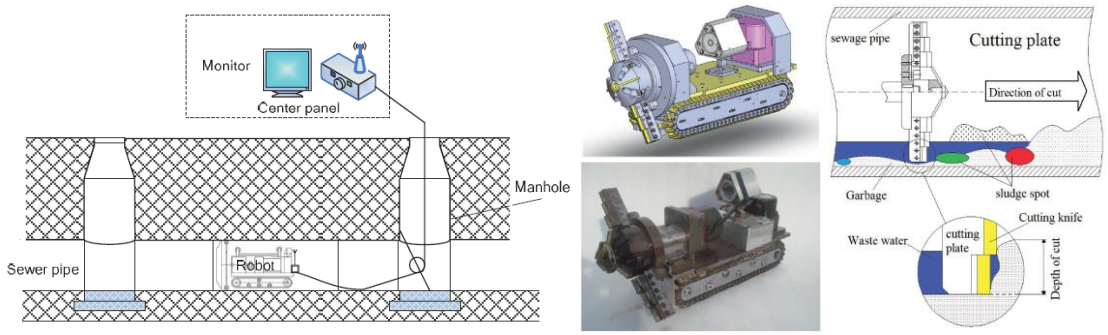

Figure 2.12: A crawler type pipe cleaning and inspection robot [16]

Nguyen T. T. et al [16] have mentioned that the three most important criteria which allow the in-pipe mobile robot to locomote on their deployed terrain are the capability of waterproof, sinkage and the traction on the ground, and all these criteria mostly depend on the sludge properties such as granularity, stickiness and hardness, and also on the weight of the mobile robot itself as well as the contact area and condition between the robot and the terrain.

In order to increase robot traction and stability, as many wheels as possible touching on the ground should be realized. Therefore, a robot designed by Nguyen T. T. et al [16] is based on the tracking mobile robot. The track size should be maximized without affecting the robot turning ability to avoid sinkage in dreg or sludge.

This robot is designed to inspect and clean the Ho Chi Minh City's sewage networks

with 300 to 600mm diameter. This design is aimed to shear the rigid dregs or sludge which cannot be removed by high pressure water jet. During the operation, the robot rotates the cutting plate mounted on an electrical-powered roller brush to cut off the rigid substances and simultaneously the water jets out from the robot to avoid dust generation. The cutting plate is made of High Speed Steel with a length of 280mm and a width of 30mm. High speed steels are high-performance steels with high wear resistance and they have high hardness at temperature up to 500^{o}C [17].

In this design, a cable is tethered to the robot and the usages of the cable are as follows:

- Provide energy supply and commands transmission
- Enable user to pull the robot out of pipe in case the robot get stuck
- Used as a measuring line for the travelled distance

Figure 2.13: A crawler robot from DrRobot [18]

The DrRobot has pioneered research in autonomous navigation and dynamic bipedal robotics that provides high performance and cost effective robots for end-users. DrRobot has commercialized their robots and they are currently available on the website. The Jaguar series robot is equipped with a 3 DOF robotic manipulator and a 1 DOF gripper which is able to reach a maximum distance of 707mm. The maximum payload of gripper is 4kg at max reach. Four tracked articulated arms mounted on the

sides of robot could convert the robot into various configurations to overcome different terrain challenges.

Figure 2.14: Quest Inspar's PipeArmor robot [19]

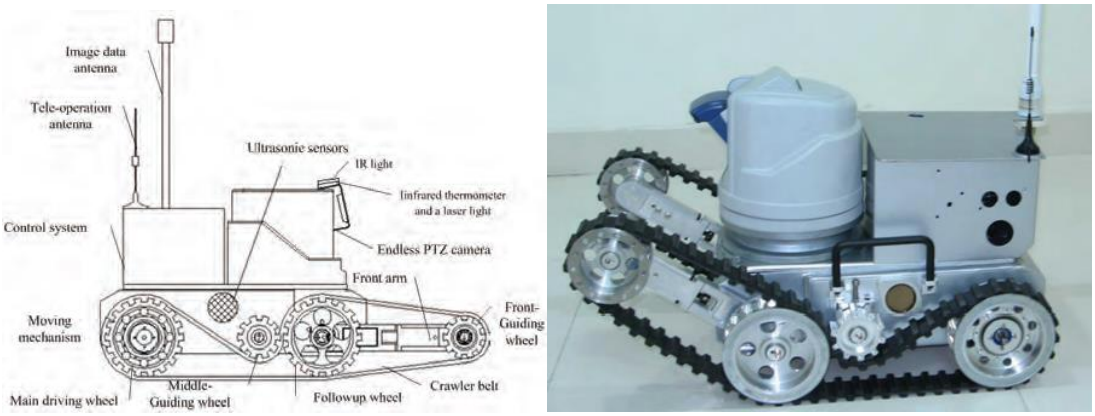

Figure 2.15: A cable-tunnel inspecting robot with tracks [20]

Fu Z. et al [20] have developed a cable-tunnel inspecting robot which consists of a control system and a moving mechanism. A symmetric double-crawler is attached to the moving mechanism. The front arm is able to rotate ranging from 0 to 90 degree. During the deployment into tunnel, the robot's front arm will rise to 90 degree to pass through the inlet of small manhole. When it needs to cross an obstacle, the front arm will adjust its angle based on the height of the obstacle.

2.1.1.4 Cylindrical type

The cylindrical type in-pipe robot generally applies pressure on the duct wall to generate necessary traction to support itself along the pipe's center. The robot is able to accomplish a number of tasks, for examples, pipe cleaning, inspection and maintenance, by holding its structure at the center of pipe and rotating around the inner

circumference of the pipe to cover the entire 3D in-pipe space. However, the pipes may break if the forces of each wheeled leg are not balanced when the robot is moving out of its centered position. Therefore, the robot has to be calibrated at the pipe's center before the corresponding task is implemented.

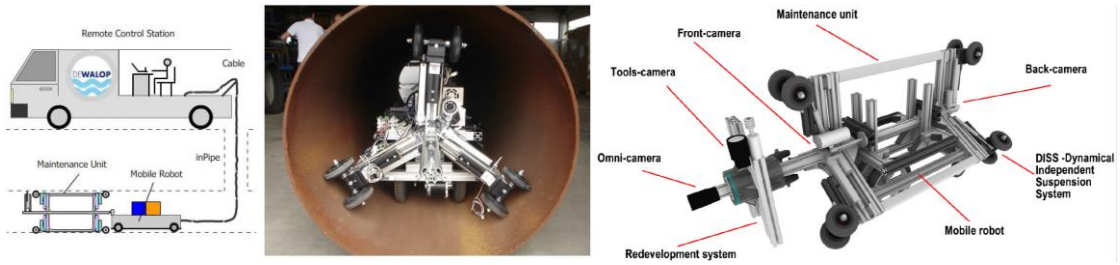

Figure 2.16: A cylindrical type robot [21-23]

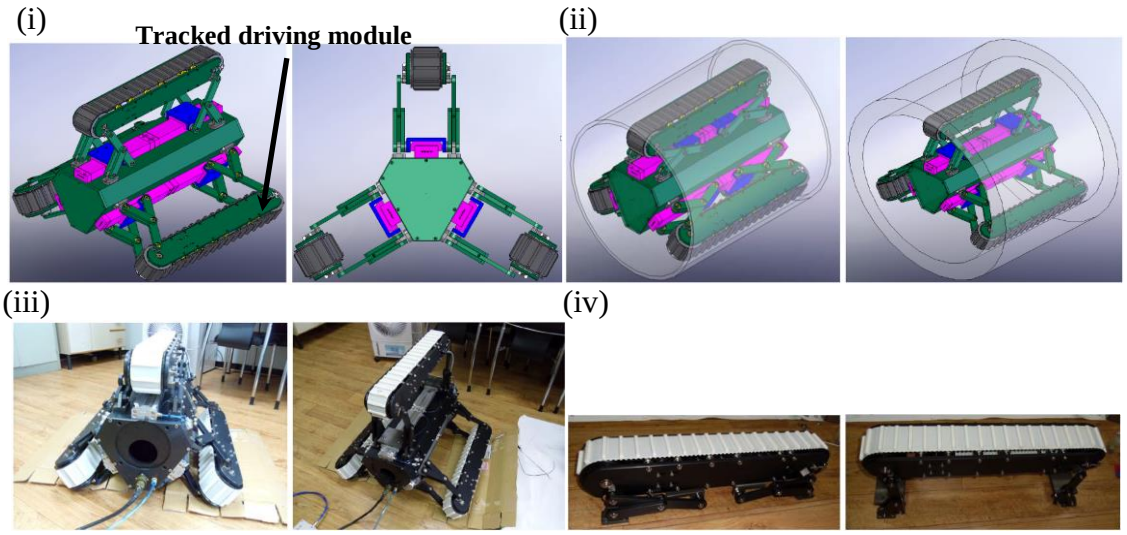

(i) Conceptual design of the in-pipe robot platform; (ii) 3D design of the in-pipe robot with adaptability to different pipe diameters(600-800mm); (iii) Prototype of in-pipe robot; (iv) Track module design

Figure 2.17: A cylindrical type robot with tracked driving module [24]

Yoon G.K. et al [24] have developed a robot which is adaptable to different pipe diameters with range of 600 to 800mm. The robot platform is integrated with a modified scissor-lift mechanism controlled by pneumatic cylinder actuators. This mechanism minimizes the distortion forces (generated when the robot moves over obstacles) while maximizes the traction forces (generated when the robot pulls the cleaning equipment along the pipe). In order to control the pushing force over the pipe wall for its mobility, two linear pneumatic cylinder actuators each equipped with three position sensors are utilized in each tracked driving module. However, more

operational functions are required for this robot, such as dynamic adaptation to external disturbances, attitude control and user-friendly remote control. Besides, cleaning tools are also needed to be further developed and integrated into the robot platform.

Figure 2.18: An Autonomous robot for inspection and maintenance of large-sized pipes [25]

Figure 2.18 shows a 300kg autonomous robot that can inspect, repair and maintain large dimension pipes. Adrian Tomoiaga of Romania, one of the inventors of this robot, received Geneva inventions award on April 14, 2016 during the 44th International Exhibitions of Inventions in Geneva. The robot is able to perform eleven tasks that are considered new at an international level and able to use hoses, hydro-blasting or high pressure spray in a continuous rotation. The robot will now be commercialized. It will be built by a factory in Borsa and the components will be assembled in Switzerland [26]. No articles or papers mentioned about the size of the robot and what size of pipe it is designed for. However, by judging from the scale of this robot in the picture, it should be designed for pipe diameter ranging from 2 to 3-meter. According to the media, there is already an interest and demand for this robot from several countries in the Middle East.

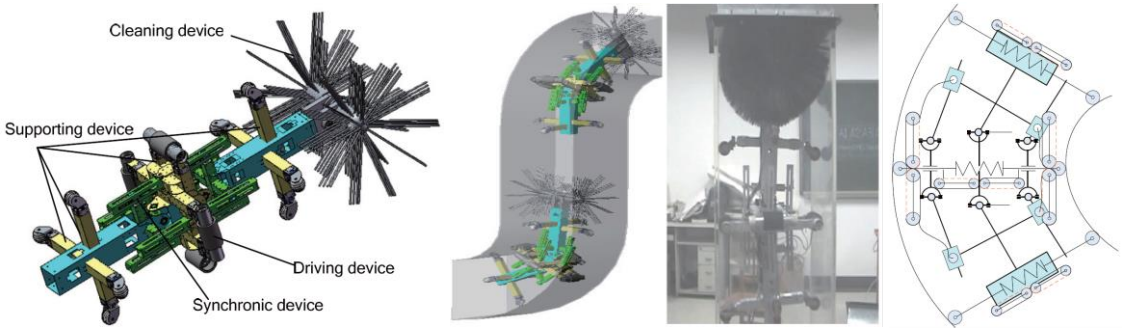

Figure 2.19: A pipe cleaning robot for air conditioning system [27]

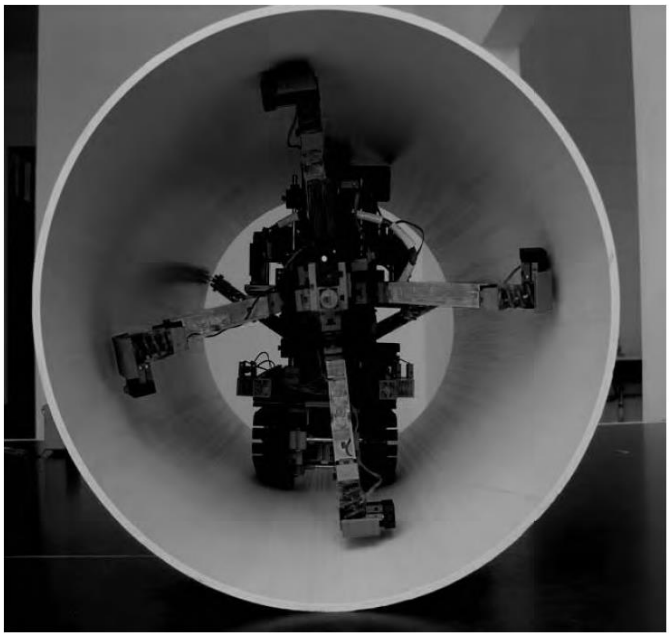

Figure 2.20: A Pipe Cleaning & Inspection Robot based on ATmega64 [28]

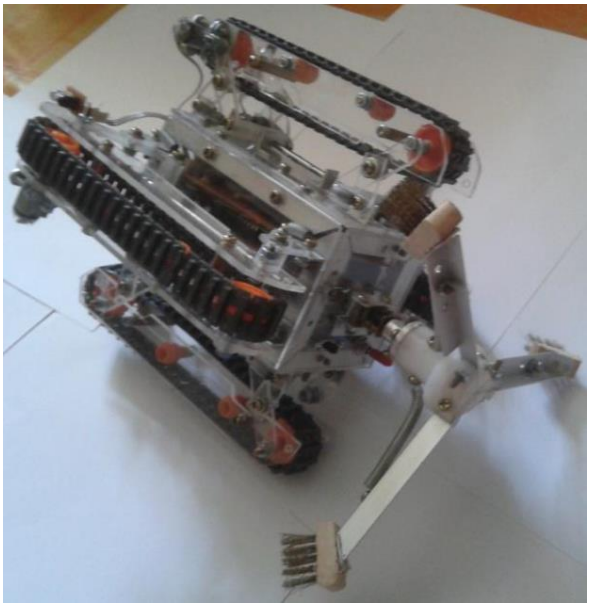

Figure 2.21: A fully autonomous pipeline cleaning robot [29]

Figure 2.22: MRINSPECT IV [30]

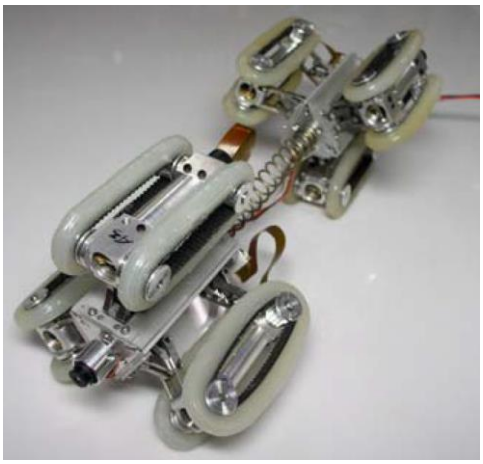

Figure 2.23: A pipeline inspection robot [31]

Figure 2.24: Tractor downhole crawling robot [32]

2.1.1.5 Legs or articulated foot type

Figure 2.25: Big Dog from BostonDynamics [33, 34]

Small amount of related research on legged robot can be found to fulfill the tunnel maintenance requirements. Legged robotic systems seem to be too complicated for practical application, and provide a poor load-carrying capacity [35]. BigDog, developed by Boston Dynamics [33], is a four-legged rough-terrain robot that is articulated like animal. The engine drives a hydraulic pump which delivers high pressure hydraulic oil to the robot's leg actuators, so that it is able to absorb shock and recycle energy from one step to the next. The system balances the robot, does navigation and manages locomotion on different terrains. It can stand, walk with a crawling or trotting gait, and squat down [34].

2.1.1.6 Inchworm type

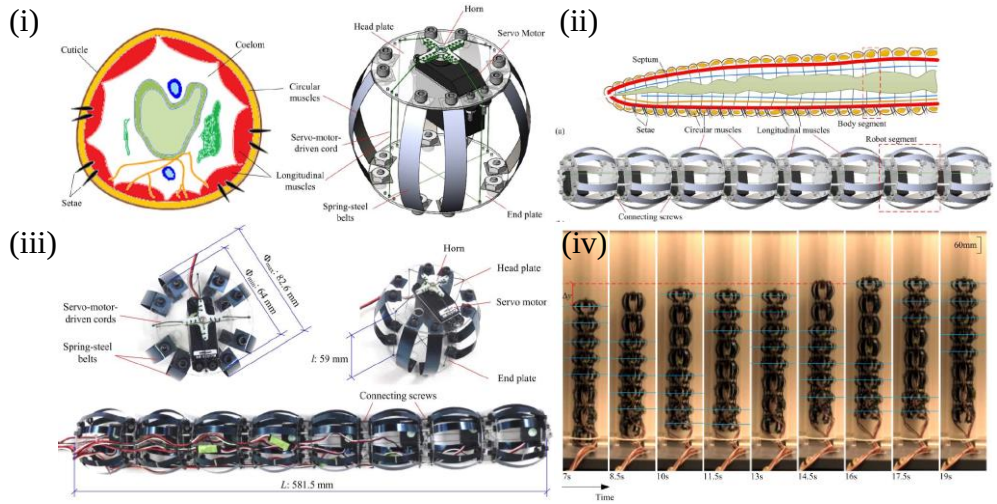

(i) Cross sectional comparison between an earthworm and a single segment of an earthworm-like robot; (ii) Longitudinal comparison between an earthworm and the eight-segment earthworm-like robot; (iii) Prototype of the earthworm-like robot; (iv) Motion testing of the robot

Figure 2.26: A inchworm type robot [36]

Fang H.b. et al [36] have developed a servomotor based actuation mechanism which mimics the alternating elongation and contraction of a single earthworm's segment. Servomotor-driven cords and spring steel belts are applied in each robot segment to imitate the longitudinal and circular muscles of the earthworm. Each robot segment is able to contract and relax like an earthworm's body segment. Figure 2.26 shows a multi-segment robot with eight identical segments in series. It is designed to carry out specific tasks in hazardous environment and confined space. In order to adapt to the change of environment, locomotion characteristics such as undesired anchor slippage

and average speed can be significantly tailored by changing different gait parameters.

The single segment of this robot consists of two transparent acrylic plates namely head plate and end plate, a servo motor with control horn, two servomotor-driven cords and eight spring-steel belts. The servomotor where the horn is fixed is mounted on the head plate. The crossed servomotor-driven cords route through the two plates and attach to the horn.

When the servomotor is actuated, the horn rotates to a predefined angle and thus tensions the cords. By doing this the distance between the two plates is reduced and then the spring-steel belts are bent. As a result, the segment is contracted axially and expanded radially. When the servomotor reverses back to its original position, the cords are loosened. The spring-steel belts will spring back and this leads to the recovery of the space between the two plates. Therefore, the segment is extended axially and contracted radially. Each segment can be actuated independently. As a result, by alternately actuating the forward and reverse rotational direction of the servomotor, the motion of the robot segment can be achieved in a similar way with an earthworm's body segment.

2.1.1.7 Helical type

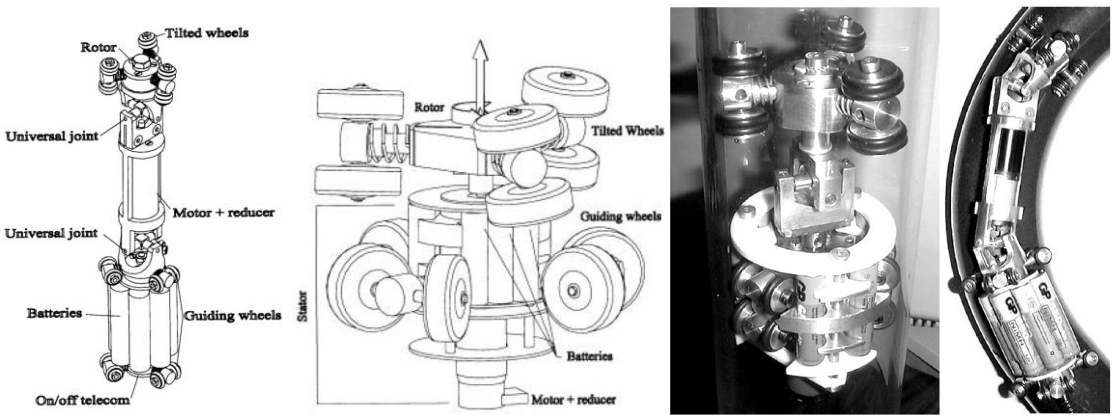

Figure 2.27: A helical type robot [37]

This design attempts to reduce the electromechanical complexity by using a single actuator to achieve mobility in the pipeline. The rotor is placed on the shaft of the actuator and the stator is equipped at the back of actuator. When the actuator shaft

rotates, the tilted wheels on the rotor follow helical trajectories and drive the entire robot to move forward while the stator follows the movement axially along the tube thanks to the guiding wheels. The actuator's rotational direction decides the moving direction of the robot.

2.1.1.8 Snake type

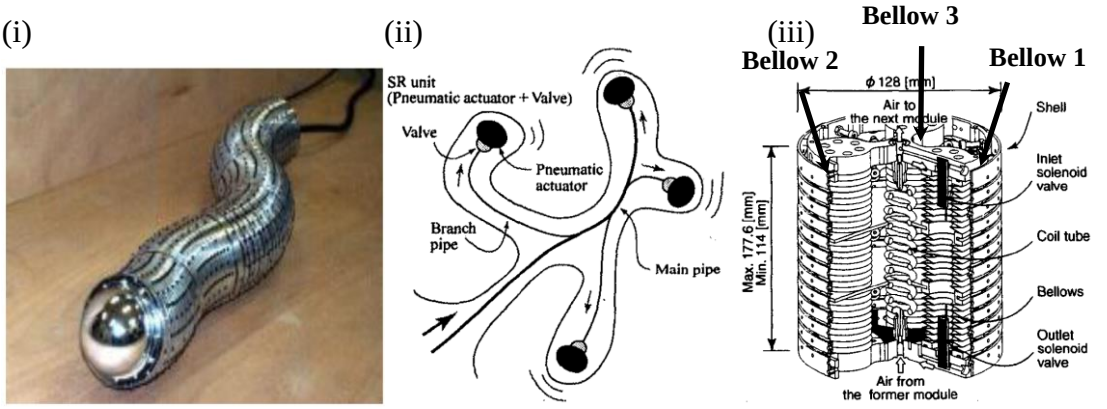

(i) A multi-DOF flexibly-deformable rope-like robot; (ii) Concept of configuration of pneumatically driven system; (iii) The mechanism design of single module

Figure 2.28: A snake type robot [38, 39]

A multi-DOF rope-like robot developed by Hidetaka O. et al [38, 39] is categorized as a hyper-redundant mobile robot. This robot is composed of six serially-connected pneumatic modules where each module consists of pneumatic actuators, displacement sensors, valves, microprocessor and springs. Each module has three bellows which are arranged equally around the circumference and it is able to perform 3 DOF motion.

Normally for most of the conventional pneumatically driven robots, the air control valves are mounted outside of the drive mechanism to make it smaller and lighter. However, by doing this way, the robot system composed of many actuators will engage the difficulty of maintaining its shape because all the pipelines from pneumatic actuators need to be arranged to the valves outside of the drive mechanism. Therefore, in this design, six on-off solenoid valves for the inlet and outlet of air are mounted at each end of the bellows respectively in each module. A main pipe for compressed air supply is connected into the body of the robot. The compressed air is provided into each bellow through the branch pipe. By controlling the air intake of each bellow through the control valve, the module can achieve the desired motion.

2.1.1.9 Variable velocity PIG type

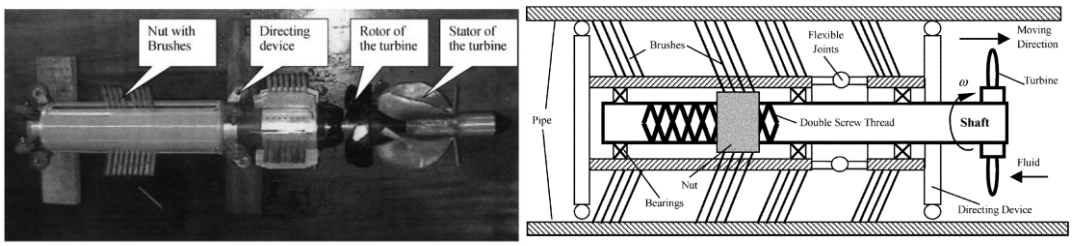

Figure 2.29: Basic structure of hydraulic brush PIG [35]

Generally, it is very hard for wheels robotic systems to generate enough traction force to move against a fluid with high flow rate. A VVPIG robot designed by Zheng Hu et al [35] is able to move with and against the direction of the flowing fluid in the pipe effectively via a turbine and a reverse-traverse screw mechanism. This design is distinguished from the conventional PIG type of robot which can only follow the flowing fluid. Many oil and gas industries benefit from this robot of its valuable bidirectional capability.

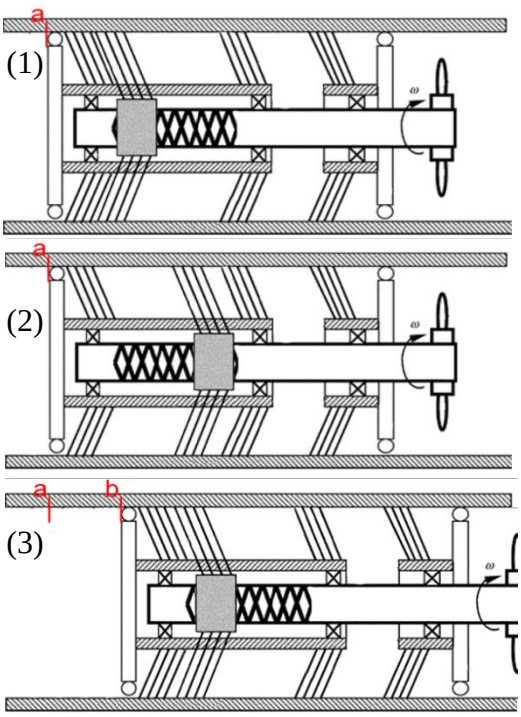

Figure 2.30: The motion of VVPIG robot from point a to b

The directing device integrated with wheels keeps the robot in the middle of the pipe. The reverse-traverse screw thread mechanism transforms the rotational torque of the turbine which generated by the fluid flow into the translational propulsion force for robot movement. Besides, the reversing nature of the screw converts the turbine's rotating motion into the nut's reciprocating motion on the shaft. Due to the fact that the brushes with rearward-pointing bristles can move forward easily but are difficult to move backward, the robot can be able to crawl upstream or downstream depends on the initial direction of the bristles.

As shown in Figure 2.30, the working principle of the mechanism is as follows:

(1) The turbine is rotated by the fluid flow, and which will then drive the transmission shaft rotating at the same speed.
(2) When the nut is in the forward driving screw thread, it will be pushed forward (to the right) because the brushes attached to the nut can be able to slide towards along the pipe while the brushes on the body of the PIG is stationary against the pipe wall.
(3) When the nut arrives at the end of the screw thread, the nut will be moving backward conversely. Since the rearward-pointing brushes on the nut are hardly to move backward, the robot body will begin to move forward instead.

Mihaita HORODINCA et al [37] have mentioned that broad categories of robotics system can be identified based on the pipe size:

(1) Generally, for small size of pipeline, the concept of the inchworm and snake robot has been followed in many projects due to its capability of axial motion in the confined space of pipeline.
(2) For medium pipes, classical electromechanical systems have been proposed with various wheels and tracks architectures which involving more or less complicated kinematical structures. Cylindrical and helical type of robots also can be adopted in this category.
(3) For large size piping, tube crawlers and wheel type of robots have been proposed.

2.1.2 Comparison of Pipe and Tunnel Robots

The comparison of various types of Pipeline and Tunnel Inspection Robots is shown in Table 2.1. Table 2.1 implies that most of the existing pipeline and tunnel robots are only applicable to small or medium pipelines. It is hard to identify any single robotic technology that can perform maintenance in large tunnel (more than Dia. 3000mm) with multifunction. This shows the possible gaps in the existing tunnel robot design that potential contributions can be approached by developing a tunnel robot for long distance maintenance in large-diameter tunnel.

Type	Pros	Cons	Robot	Capability	Applicable Pipe Size
PIG	• Simple mechanism design • No power supply required	• Keep rotating along its central axis when moving • Poor performance on various conditions like low fluid flow or complex pipe system • Only moves along the direction of fluid	[5, 6]	Inspection	ϕ25-150mm
			[7]	Inspection	NA
Wheels	• Common design • Low maintenance costs • Lower cost than tracks	• Complex steering mechanism • Poor performance on certain terrains • High centering when travelling over uneven terrain	[8]	Inspection & Cleaning	ϕ 1600-2600mm
			MAKRO [9]	Inspection	ϕ 300-600mm
			[10]	Inspection & Cleaning	NA
			[11]	Inspection	NA
			[12]	Inspection	NA
			[13, 14]	Inspection	ϕ 9000mm
Crawler	• Handles more aggressive terrain	• Less energy efficiency • Expensive	[15]	Inspection	Min. 381mm
			[16]	Inspection & Cleaning	ϕ 300-600mm
			[18]	Inspection	NA
			[20]	Inspection	700x700mm
			[19]	Repairing	ϕ 152.4-4419.6mm
Cylindrical	• Able to move forward and backward freely in small diameter pipe • Adaptable to small pipes with different diameters	• Calibration at the center of pipe is needed before the operation • Mainly suitable for precise motion in small pipe • Not suitable for complex pipe structures with low payload	[21-23]	Inspection	ϕ 800-1000mm
			[24]	Inspection	ϕ 600-800mm
			[25, 26]	Inspection, Cleaning & Repair	NA
			[27]	Cleaning	Rectangle 300-600mm
			[28]	Inspection & Cleaning	ϕ 300-600mm
			[29]	Cleaning	ϕ 150mm
			[30]	Inspection	ϕ 100mm
			[31]	Inspection	ϕ 80-100mm
			[32]	Inspection	NA
Legs	• Able to cope with different in-pipe environment	• Relatively complicated for practical application • Provide poor load-carrying capacity • Instability during locomotion	[33, 34]	-	NA
Inchworm	• Light weight • Cheap	• Not effective due to its low speed • Poor reliability	[36]	-	ϕ 103.5mm
Helical	• Relatively less actuators needed • Able to move forward and backward freely in small diameter pipe	• Not effective due to its low speed • Mainly suitable for precise motion in small pipe • Not suitable for complex pipe structures with low payload	[37]	Inspection	ϕ 40-170mm
Snake	• No motors and wheels needed • Move horizontally like normal wheeled robot motion	• Need more energy for operation	[38, 39]	-	NA
VVPIG	• No power supply required • Able to move with either along or against the direction of the flowing fluid	• Poor performance on various occasions like low fluid flow or complex pipe system	[35]	Cleaning	NA

Table 2.1: Comparison of Pipeline and Tunnel Robots

CHAPTER 3: CONCEPTUAL DESIGN OF ROBOTIC PLATFORM

3.1 Design Requirements

There are various design requirements that serve as a guide to design the robotic platform. The robot must satisfy various constraints to deal with the challenges so as to achieve full functionality and robustness. Among the various factors being considered are:

(i) Robot reliability

This criterion is to ensure that the robot can maneuver successfully without stalling or being trapped in the tunnel. Robot can cope with various tunnel conditions from dry, muddy and partially filled water while sudden breakdown of robot mechanism has to be minimized. Moreover, the robot can carry out the essential inspection task in the trunk sewer. It can acquire video images suitable for real-time visual inspection of the tunnel bore without interruption.

(ii) Structural rigidity

It is defined as how strong the structure of robot can be, and how much external impact the structure can be able to withstand. The robot requires adequate weight to maintain maneuverability in slippery environment, so the structure has to be strong enough to overcome the load on itself. A good structural design also should avoid any protrusion on the design so that the robot will not get stuck at the sludge or debris in the tunnel and at the intermediate platform in the access shaft.

(iii) Modular design

It is defined as how easy it is to extend or improve the robot further. Robot that is designed approaching its minimum size for the access of 60cm x 60cm manhole opening might not have any extra space to attach other device if needed. Despite other additional device is attached, the design of modularity will be more complex.

(iv) Motion control of robotic platform

It is defined as how well and reliable the mechanism can move straight in the tunnel. For the two- or four-wheel drive, every wheels are hard to achieve the exact same rotational displacement without encoder and hard to travel in straight line on a curved surface due to the software program or mechanism limitations as well as the environment constraints. Moving in a straight line makes it more stable and efficient in the maintenance task.

(v) Management of robot weight

The robot cannot be too heavy as it may damage the water-proof lining on the tunnel surface and is not convenient for robot transportation and deployment. A light-weight robot design may not have enough traction force for locomotion and can hardly move stably in the tunnel.

(vi) Ease of fabrication and maintenance

It is measured by the number of mechanical parts in the design of robotic platform. Simple design with fewer parts is easy to fabricate and assemble. It can also be measured by the shape of the parts that need to be fabricated. Simple shape like straight edges and circular holes are easier to fabricate. Besides, simple mechanism is easier to troubleshoot without any guidance from user manual.

3.2 Morphological Chart

From the literature review in Chapter 2, the sub-functions of the tunnel robot can be defined. The next step is to find out possible design for each of the sub-functions to form the morphological chart. The morphological chart of each of the sub-functions is shown in Table 3.1. On the left side of the chart, the functions are listed. Different mechanisms which perform the corresponding functions are listed on the right side. The idea generation is accomplished by creating single system from different mechanisms as shown in the morphological chart.

Body Configurations	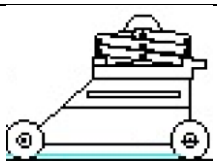		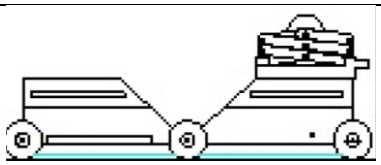		
	Single Segment		**Multiple Segments**		
Locomotion Mechanisms	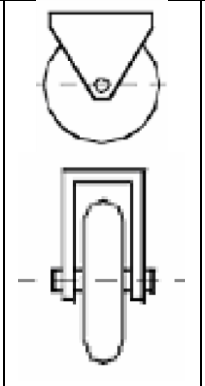	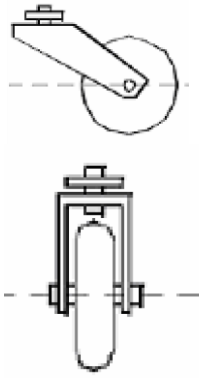	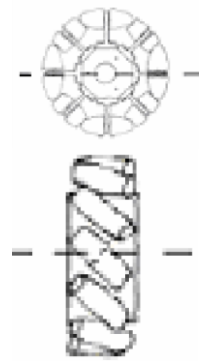	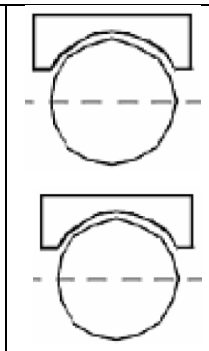	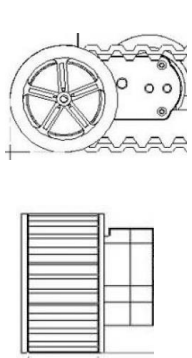
	Standard Wheel	**Castor Wheel**	**Swedish Wheel**	**Spherical Wheel**	**Tracked Wheel**
Number of Wheels in each segment	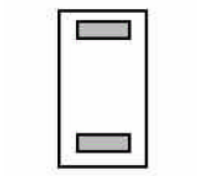	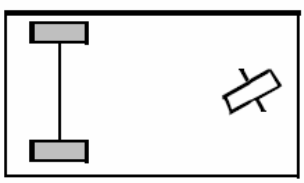	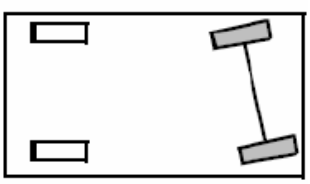		
	Two-Wheel	**Three-Wheel**	**Four-Wheel**		
Wheel Configurations	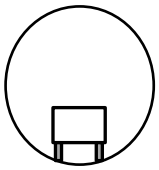	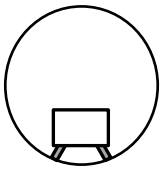	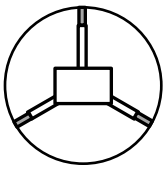		

Table 3.1: Morphological chart of the tunnel robot

3.3 Embodiment Design

From the morphological chart in the previous section, various paths could be selected to generate various concepts of the robot design. The different paths for tunnel robot design are illustrated in the Table 3.2.

Based on the studies of existing pipeline and tunnel robot, four conceptual designs have been generated from these paths respectively. The four concepts will be depicted in the following sections.

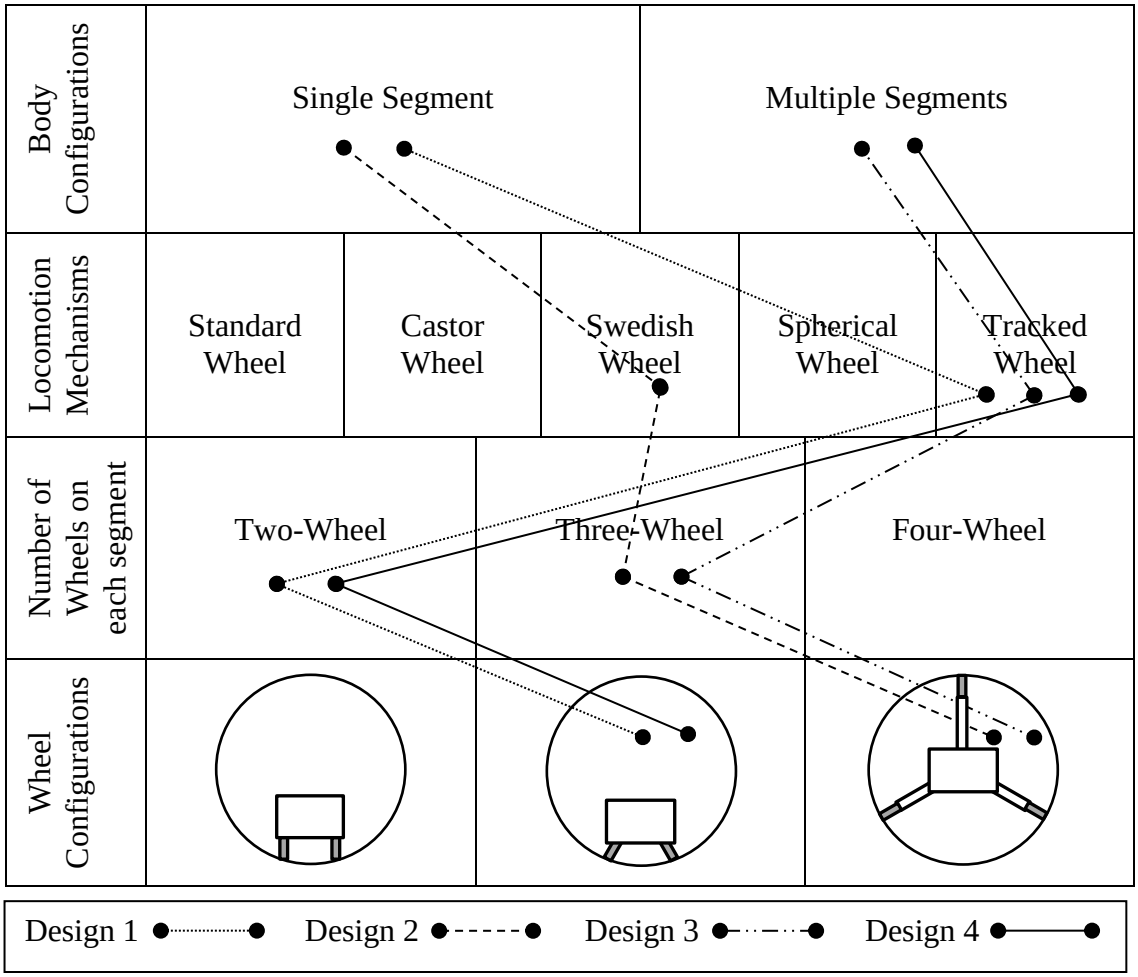

Table 3.2: Paths taken for different concepts of tunnel robot

3.4 Conceptual Design 1

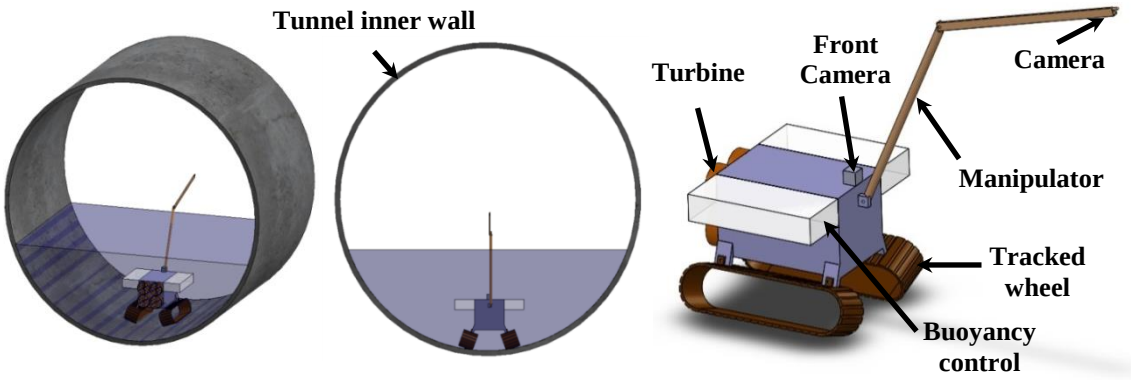

Figure 3.1: Conceptual design 1

Conceptual design 1 is a common tracked robot with a manipulator arm where camera will be mounted on the end effector. Turbine and buoyancy system will be integrated to this design so that the robot is able to swim along the tunnel during rainy season. It is adaptable to pipeline with different diameters and is able to handle more aggressive terrain. The manipulator arm needs to be long enough so that the working envelope of the arm can cover the tunnel surface.

3.5 Conceptual Design 2

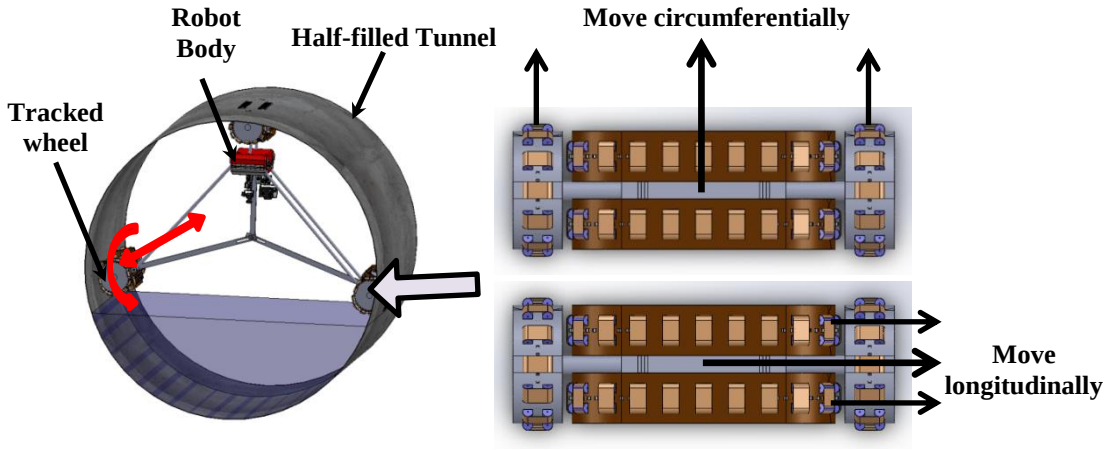

Figure 3.2: Conceptual design 2

The second design is able to move along the upper part of tunnel so as to get rid of the sludge accumulated at the lower part of the tunnel as well as the influence of fluid flow in the tunnel. It equips with special tracked wheels which have the same working

principle as Swedish Wheel. The Swedish Wheel is made up of a bunch of small rollers which can move vehicle in any direction by varying the speed of rotation of each wheel. In this design, three wheels expand radially and compress the inner wall to generate sufficient traction force for its locomotion. The wheels are able to move circumferentially to balance the horizontal position of the robot while the longitudinally movement of the wheels allow robot to locomote along the tunnel. The study of the traction force has to be done to ensure the tracked wheels can support the robot body and yet not too large to damage the waterproof-coating on the tunnel wall.

3.6 Conceptual Design 3

In this design, turbine is adopted to the end of robot body to stabilize the motion of the robot when it moves against water flows. It comprises of three tracked driving module and each driving module equips with camera and nozzle head. The robot follows helical trajectories to drive forward and every single area of the inner surface can be investigated thanks to the tilted tracked wheels. The nozzle is much closed to the wall so that low pumping head is enough.

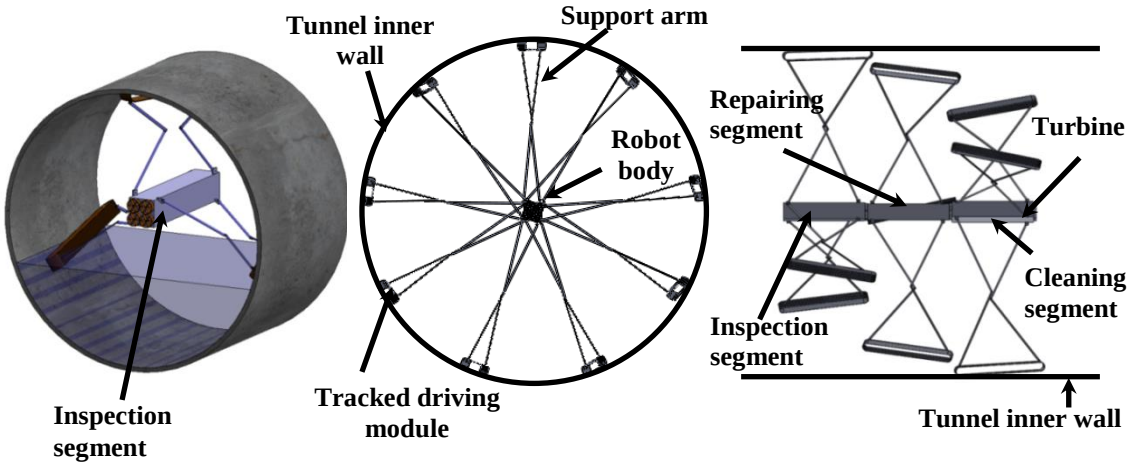

Figure 3.3: Conceptual design 3

The disadvantage of this design is that the support arms have to be strong enough to hold the robot at the center position; otherwise the uneven applied force on tracked wheels may damage the inner wall. Alternately, more detachable identical segments can be assembled in series to perform different tasks individually, such as inspection, cleaning and repair. The inner surface of tunnel is fully covered by robot's helical

trajectories, therefore inspection, cleaning and repairing for any point on the wall is possible.

3.7 Conceptual Design 4

This design which moves in helical trajectories is similar to the Design 3 but it doesn't have the main robot body. It consists of a number of tracked driving modules, each module equipped with camera, nozzle and repairing equipment.

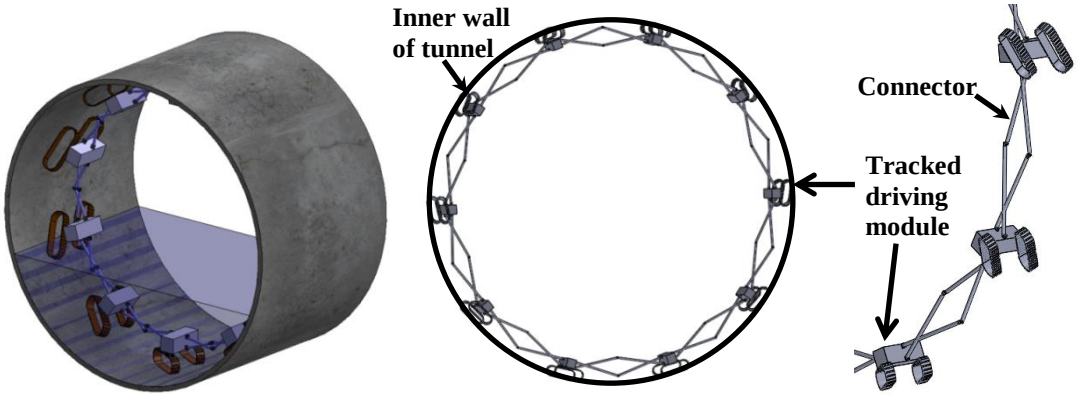

Figure 3.4: Conceptual design 4

No turbine is required for the stabilization of the robot because the modules are closed to the wall, partially or fully filled in-pipe condition will have relatively less effect on the motion control due to fluid viscosity. In other words, the fluid flow closed to the tunnel wall has the minimum velocity and it hardly affects the motion of the robot.

3.8 Robot Design Evaluation

Selection criteria are developed to select a design that best suit to the project needs. These criteria can be obtained from the design requirements explained in earlier chapter. However, not all of these requirements are equally important, and hence a weighted average is assigned to each of the criteria according to its importance. Higher weighted average is assigned to criteria that are more important compared to the others. The developed selection criterion for tunnel robot with the weighted average is shown in Table 3.3.

No.	Criteria	Weighted Average
1	Robot reliability	25%
2	Structural rigidity	20%
3	Modular design	20%
4	Motion control of robotic platform	15%
5	Management of robot weight	10%
6	Ease of fabrication and maintenance	10%

Table 3.3: Weighted average of the selection criteria for robotic platform

Concept selection is a process of evaluation the design concepts. It compares the strength and weakness of each concept. To select the best concept among the four conceptual designs, a matrix evaluation table is needed. A number ranging from 1 to 5 is assigned to each design for respective criteria. The description of each rating is as follows:

1 – Poor, unsatisfactory

2 – Tolerable, acceptable

3 – Moderate

4 – Suitable, good

5 – Ideal, very good

After that, these values are multiplied with the weighted average to obtain the *"W.V"*. For each concept, all the *W.V.* value of each criterion is summed. The concept with the highest sum of *W.V* value will be the one that has the best solution for the challenges of tunnel inspection. The construction of the matrix evaluation table is shown in Table 3.4.

Criteria	Weight (%)	Design 1		Design 2		Design 3		Design 4	
		Values	W.V.	Values	W.V.	Values	W.V.	Values	W.V
Robot reliability	25%	4	1	3	0.75	3	0.75	2	0.5
Structural rigidity	20%	4	0.8	3	0.6	3	0.6	2	0.4

Modular design	20%	3	0.6	3	0.6	5	1	4	0.8
Motion control of robotic platform	15%	3	0.45	4	0.6	5	0.75	5	0.75
Management of robot weight	10%	5	0.5	3	0.3	3	0.3	2	0.2
Ease of fabrication and maintenance	10%	5	0.5	3	0.3	4	0.4	2	0.2
			3.85		**3.15**		**3.8**		**2.85**

Table 3.4: Matrix evaluation table for the four concepts of robotic platform

From Table 3.4, it can be seen that the Design 1 has the highest summation of W.V. value. After careful consideration, it is selected for further development because it has common design, less fabrication cost and potential feasibility to withstand challenging environment in the large-diameter tunnel to undertake the maintenance task.

3.9 Preliminary Design of Robotic Platform

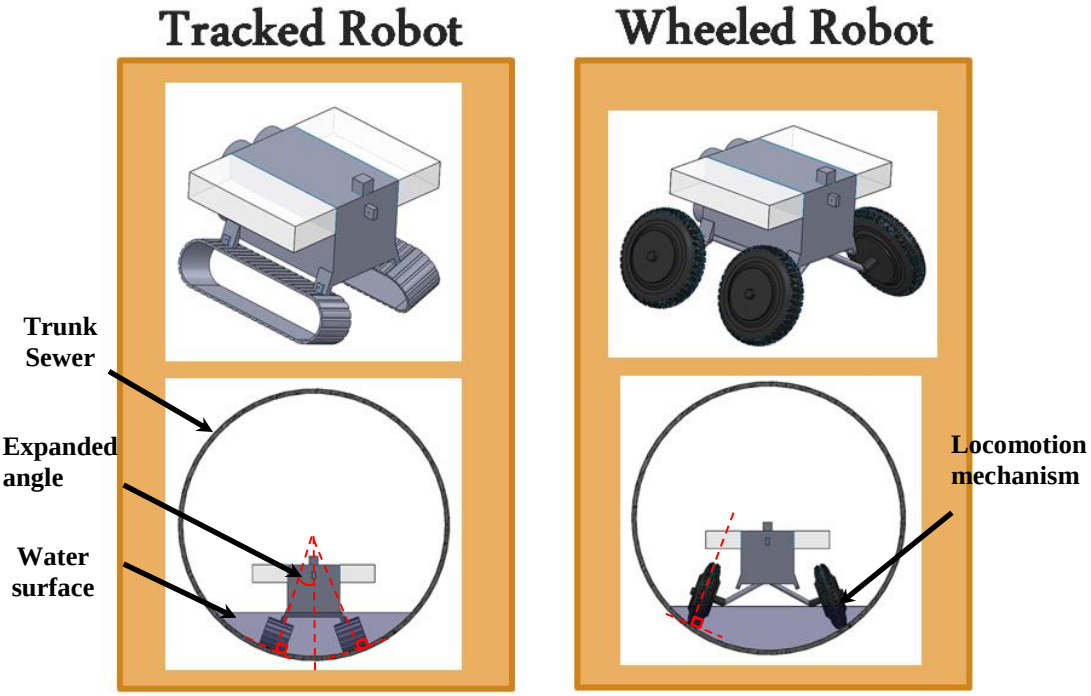

Figure 3.5: Tracked and Wheeled Robot Design

Two preliminary designs of the robotic platform, track-based and wheel-based robot, are carried out and simulated in 3D model to evaluate the functionality and feasibility of the design concept.

Figure 3.5 shows the conceptual design of robots in isometric view and the relative dimension of the robotic platform to that of the trunk sewer when it is placed inside. When the robot is being deployed into the sewer through the vertical shaft, the wheel frames of robotic platform expand to certain angle which is perpendicular to the tunnel surface before landing onto the sewer. This helps to allow robotic platform acquires better traction force over the sewer surface and also to get rid of the sludge at the bottom. The conceptual design of the robot chassis and the actuation mechanism to control the angle of the wheel frames will be covered in the following chapters.

3.9.1 Mounting Frame Design

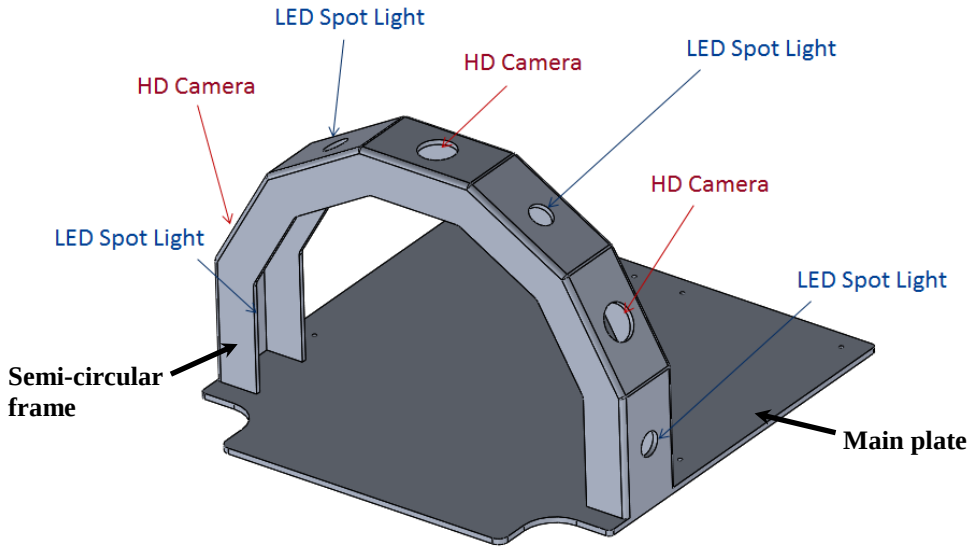

Figure 3.6: The Design of Mounting Frame

The mounting frame is in the form of a semi-circular arch with a main plate as shown in Figure 3.6. The semi-circular frame and the main plate may be welded together into single mechanical part to increase the structural rigidity. The frame is designed for the mounting of three HD cameras and four LED spot lights, forming an inspection array radially at equal angle apart and facing towards the inner circumference of the sewer to completely cover the surface of the sewers above the water level. The main plate is the main support structure of the robotic platform - all the mechanical parts will be

assembled based on the main plate, for instance, front and rear camera, enclosures, wheel frames, ballast, etc.

3.9.2 Conceptual Designs of Wheeled Robot

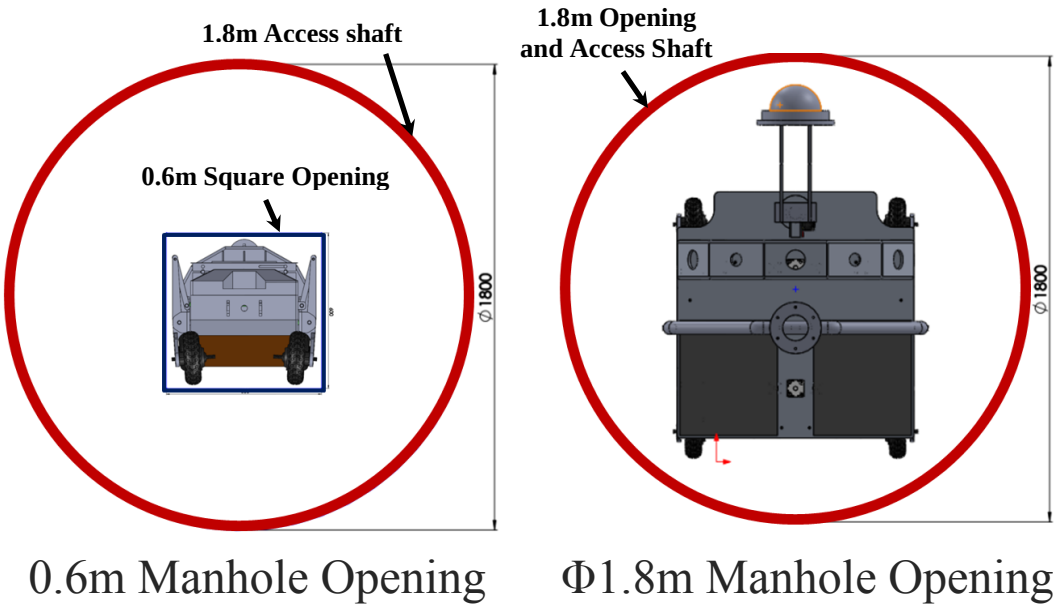

Figure 3.7: Comparison of inspection robot and manhole opening (Top view)

Two mobile robotic platforms are proposed to cater for two different sizes of manhole opening. The relative dimension of the inspection robot and the manhole opening is shown in Figure 3.7. It shows the top view of the manhole opening and the configuration of the robot when being deployed vertically into the sewers. The small robot on the left is able to access the 0.6m opening of trunk sewer. The overall size of the inspection robot on the right is designed to access the entrance of DTSS with diameter of 1.8m.

3.9.2.1 Robot Design for 0.6m Opening

Due to the fact that this robot has to be small enough to access the 0.6m opening, the wheel frames of the small robot needs to be able to expand horizontally to the sides of the sewer to increase the clearance between the wastewater and the robot chassis so as to avoid sludge along the pipe and to increase the robot stability. Two small wheels mounted in between the hub motors are utilized to prevent hard debris or other obstacles stuck at the center position.

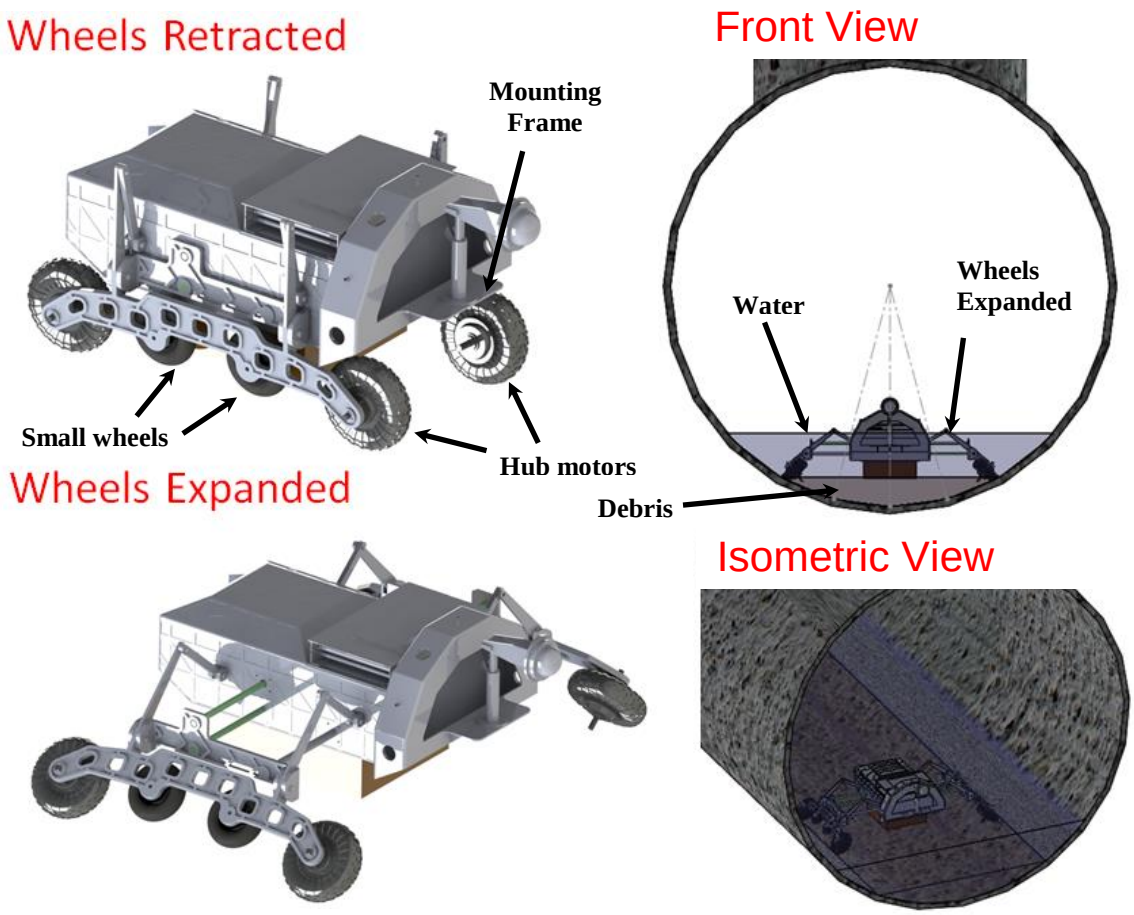

Figure 3.8: Robot Design for Small Manhole Opening

The front view in Figure 3.8 shows that the water level is too high for the robot. The robot is almost immerged into water. Also, the humidity inside sewers is normally wet and the presence of vapor may cause the image captured to be misty if the camera is too far away from the target surface. Therefore, for larger diameter sewers, a lifting mechanism, as shown in Figure 3.9, is designed to lift the inspection array up above water surface so that the view of the cameras will not be blocked by water and the camera can be as near to the target surface as possible. Using lifting mechanism to move up the camera array may increase the center of gravity and it would risk dangling and destabilizing the robotic platform. The quality of the image captured and the mobility of the robot will be affected consequently.

.

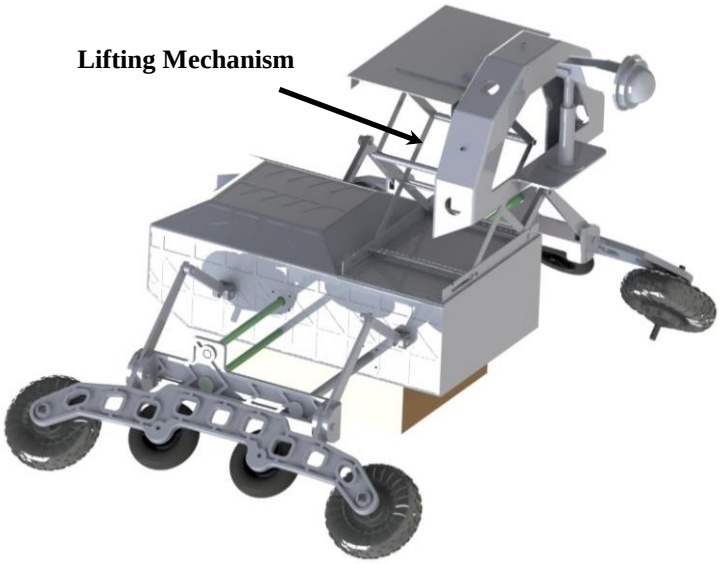

Figure 3.9: A lifting mechanism on the robot platform

After the evaluation of this design, it is a bit complicated because of the extensible wheels mechanism, and we also need to squeeze every component into limited space in the robot body. As shown in Figure 3.10, limited space can be utilized for the mounting of other electrical components such as controller, transformer box, motor drivers, etc.

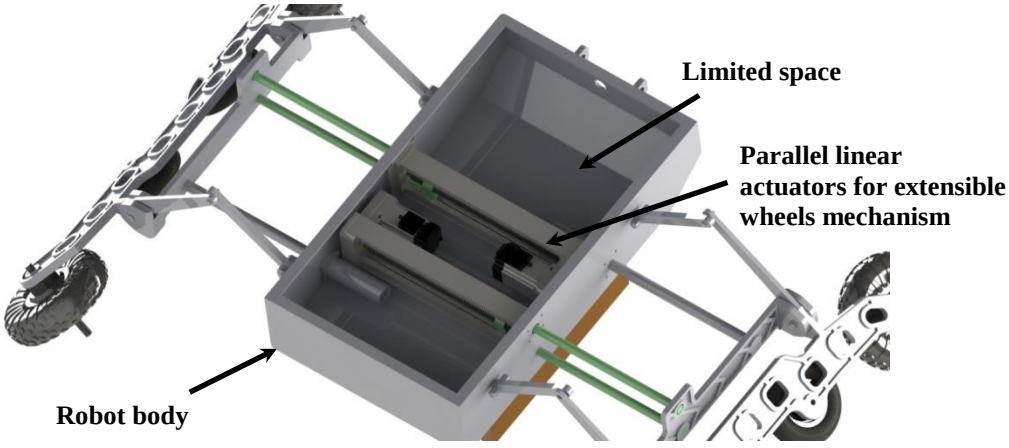

Figure 3.10: Configuration of the Actuators

3.9.2.2 Robot Design for 1.8m Opening

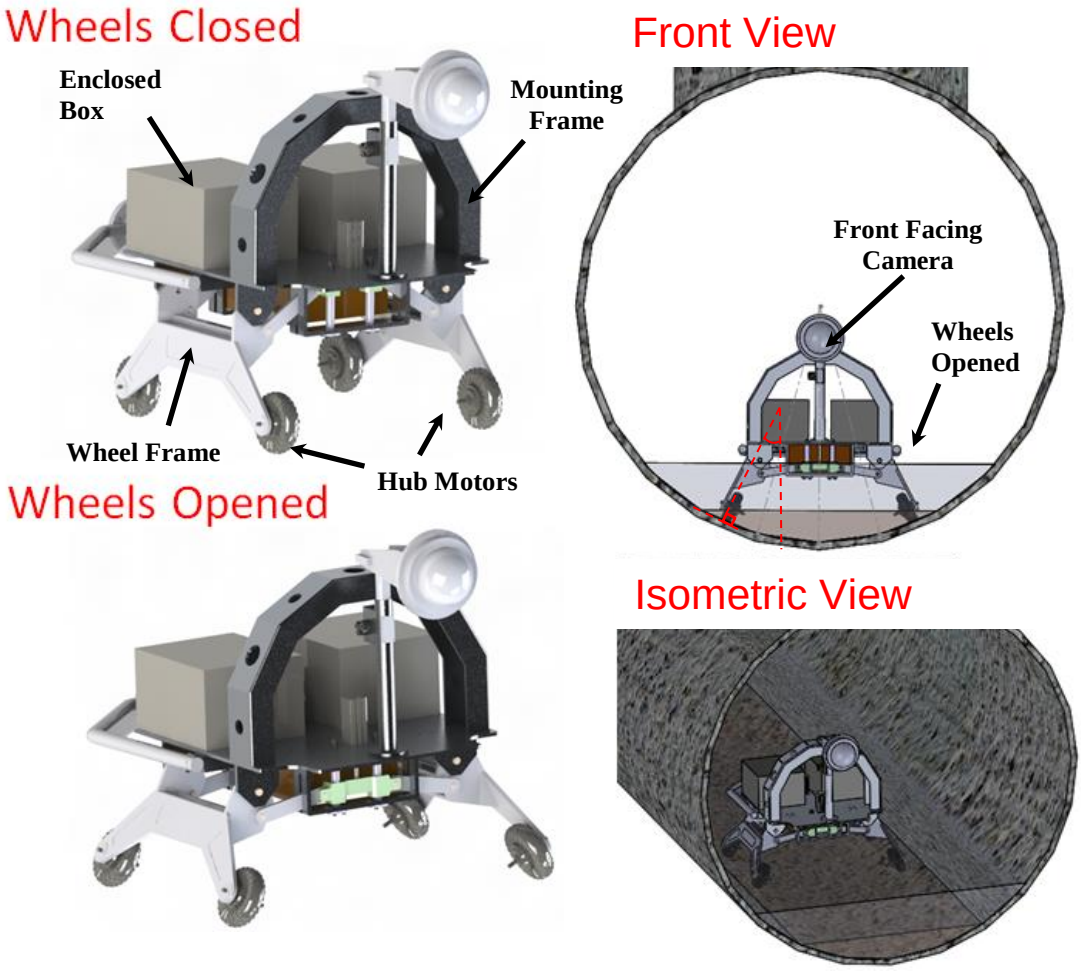

Figure 3.11: Robot Design for Large Manhole Opening

In Figure 3.11, it is seen that two water-proof enclosed boxes fixed on the main plate are used to house the electrical components such as drivers and controller. The front facing camera is at a high position in the sewers, allowing an unblocked field of view of the sewer for navigation. Also, it has low center of gravity and has large base to increase the robot stability. The figures on the right illustrate the situation when the robotic platform is deployed in the trunk sewer. In this design, the platform of the robot is to be kept well above the water surface.

The Figure 3.12 shows the design of the chassis and actuation for the wheeled robot. The locomotion can be tilted to certain angle to avoid the possible presence of soft debris along the bottom of the 3-meter trunk sewers. This is achieved via a slider-crank mechanism which is used to transform translational motion into rotational motion.

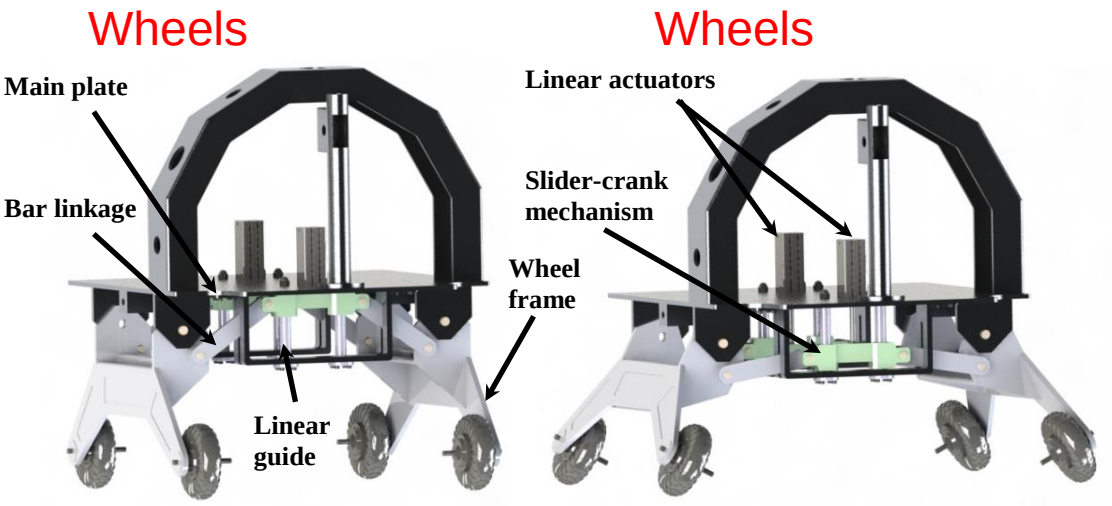

Figure 3.12: The actuation mechanism to control the angle of wheels

The slider-crank mechanism has a well-known application in engines, which is used to transform translational motion into rotational motion. As depicted in Figure 3.13, the wheel frame (1) is attached to the main plate (4). The bar linkage (2) links the wheel frame to the linear guide (3). By pushing the linear guide up and down, we could realize the rotational motion on the wheel frame.

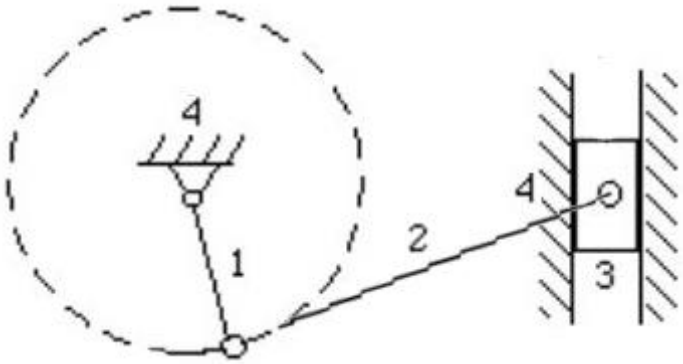

Figure 3.13: Slider-Crank Mechanism

Careful evaluation and consideration has been taken place between the two designs and the latter robot design is consequently selected for further development.

3.9.2.3 Robot Weight

Robot weight is one of the most important factors affecting the mobility of a robot. Determining the weight of the robot is necessary so as to ensure the motors are strong enough to move the robot as well as the robot weight is within the load capability of the

hoisting mechanism. Also, it helps in umbilical selection as the cable breaking strength has to be larger than the robot weight. In order to estimate the weight of our robot, the related information of the existing pipeline robots is summarized. Based on the given mass and volume of the robots, we can estimate the density of each robot. Assuming the size of our robot is 1 meter cube, we can then estimate the weight of our robot, which is 180.7kg.

Robot	Photo	Mass (kg)	Size LxHxW (mm)	Density (kg/m^3)	Robot	Photo	Mass (kg)	Size LxHxW (mm)	Density (kg/m^3)
[8]		2500	3500x1500 x1500	317.4603175	[30]	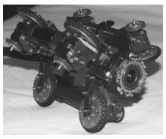	0.7	150 w/ Dia. 85mm	205.598081
[20]		3	420x300x320	74.4047619	[18]		20	615x265x573	214.1679028
[34]		109	1100x1000 x300	330.3030303	[37]		1.3	163 w/ Dia. ?	N.A.
[36]		0.576	581.5 w/ Dia. 64mm	76.9773478	[27]		N.A.	N.A.	N.A.
[24]		80	680 w/ Dia. 340mm	323.9465563	[29]		0.7	139.7 w/ Dia. 165.1mm	58.51370727
[27]		4	1000x400x 400	25				**Average**	**180.7079672**

Table 3.5: A summary of robot weight

CHAPTER 4: DETAILED DESIGN OF ROBOTIC PLATFORM

4.1 Platform Design

It is important to identify critical issues such as unreliable technology and high risk of failure in the design. Some of the state of the art design concept have been reviewed and applied to the preliminary platform design in order to increase the chance of success, for examples, the tilted wheel frame and the inspection array follows the same concept as the robot in Figure 2.5 and Figure 2.10 respectively. The proposed conceptual design in the previous section is detailed enough to justify if it is a good solution to the intention and task, and shows an acceptable probability of realisation and success. The concept has been revisited in order to re-evaluate and refine previous decisions in the light of the design parameters. However, some of the parameters in the aspects of mechanical design are too subjective, such as size, shape or thickness. Therefore the intuition and experience which can be accumulated from continuous design simulation and evaluation, such as using finite element analysis to check the structure rigidity, may take place to find approximate solutions to bring the conceptual design to the detailed design.

The design of the robotic platform will be in phases, the main focus is the functionality at current stage to be followed by robot modularity. Figure 4.1 illustrates the prototype that is being designed and to be fabricated in the first phase for feasibility testing. The main components are the main plate, wheel frames, inspection array and drawbar. The linear actuators are used to expand the wheel frames from a closed position for deployment to perpendicular position to the tunnel wall for better traction force. The semi-circular frame is designed for mounting of three HD cameras and four LED spot lights, forming an inspection array radially in the tunnel for tunnel investigation. The

coverage of each camera and LED would overlap each other to provide seamless images and illumination. A front pan-tilt camera and a rear camera will be integrated for navigation purpose. The drawbar is for hoisting the robotic platform.

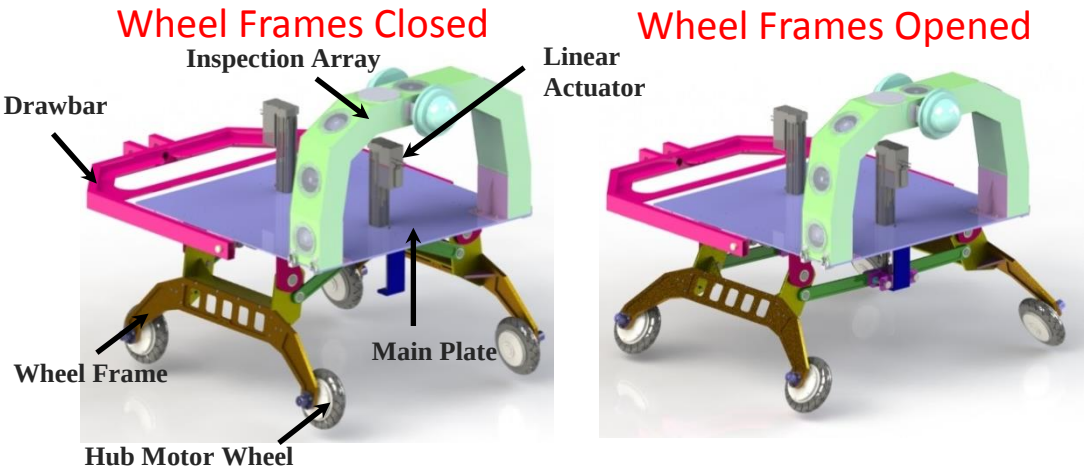

Figure 4.1: First prototype of robotic platform

The access to the trunk sewer is through a 1.8m vertical access shaft with a 600mm x 600mm manhole opening, as shown in Figure 4.2. Apart from the small opening, there are also intermediate platforms along the vertical access shaft. The top view of the trunk sewer is shown in the figure below and it is clear that the robotic platform is not able to access the manhole opening. Subsequently, as mentioned previously, a modular form of the prototype will be designed and built. The components of the robotic platform will be able to be deployed through the 600mm x 600mm manhole opening of the trunk sewer and assembled at the bottom of the access shaft.

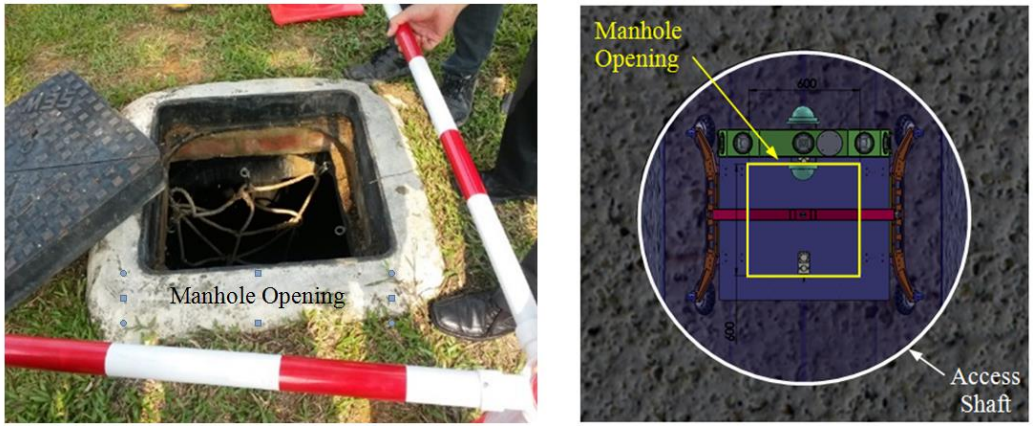

Figure 4.2: Top view of access shaft

Figure 4.3 illustrates the relative dimensions of the robotic platform in the 3-meter trunk sewer. The water level is assumed to be up to 500mm high and the height of the debris is up to 200mm as the current prototype is designed mainly for upstream tunnel where water is partially filled up. It is seen that the main plate and the inspection array are above the water level, ensuring that the field of view of the cameras and LEDs are not blocked.

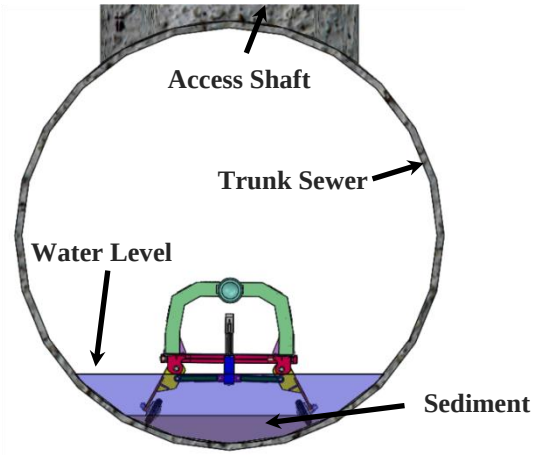

Figure 4.3: Front view of robotic platform in 3m trunk sewer

4.2 Design of Inspection Array

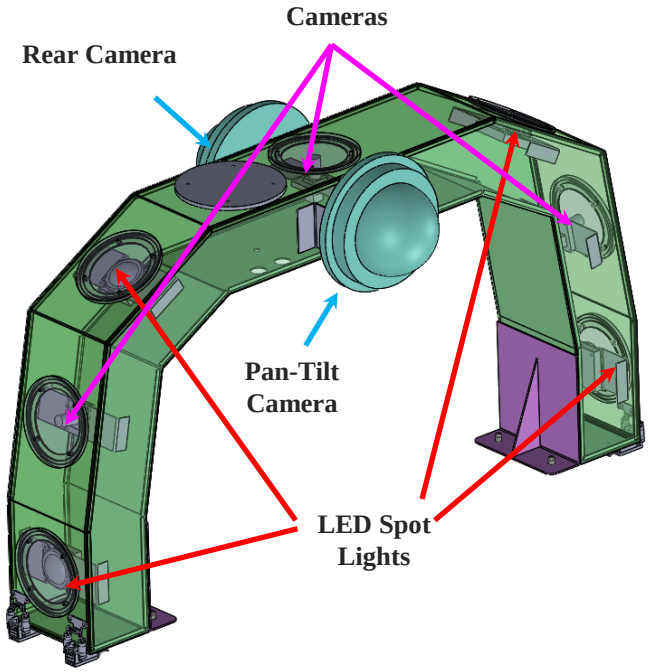

Figure 4.4: The configuration of inspection array

The configuration of the inspection array comprises of three HD cameras and four LED spot lights, as shown in Figure 4.4. The HD cameras are used to capture images of the inner surface of the sewer and the LED spot lights are for illumination. The cameras and LED spot lights are specially arranged in a semicircular arch so as to capture the tunnel surface above the water level while minimizing shadow in the images. The cameras and LED spot lights would be mounted at fixed angles and their coverage would overlap each other so that the images captured by this inspection array could be post processed to form a seamless image.

4.2.1 Camera Array

The field of view of the camera needs to be determined so as to optimize their placement on the semicircular arch in capturing the images of tunnel surface. Figure 4.5 interprets the setup of the experiment. The camera is placed 500mm away from the wall. The horizontal and vertical views of the camera can be marked on the wall and the corresponding distances can be measured. The measured height and width of the view are 540mm and 1350mm respectively. The horizontal θ_H and vertical θ_V field of views of the camera can then be found through trigonometric functions. The horizontal field of view θ_H can be obtained as

$$\theta_H = 2 \times \tan^{-1}\left(\frac{\frac{1350mm}{2}}{500mm}\right)$$
$$= 106.94°$$

In the same way, the vertical field of view θ_V can be derived, that is

$$\theta_V = 2 \times \tan^{-1}\left(\frac{\frac{540mm}{2}}{500mm}\right)$$
$$= 56.74°$$

The semi-circular frame in Figure 3.6 has been redesigned to provide better coverage of the tunnel surface. As shown in Figure 4.6, the three cameras are rearranged to appropriate angle and position to cover the inner tunnel surface above the water level with some overlap, enabling the images to be stitched.

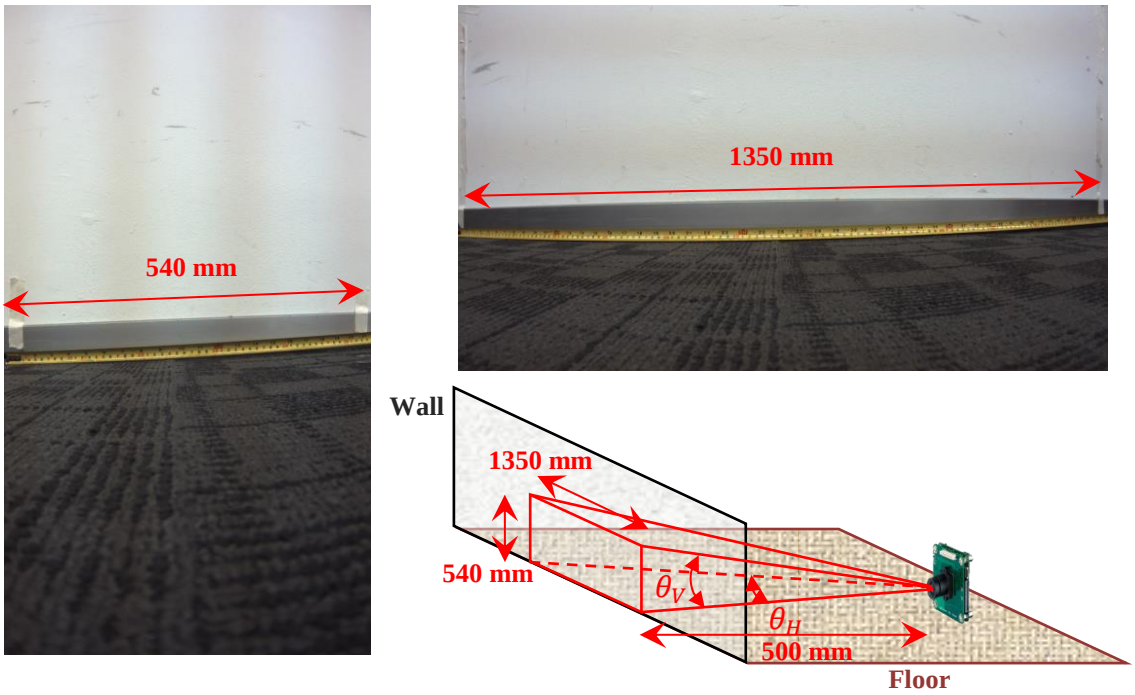

Figure 4.5: The experimental setup for field of view of camera

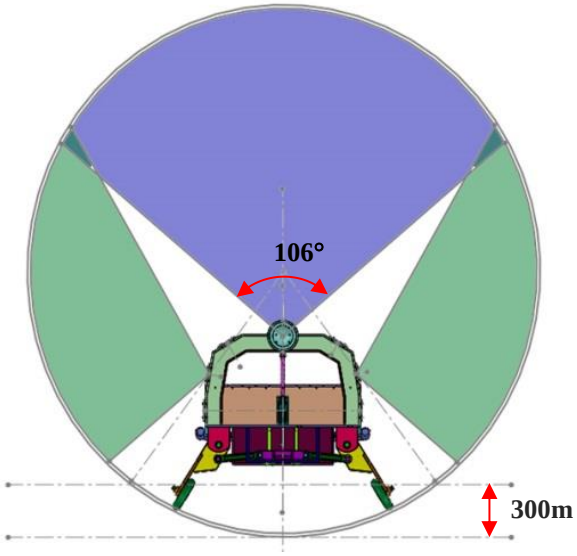

Figure 4.6: Coverage of cameras in 3m tunnel

4.2.2 Light Array

Four LEDs spot lights will be mounted on the inspection array for illumination. The purpose of using LED spot lights is to reduce the power consumption. In addition, the light intensity of LEDs can be easily controlled by using different lenses to ensure appropriate brightness for the environment.

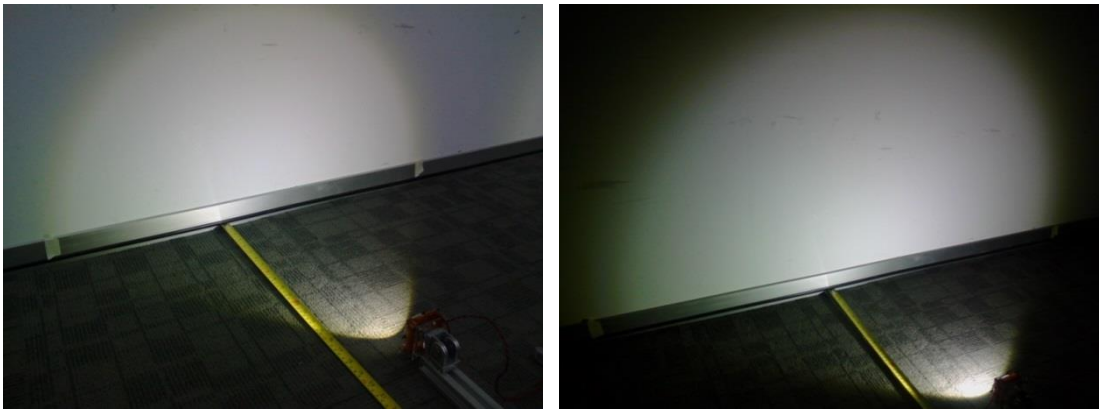

(a) (b)

Figure 4.7: The beam angle of LED with (a) 80^o lens and (b) 100^o lens

Figure 4.7 shows that the LED equipped with 100^o lens has wider beam angle than that with 80^o lens. However, the LED with 100^o lens appears to have lower light intensity. An experiment is carried out to measure the light intensity of LED with no lens, 80^o lens and 100^o lens, at distances of 1m, 2m and 3m apart from the light meter. The voltage and current used in this experiment are 12V and 0.7Amp respectively. The measurements are summarized in Table 4.1.

	Intensity (lux)		
Distance from light meter	**No Lens**	**100^o Lens**	**80^o Lens**
1m	190	272	480
2m	48	65	119
3m	20	30	54

Table 4.1: Measurement of light intensity with and without lenses

From Table 4.1, it is seen that the LED without lens has the lowest intensity for all cases because of light dissipation over distance. Although the 80^o lens has the best light intensity in this experiment, the LED with 100^o lens is considered more desirable as it has wider angle of illumination with sufficient intensity.

The layout of the LEDs on the inspection array is shown in Figure 4.8. Four LEDs with 100^o lens are used. The figure shows that the light array is able to cover the inner surface of the trunk sewer surface above the water level with overlap to ensure good illumination for image capturing by cameras.

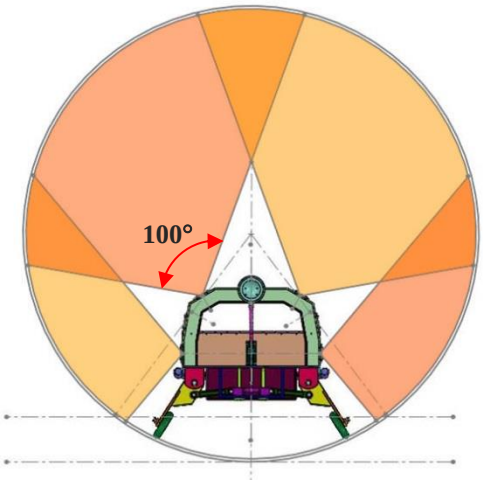

Figure 4.8: Coverage of LEDs in 3m tunnel

4.3 Design of Enclosures

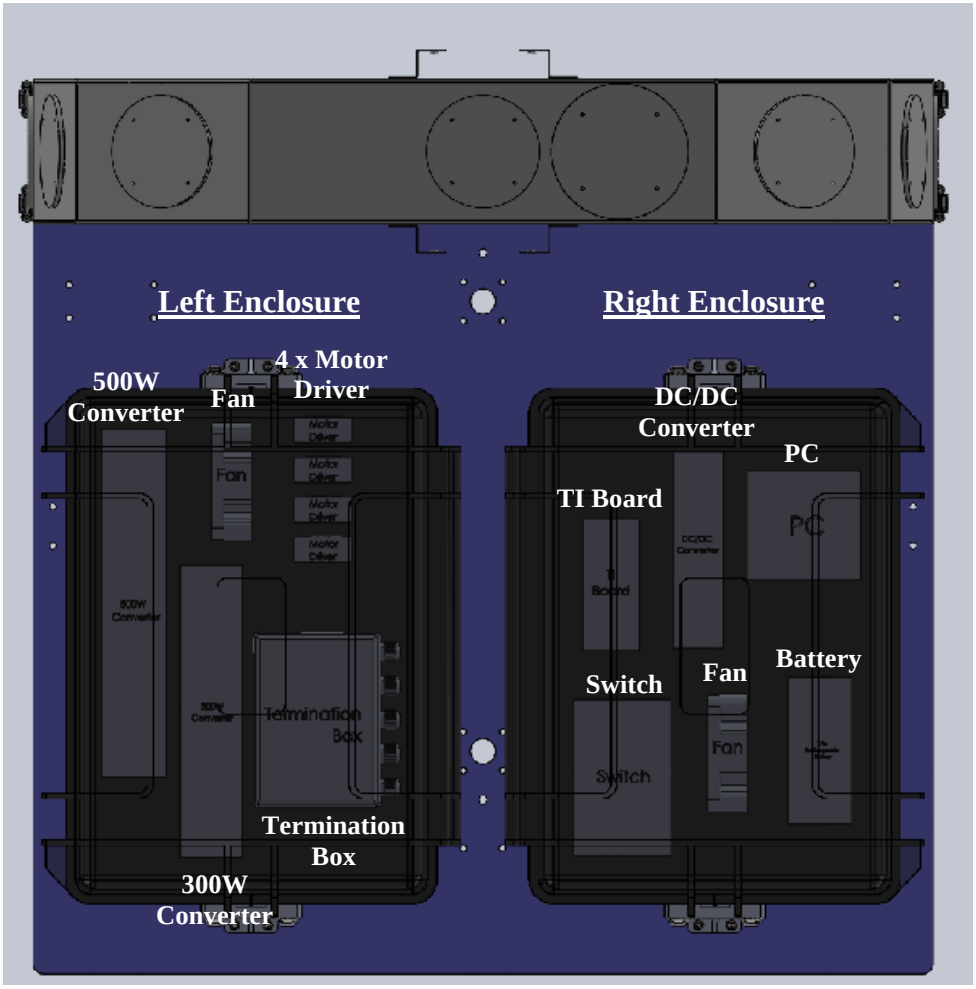

Figure 4.9: The layout of electrical components in the enclosures

Two water-proof enclosures as indicated in Figure 4.9 are fixed on the main plate to house the electrical components. The enclosures equipped with the necessary cable glands for easy and fast connection or disconnection. The high voltage components are mostly housed in the left enclosure and low voltage components in the right enclosure for easy management of wiring and for the sake of safety. In addition, it also helps to ensure the operation of the high voltage components do not interfere with other components, for instance, the AC to DC converters that normally heated up rapidly during operation can be isolated away from other electronics.

The enclosure as shown in Figure 4.10 has waterproof and dustproof IP67 certified watertight seal around lid. It has automatic pressure release valve to adjust the pressure in the enclosure to the atmospheric pressure. The electrical components will be mounted underneath the main base plate for the ease of maintenance. It also helps to reduce the temperature generated by electrical components through conduction and provides a large surface area for convection to efficiently carry away heat. A ventilation gland will be mounted on lid to release hot air to the atmosphere from the enclosure.

Figure 4.10: The main base plate for components mounting

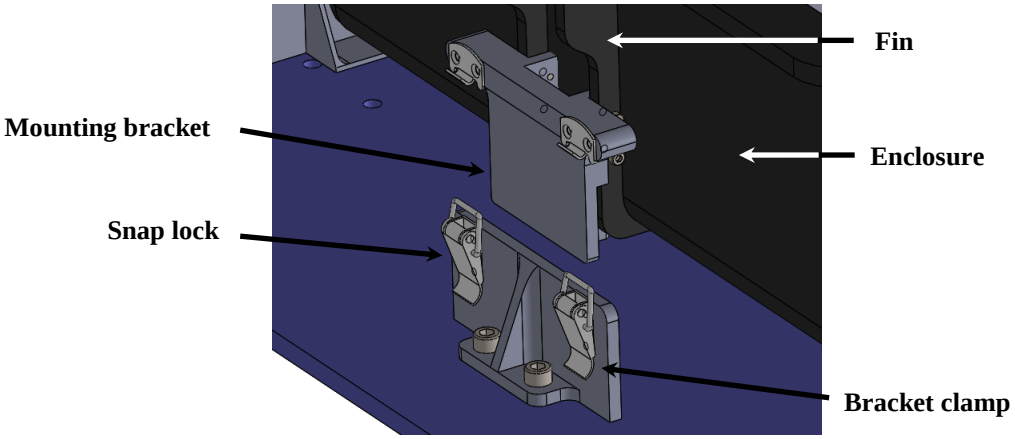

Figure 4.11: Enclosure mounting on the main plate

The enclosure is clamped externally without too much modification. Figure 4.11 illustrates the mounting bracket which is attached to the fin of the enclosure instead of mounting onto the case body. Minor modification can retain the performance in waterproofness with good durability. Two snap locks are fixed on the bracket clamp which is mounted on the main plate. With the snap lock in place it can lock or unlock the mounting bracket to make the enclosure becomes detachable and portable.

4.4 Force Analysis

The buoyancy force at high water level in the trunk sewer may cause robotic platform to lose its stability and maneuverability. It is necessary to ensure that there is sufficient downward force to keep the hub motor wheels in contact with the tunnel wall.

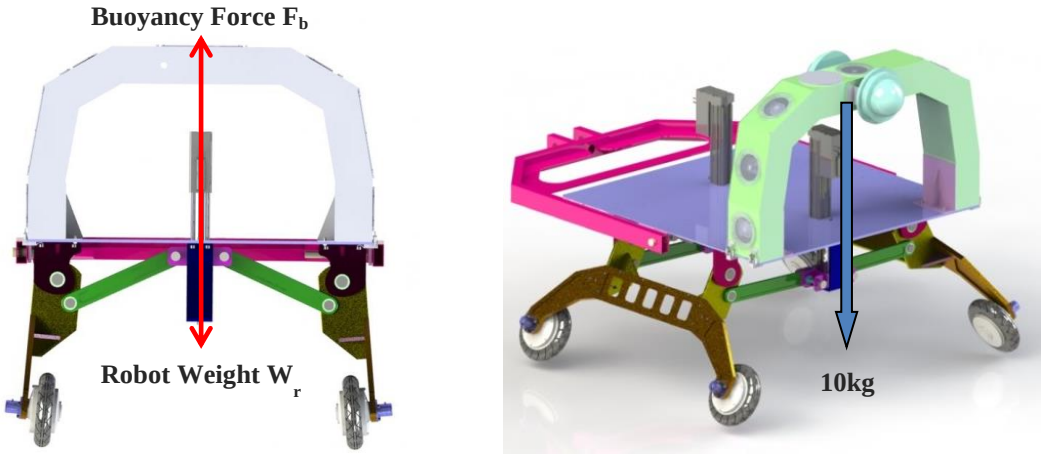

(a) (b)

Figure 4.12: (a) Force diagram of robotic platform and (b) Mounting of inspection array

The volume of the prototype obtained in the CAD software is $0.0225m^3$. The highest buoyancy force occurs when the robotic platform is completely submerged in the water. The highest buoyancy force, noted as F_b, is determined based on the volume of the robotic platform.

$$F_b = \text{Density x Volume}$$
$$= 1000kg/m^3 \text{ x } 0.0225m^3$$
$$= 22.5kg$$

The weight of the robotic platform W_r can be found by

$$W_r = 0.0225m^3 \text{ x } 27000kg/m^3 \text{ (Aluminium Alloys)}$$
$$= 60.75kg$$

From the calculations above, it is seen that even when the robot is fully immerged in the water, it will still have 38 x 9.8 N of downward force to keep the wheels to be in contact with the tunnel wall for locomotion.

4.5 Material Selection

There are two types of materials are used for the fabrication of the robotic platform. The drawbar is made by Stainless Steel. Other than that, all the mechanical components are made by Aluminium Alloy 6061.

4.5.1 Properties of Aluminium Alloy 6061

Aluminium Alloy 6061, containing silicon and magnesium as its main alloying elements, is a precipitation hardening aluminium alloy. Aluminium Alloy 6061 is well-known for its excellent machinability where making it versatile for a broad range of applications. It is widely used for construction of aircraft and yacht structures as well as bicycle frame and components. This material has medium to high strength, good surface finish and toughness, light weight and excellent corrosion resistance to atmospheric conditions [24]. Therefore, Aluminium Alloy 6061 has been selected for the fabrication of the parts of proposed robotic arm so as to make the overall weight of

the manipulator as light as possible. Although the rigidity of the aluminium alloy is not extremely high, it is adequate to withstand the body force and the pulling force of the cables. The properties of Aluminium Alloy 6061 are shown in Table 4.2.

Properties	Units	Aluminium Alloy 6061
Elastic Modulus	N/mm^2	69000
Poisson's Ration	-	0.33
Shear Modulus	N/mm^2	26000
Density	kg/m^3	2700
Tensile Strength	N/mm^2	124.08
Yield Strength	N/mm^2	55.15
Thermal Expansion Coefficient	$10^{-6}/K$	24
Thermal Conductivity	W/(m.K)	170
Specific Heat	J/(kg.K)	1300

Table 4.2: Properties of Aluminium Alloy 6061 [40]

4.5.2 Properties of Stainless Steel

Stainless steel is a type of alloy steel that has unique stainless and corrosion resisting properties. It offers excellent impact and fatigue resistance, and retains shock resistance and strength even at high temperatures. Products made with this material generally last a longer time due to higher hardness and lower maintenance [41]. Stainless steel is more expensive than other standard grades of steel but it is more economically applicable if life-cycle and service life are considered [42]. The properties of Stainless Steel are shown in Table 4.3

Properties	Units	Stainless Steel
Elastic Modulus	N/mm^2	190000-210000
Poisson's Ration	-	0.27-0.30
Density	kg/m^3	7750-8100
Tensile Strength	N/mm^2	515-827
Yield Strength	N/mm^2	207-552
Thermal Expansion Coefficient	$10^{-6}/K$	9.0-20.7

Thermal Conductivity	W/(m.K)	11.2-36.7
Specific Heat	J/(kg.K)	420-500

Table 4.3: Properties of Stainless Steel [43]

4.6 Finite Element Analysis

Deformation is critical to the robot deployment and operation because it will cause the joints stuck due to improper contact. A break occurs after the mechanical parts have reached the end of the elastic and plastic deformation ranges if sufficient loads are applied. This may lead to the malfunction in the robot. Therefore, Finite Element Analysis, which has been broadly used in the recent years, is conducted to simulate the rigidity of the robot structure. FEA is a powerful tool to get better understanding on the performance of the structure [44].

The first step in the analysis is to build up the solid models of robotic platform and drawbar respectively. A CAD model was developed using the Solidworks software. Models of each component were created and assembled to demonstrate the functionality of the design. After completing the solid modeling, the model was transferred into the Ansys software and converted to a parasolid file [45]. The surfaces of the model were then meshed with triangular 2D elements, as shown in Figure 4.13.

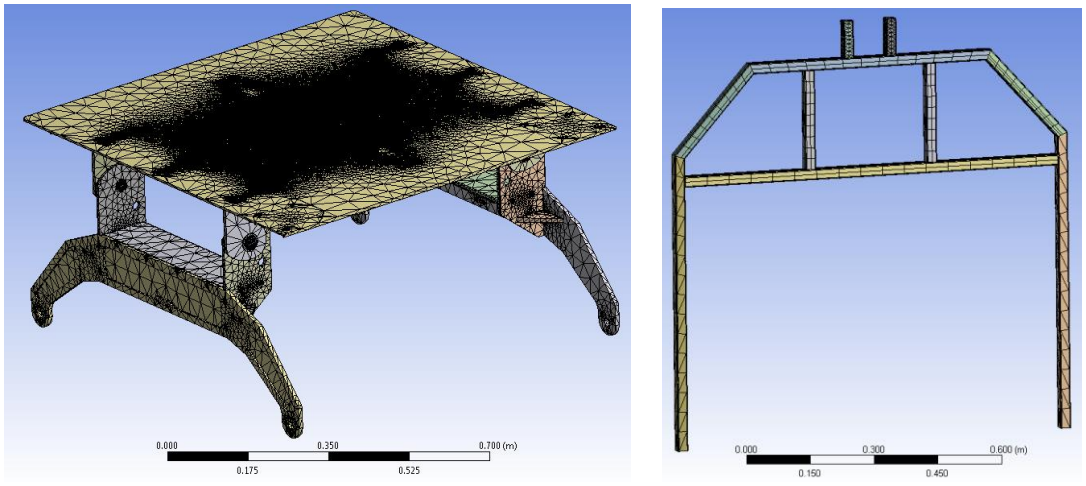

Figure 4.13: Finite element model of Robotic Platform and Drawbar

It is important to analyze the stiffness of the model accurately as it generally governs the essential behavior of the structure as a whole. Out of all the variety of components in tunnel robot, the drawbar is most likely to be failed because it may encounter the highest loading force, hereby having high chance to be deformed or broken.

The maximum stress value in the Von-mises analysis is recommended to be used as a failure criterion. It can reflect various materials and geometrical factors which may affect the strength of the structure [46]. Deformation analysis is the observations of the geometrical changes of a body in the time interval [47].

4.6.1 Structural Analysis of Robotic Platform

The main components of the robotic platform are made from aluminium such as the wheel frame and the main plate where the inspection array will be mounted on. The thickness of the main plate is 5mm with 3mm stiffeners underneath. As shown in Figure 4.12, the inspection array is fixed at the edge of the main plate. The weight of the inspection array is 10kg. Structural analysis is carried out to ensure the deformations and stresses on the robotic platform are tolerable. The factor of safety used in the structural analysis is 2.

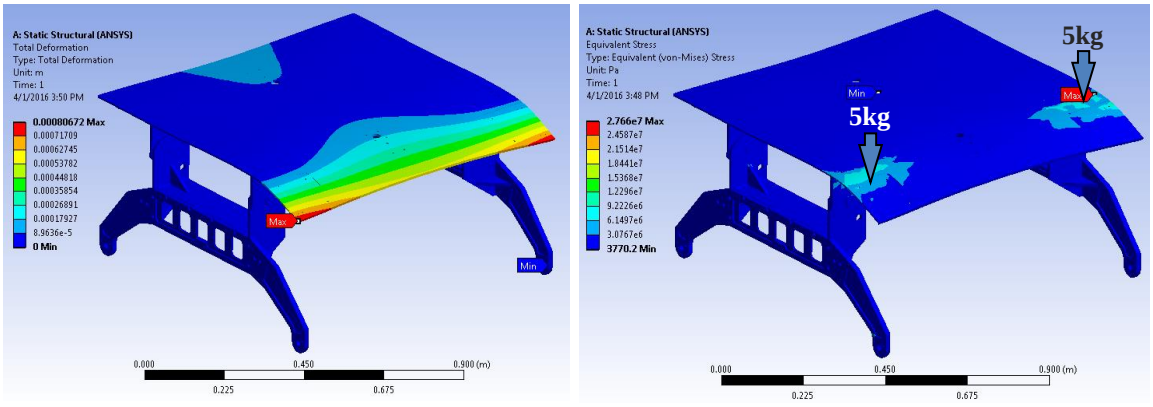

(a) (b)

Figure 4.14: (a) Deformation analysis and (b) stress analysis of robotic platform

As shown in Figure 4.14, the main deformation occurs at the edge of the main plate but it is only 0.8mm and negligible. The maximum stress that the main plate experienced is 27 MPa, which is half of the maximum yield strength of aluminum (55 MPa).

Therefore, the current design of the main plate is able to withstand the loads and has low chance to cause failure.

4.6.2 Structural Analysis of Drawbar

The drawbar is used to lower or lift the robotic platform into or out of the sewer tunnel through the access shaft vertically. It is the only structure to withstand the weight of the entire robotic platform during the deployment and retrieval of the robotic platform, hence it may encounter high loading force and hereby having high chance to be deformed. The analysis of drawbar design is therefore necessary to understand the potential areas of stress concentration that may lead to structural failures. We assume the weight of the robotic platform is 100kg which is the load drawbar has to withstand. The drawbar will be built with steel with high yield strength. The safety factor defined in the analysis is 2. The mounting holes as labeled in Figure 4.15 are where the drawbar is hinged to the robotic platform. The area closest to the mounting holes encounters the highest deformation. The deformation is found to be very small that it can be ignored (0.0668mm). From the stress analysis, the maximum stress is found to be 43MPa, which is much smaller than the maximum yield strength of steel (250 MPa).

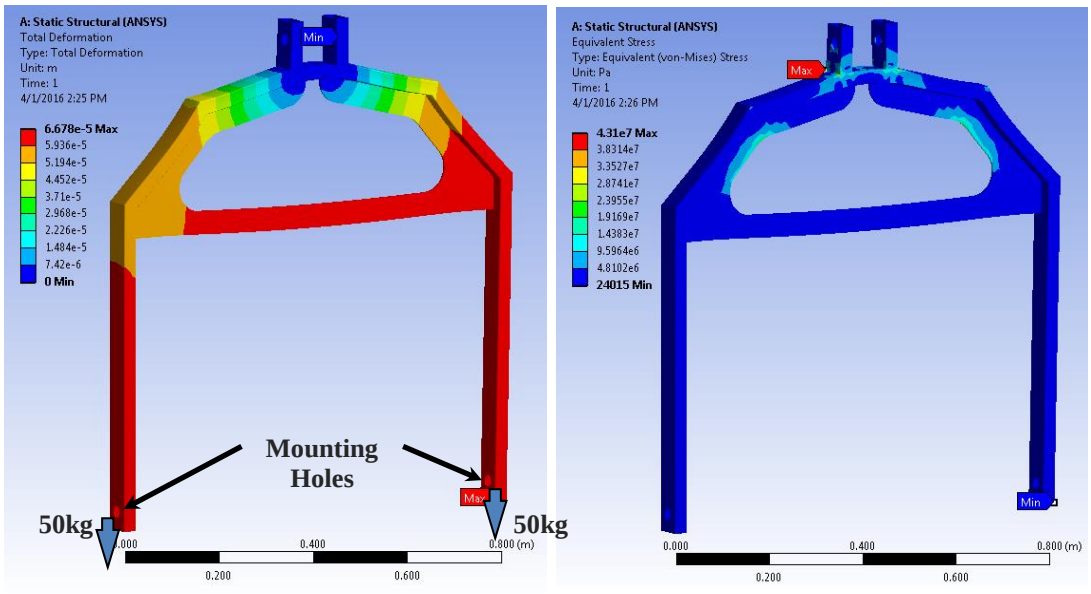

(a) (b)

Figure 4.15: (a) Deformation analysis and (b) stress analysis of drawbar

Base on the analysis above, we can conclude that the structures of the robotic platform is adequate to withstand the load of robotic platform.

4.7 Modular Robot Design

The first prototype is not able to go through the small manhole opening, thus the modular robotic platform, as shown in Figure 4.16, has been designed for further development in the next phase. The sealed enclosures are used to house the electrical components. It will be pressurized through the Schrader Valve and the inner pressure could be inspected through pressure sensor inside the enclosures. Pressure drop in the enclosures indicates leakage and the inspection task would be terminated immediately. The red circle in Figure 4.16 (b) represents the access shaft and the blue square is the 600mm manhole opening. The robotic platform will be disassembled and folded beforehand during the deployment process. After the robotic platform is deployed into the trunk sewer through the small opening, the main plate will be unfolded and assembled back by worker within the interior of the trunk sewer.

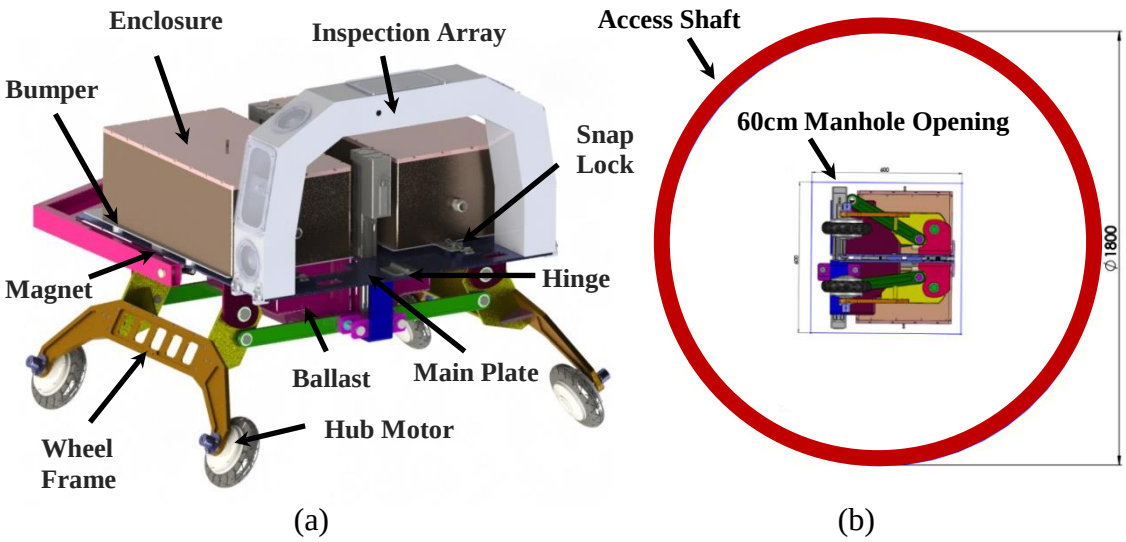

Figure 4.16: Design of modular robot (a) before disassembly and (b) after disassembly

The main plate consists of four small plates in the modular design and each plate is connected by heavy load hinges so that the main plate is foldable to reduce the overall size. Figure 4.17 illustrates the mechanical components on the main plate for folding purpose. The snap locks and magnets are strong and rigid enough to hold the position of the small plates at certain configuration during the deploying and retrieving process.

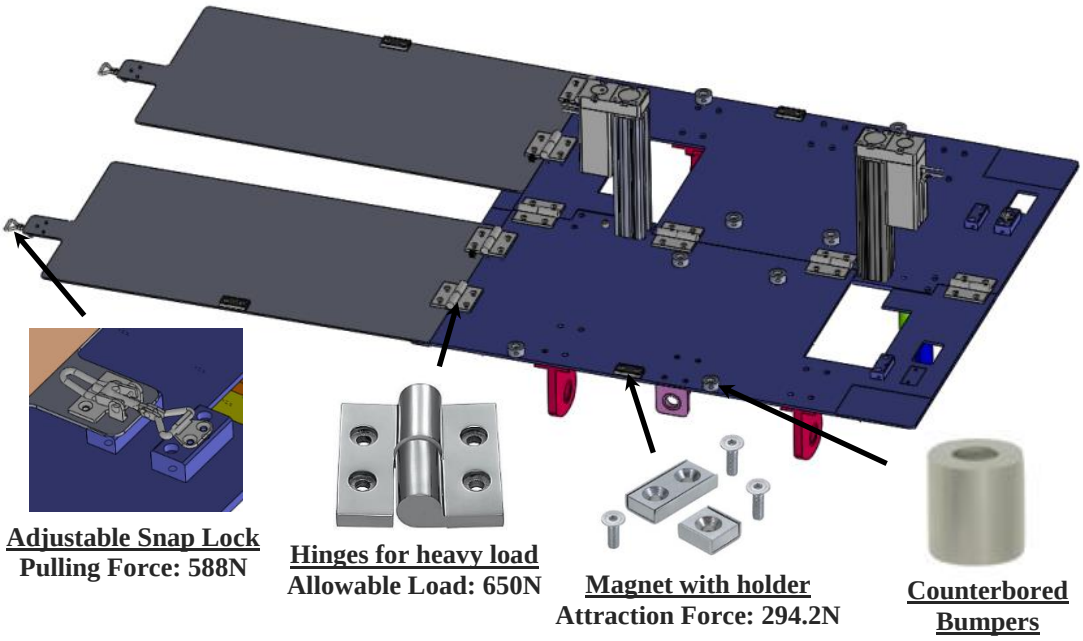

Figure 4.17: The components on the main plate

CHAPTER 5: PROTOTYPE OF ROBOTIC PLATFORM

5.1 Robot System

5.1.1 Schematic Diagram of Electrical Parts

The electrical and sensing equipment for the robotic platform has been identified and the schematic diagram is shown in Figure 5.1. The robotic platform is equipped with an onboard notebook which communicates with embedded controller, cameras, scanning profilers and hub motors through fiber transmitter and receiver. The various components such as hub motors, ballast, LEDs, pressure sensor, gas detection sensor, IMU and water sensor are connected to the embedded controller.

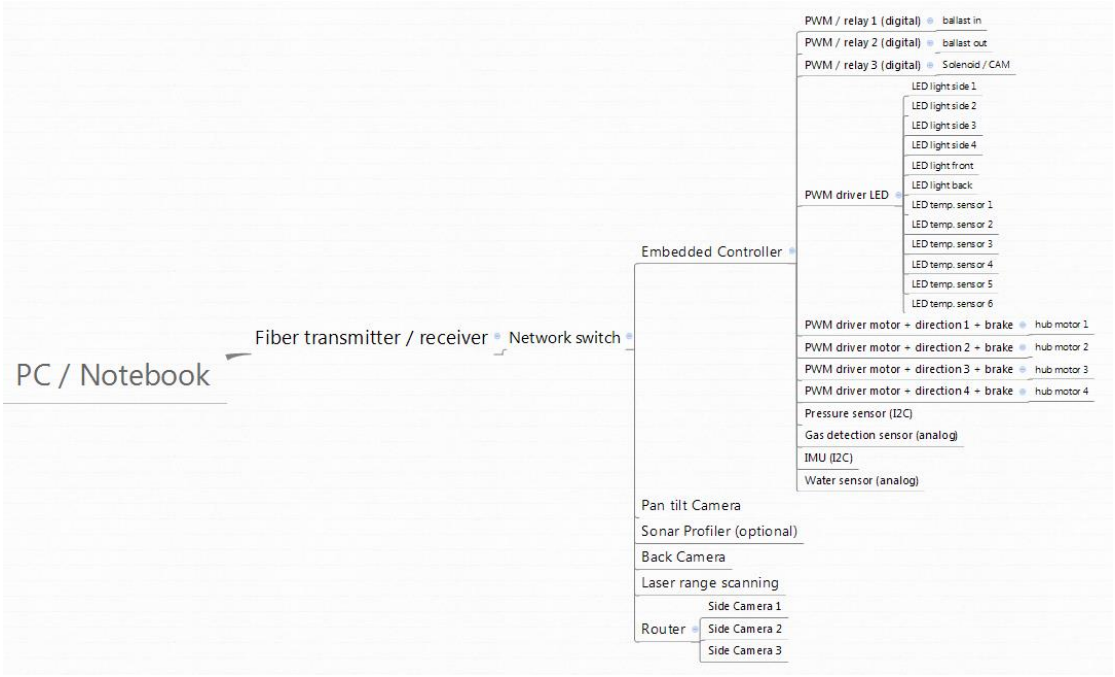

Figure 5.1: Schematic Diagram

5.1.2 Power Diagram

Figure 5.2 shows the power diagram for the robotic platform. An external 3-phase 400VAC surface power generator provides power to the surface station and the robotic platform. There will be a low current battery equipped on the robotic platform to power up the gas detection sensor, fiber transmitter/receiver, embedded controller and network switch. When the robotic platform is being deployed into the trunk sewer, only the gas detection sensor and a few components are powered by the onboard battery to continuously check the concentration of combustible gases. If the level of combustible gases is below the limit, the robotic platform is then powered up by the surface generator to carry out the inspection task.

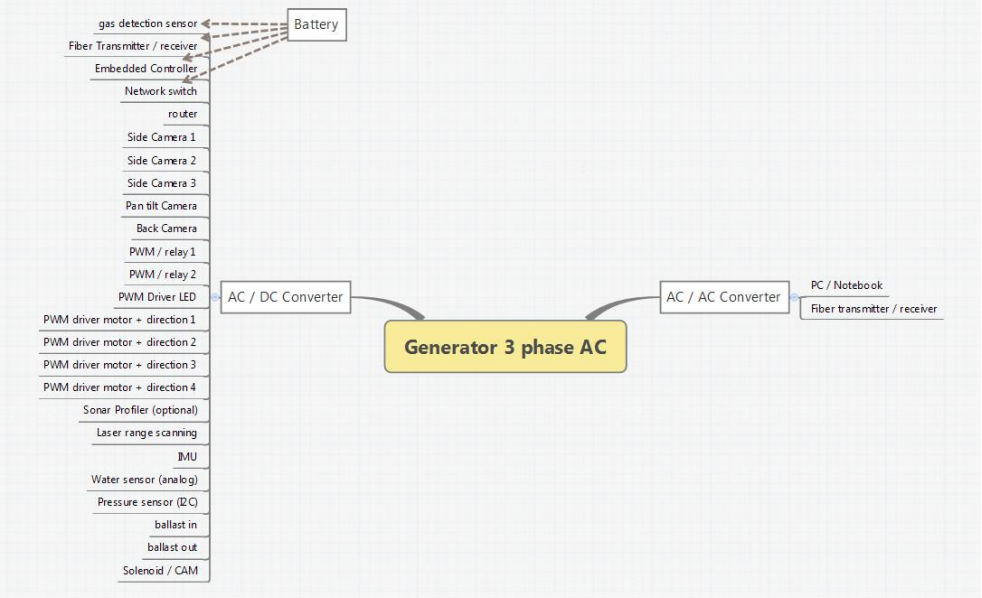

Figure 5.2: Power Diagram

5.2 Implementation for ATEX standard

The trunk sewer may fill with monoxide, hydrogen sulfide and oxygen by which any electric spark may cause explosion and significant damage. The ATEX standard describes what equipment is allowed in an environment with explosive atmosphere and it needs to be followed in this project for workplace safety. In order to fulfil the ATEX standard, the combustible gases will be checked continuously to ensure the concentration of explosive gases is always below the limit. Moreover, the robot will be

designed to meet the ATEX standard by filling the hub motors with non-conductive oil and the enclosures will be sealed and pressurized to isolate electric spark from the combustible gases.

5.3 Selection of Components

The dustproof and waterproof capability of the components is one of the crucial parts for the selection. We could refer to the IP Code which aims to provide more detailed information about the degree of protection provided against accidental contact, dust and water by electrical enclosures and mechanical casings. Two digits indicate the dustproof and waterproof conditions correspondingly which summarized in the Table 5.1.

First Digit: Protection of Solid Particle	
0	1
No protection	Protected against solids objects over 50mm (e. g. accidental touch by hands)
2	3
Protected against solids object over 12.5mm (e. g. fingers or similar objects)	Protected against solids objects over 2.5mm (e. g. tools and wires)
4	5
Protected against solids objects over 1mm (e. g. wires and slender screws)	Protected against dust, limited ingress
6	
Totally protected against dust	
Second Digit: Protection of Liquid Ingress	
0	1
No Protection	Protected against vertically falling drops of water
2	3
Protected against falling drops of water up to 15 degree from the vertical	Protected against falling drops of water up to 60 degree from the vertical
4	5
Protected against water splashing from any direction	Protected against low pressure water jets from any directions
6	7
Protected against powerful water jets	Protected against the effects of temporary immersion in water up to 1m of submersion.

8
Protected against long periods of immersion at least 1m or more depth

Table 5.1: The IP Code

Ideally, all the components that are exposed to the water in the tunnel environment should be rated at IP68. However, some equipment can hardly achieve IP68, for example, ingress of water is possible at the joint between electric motor shaft and the hub of wheel. The highest IP code of most of the off-the-shelf hub motors in the market, as of the period where this project is carried out, is IP65. This shows that hub motors are generally not waterproof, but only protected against low pressure water jets. For our first prototype, the abovementioned IP grade should be sufficient for now and further customization is required to realize fully waterproof in the next phase of robot design.

The hub motor of the robotic platform should be able to withstand at least 45kg of load each, as per the preliminary weight estimation on Page 41. Table 5.2 shows the specification of the 8-inch hub motor that was selected for the prototype.

Gearless hub motor	
Rated voltage: DC 24/36/48V	**Tyre**: 200*50-5, vacuum tyre
Rated power:180-250W	**Efficiency**: >83%
No-Load Speed: 400-1200rpm	**Gross Weight**: 3.5kg/pcs
Start Torque: 6Nm	**Rated Torque**: 18Nm
Rim size: 8 inch	**IP code:** IP65

Table 5.2: The Technical Specification of the 8-inch Hub Motor

Figure 5.3 shows the 8-inch hub motor in which planetary gear system is used to increase the rotational torque. Figure 5.4 shows the hub motor controller. Each hub motor is controlled by a controller and a total of four controllers are used. Figure 5.5 shows the 12V battery that powers the four hub motors. Figure 5.6 shows the speed throttle which is merely for manually testing the functionality of the hub motors, it will not be included as part of the final robot prototype.

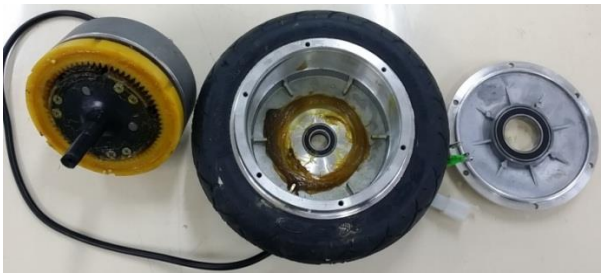

Figure 5.3: 8-inch Hub Motor

Figure 5.4: Hub Motor Controller

Figure 5.5: Battery

Figure 5.6: Speed Throttle

5.4 Mockup for Pulling Test

A mockup which has the flexibility to stretch its width was built to characterizing the performance of the proposed design. This mockup is designed to access the 60x60cm manhole opening. Figure 5.7 shows the design comparison between the prototype and the mockup. Figure 5.8 shows the actual mockup built with aluminium profiles in the 90°, 120° and 150° orientations respectively. The expanded wheel frames in the mockup serve the same functionality as that of the prototype, which is to elevate the whole structure away from the sediment and increase its stability.

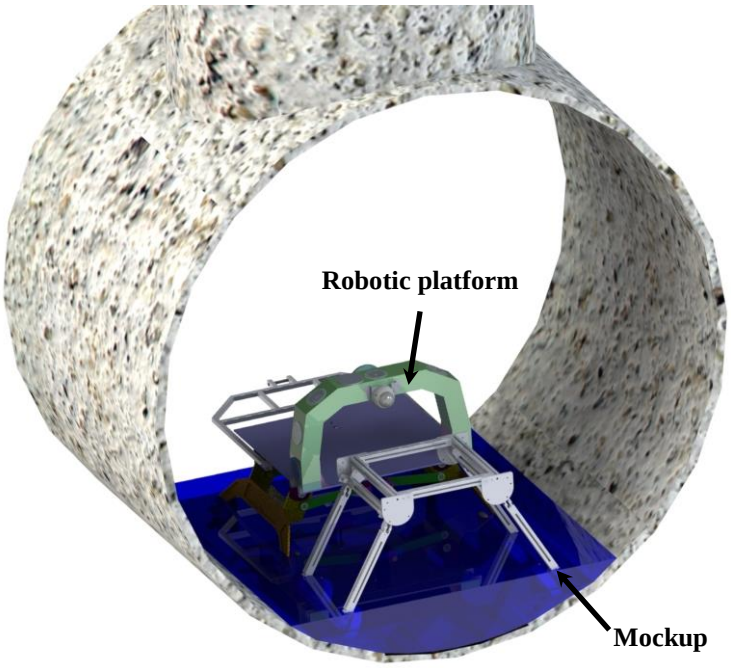

Figure 5.7: The robotic platform and the mockup

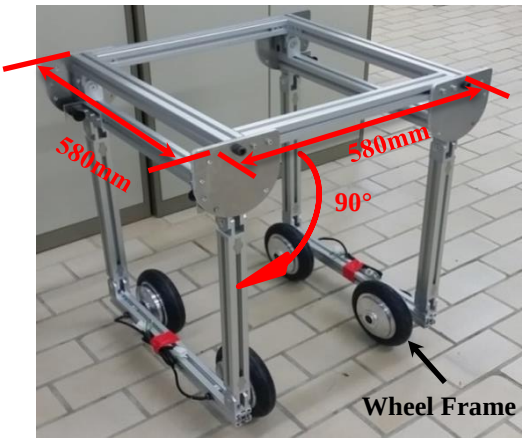

(a)

(b)

(c)

Figure 5.8: Wheel Frames at (a) 90° angle (b) 120° angle (c) 150° angle

Figure 5.9 shows all the wired electronic components on top of the mockup. After the hub motors are wired to the TI broad and to the controllers, and with some program written in laptop controller to control the relays and voltage to the motor controllers through the TI board, the four hub motors can be controlled by the keyboard to do forward, reverse and break motion.

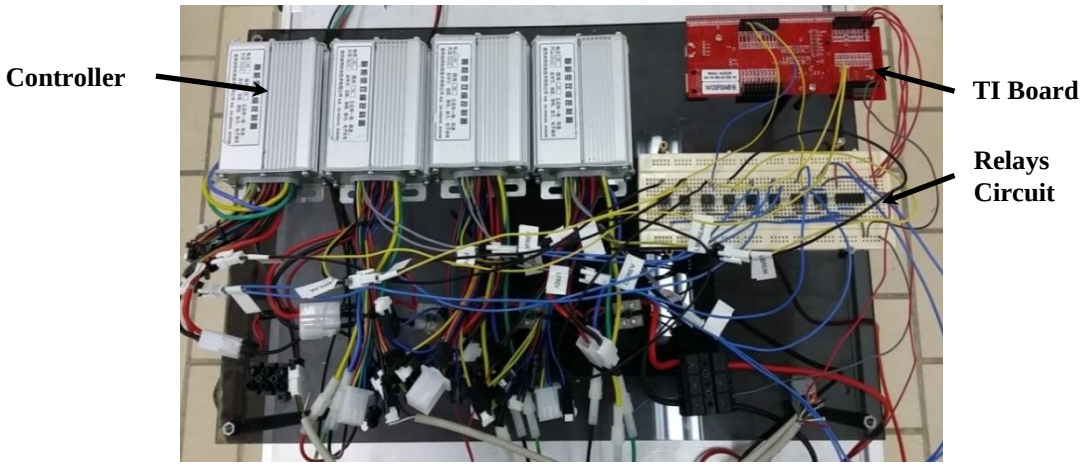

Figure 5.9: Overall view of electronic components

5.4.1 Experimental Evaluation on pulling test

After the completion of the setup of control system, an experiment was carried out to assure the structure has adequate cable pulling force with good stability and to find out the best position to hinge the umbilical cable on the robotic platform with appropriate drive wheel configuration. The mockup was pulling a 130-meter long umbilical cable away from the winch for a distance of 10 meters along the corridor. The estimated

weight of the 130-meter cable is 10kg. The cable was left slackly at the winch and the mockup was controlled to pull the cable for 10 meters before the cable became taut as the unwinding force and the friction between the cable and the winch drum were not considered in this experiment.

(a) (b)

Figure 5.10: (a) Rear cable fixing and (b) front cable fixing

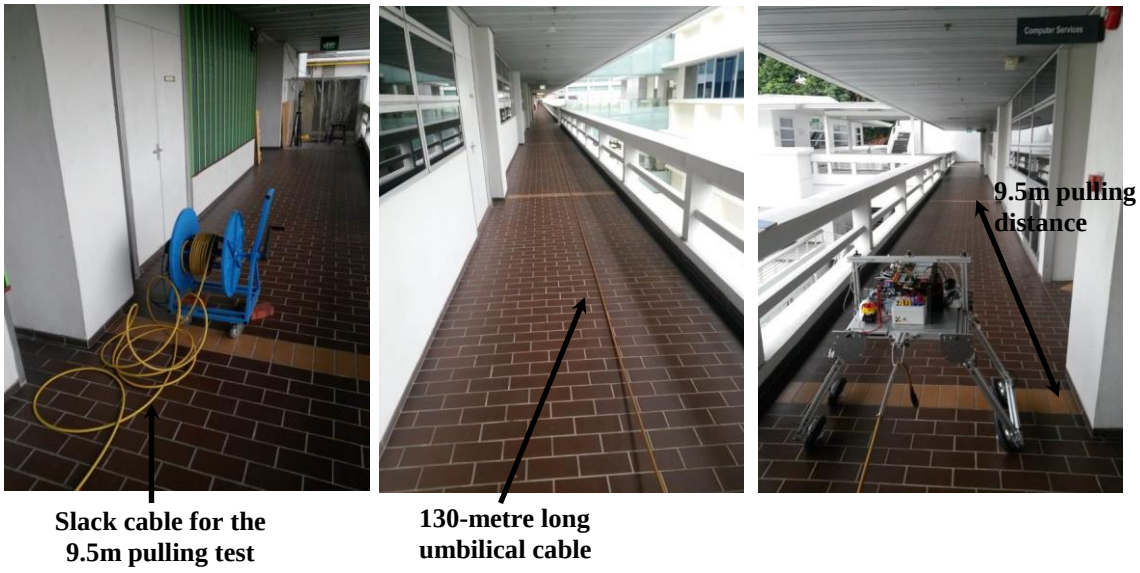

Figure 5.11: Snapshots of the various perspectives of the test environment

Back and front cable fixings with front-, rear- and all-wheel drives are tested accordingly in this experiment. The average moving speed of the mockup in each criterion was recorded as it implied how effective the mockup can be to travel the 10-meter distance. The value was obtained by the total time spent over the 10-meter distance. The mockup with front-wheel drive failed to achieve the destination in the experiment because it showed a tendency to topple down to the ground when the

wheels started to move forward. Wheel slippage occurred when driving with rear cable fixing, more time was needed for the mockup to overcome the slippage and for us to adjust its orientation to the goal direction.

The results of the experiment are summarized in Table 5.3.

		Cable Fixings	
		Front	**Rear**
Drive wheel Configuration	**Front-wheel Drive**	Fail	Fail
	Rear-wheel Drive	0.08 m/s	0.012 m/s
	All-wheel Drive	0.11 m/s	0.036 m/s

Table 5.3: Results of the pulling experiment

A number ranging from 1 to 5 is assigned in each testing criteria to indicate the pulling efficiency of the mockup. The description of each rating is as follows:

1 – Very unstable, tends to topple down
2 – Poor stability, wheel slippage frequently occurred
3 – Moderate stability, wheel slippage occasionally occurred
4 – Good stability
5 – Ideal, very good stability and fast average travelling speed

Base on the observation in the experiment, the performance of the mockup is shown in Table 5.4.

		Cable Fixings	
		Front	**Rear**
Drive wheel Configuration	**Front-wheel Drive**	1	1
	Rear-wheel Drive	4	2
	All-wheel Drive	5	3

Table 5.4: Performance of the mockup

From the experiment results, it is seen that the front cable fixing with all-wheel drive has the most desired performance for all cases. The all-wheel drive provides better control on loose and slippery surface. It has most of the advantages of both front- and rear-wheel drive. Traction is nearly doubled compared to a two-wheel-drive layout. This experiment also shows that rear-wheel drive has better performance than the front-wheel drive because the former offers better initial acceleration as the weight is transferred to the rear of the mockup upon accelerating, thus boosting traction.

The movement of the mockup is also affected by the magnitude of moment generated by cable weight and cable friction base on the position of the cable mounting. The front cable fixing point is slightly lower compared to the rear cable fixing. This helps to reduce the moment and thereby robot can obtain better stability.

5.5 Motor waterproofing

The 9.5 inch hub motors on the mockup are specified by manufacturer that it is not suitable for continuous immersion in water for 1m or more depth. In Figure 5.12, the wheels are therefore customized by applying water-repellent coatings on both ends of rotating shaft and by sealing seams with O-rings and oil seals to protect the contents. An experiment was conducted to ensure the waterproofed hub motor has the capability of resisting the ingress of water under a long run in water.

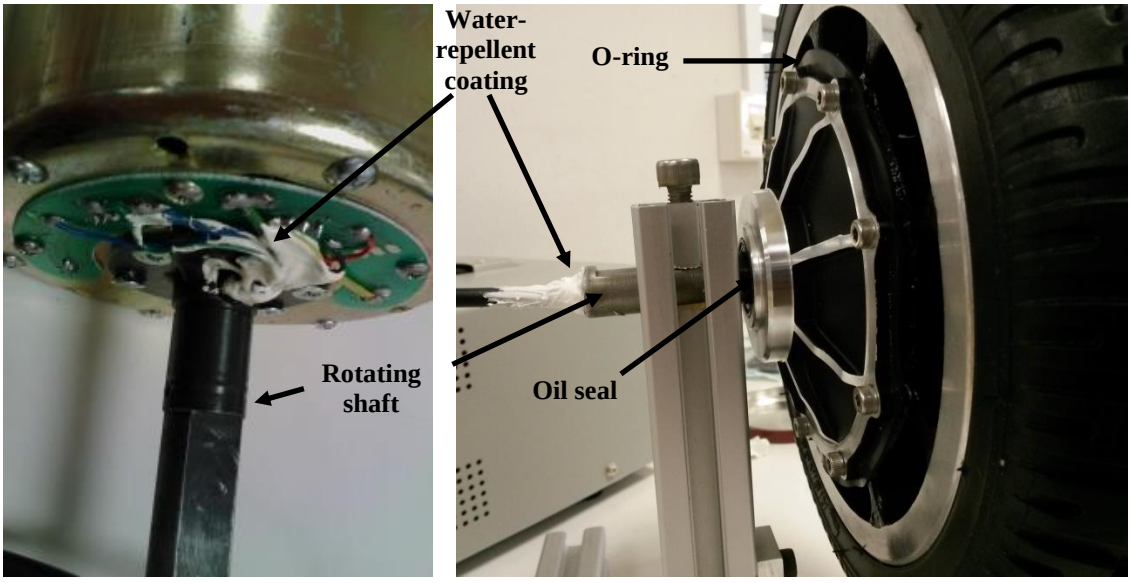

(a) Motor (b) Wheel body

Figure 5.12: Waterproofing of hub motor

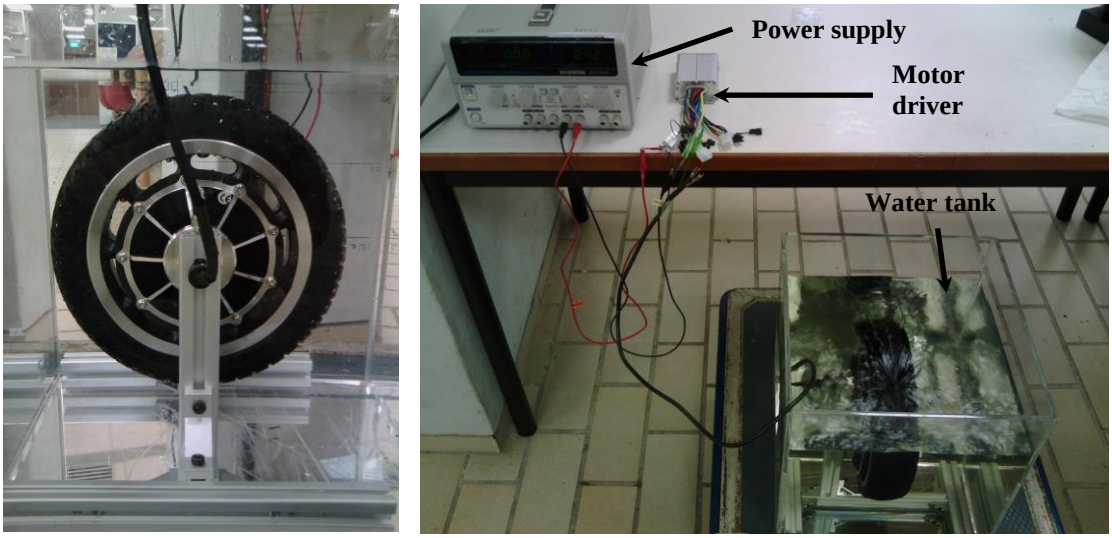

Figure 5.13: Experiment setup

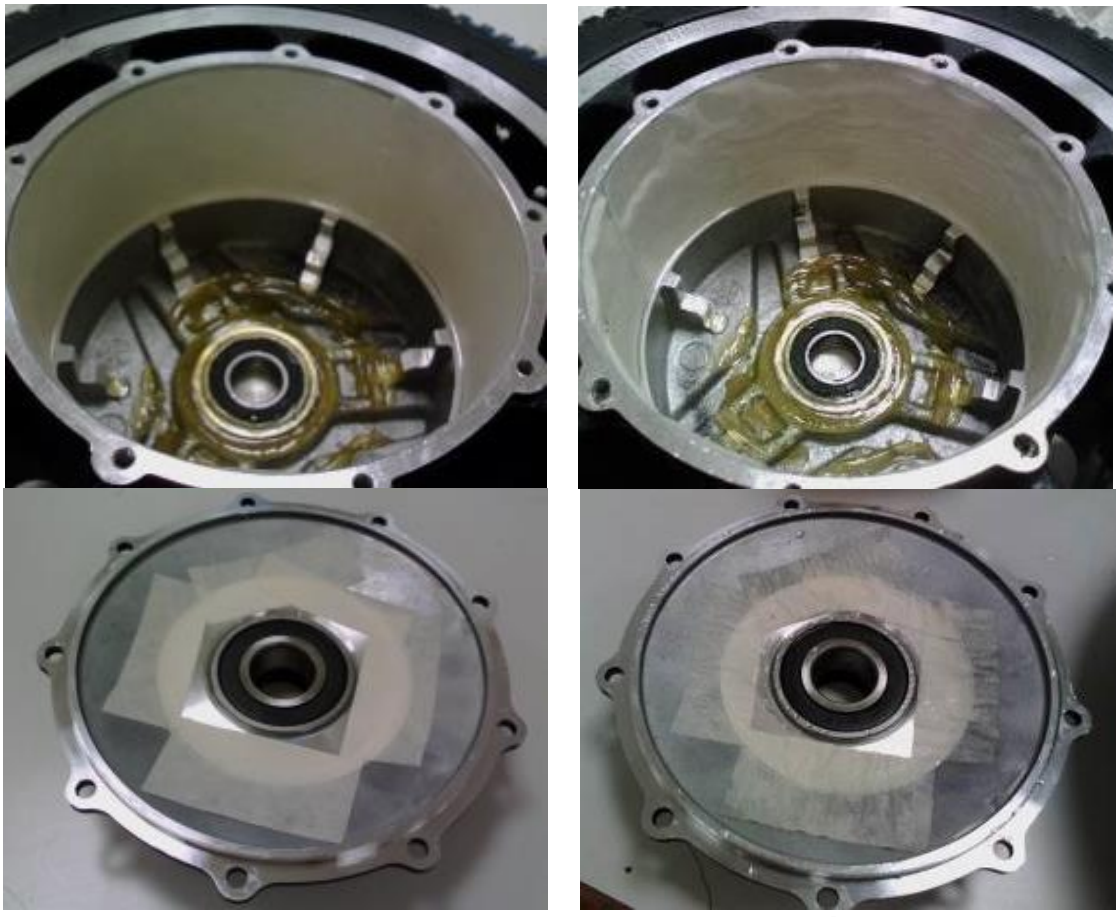

(a) (b)

Figure 5.14: (a) Before and (b) After testing in water

The hub motor was submerged fully in the water and being tested run continuously in full speed for 2 hours, the setup is depicted in Figure 5.13. Before starting the experiment, masking tape was placed in the hub motor before sealing it to easily

identify any water ingression since it absorbs and retains water when wet. In Figure 5.14 (b), it was observed that the masking tape was damp uniformly and became creased. It might be caused by water condensation. During the operation, the air sealed in the motor condensed when the temperature outside the motor was low but inside was high. There was no sign of water ingression and the wheel was still operational. The motor and water became warm after the testing because of the long period of operation. It has low chance to be overheated because water will help to reduce temperature and the inspection is normally shorter than 2 hours.

5.6 Testing of the Mockup on Curved Surface

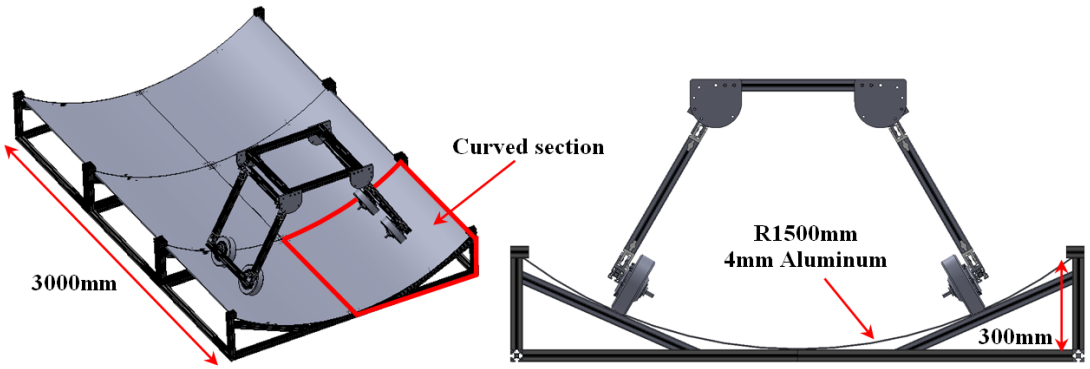

Figure 5.15: Curved Section and its dimension

A 3m long track with curved surface is designed and built as shown in Figure 5.15. It is made up of 6 modular curved sections. Each section comprises a curved plate with a 1.5m radius of curvature and an aluminum support frame. The section is designed for ease of assembly, storage and transportation. The height of the curved section is 300mm, which is the same as the water level when the trunk sewer is 10% filled. This helps to provide a visual guide on how much of the platform is submerged. Figure 5.16 shows the mockup platform resting on the fabricated curved track.

Various tests will be conducted on the curved track to assess the steering and control of the platform. In particular, tests will be done to determine if the platform can move continuously along a straight line with minimal drifting to the sides or misalignment w.r.t. the centre line, the possibility of steering the platform when there is a misalignment, and suitable control strategies for the hub motors.

Initial misalignment tests were conducted with a yaw angle of the mockup platform at 6^o w.r.t. the center line as illustrated in Figure 5.17(a). It was noted that only three wheels were in contact with the curved surface. It was observed that when the mockup platform was steered forward, it would slowly get back to alignment due to the action of its as shown in Figure 5.17(b) for both cases.

Figure 5.16: Mockup on the curved sections

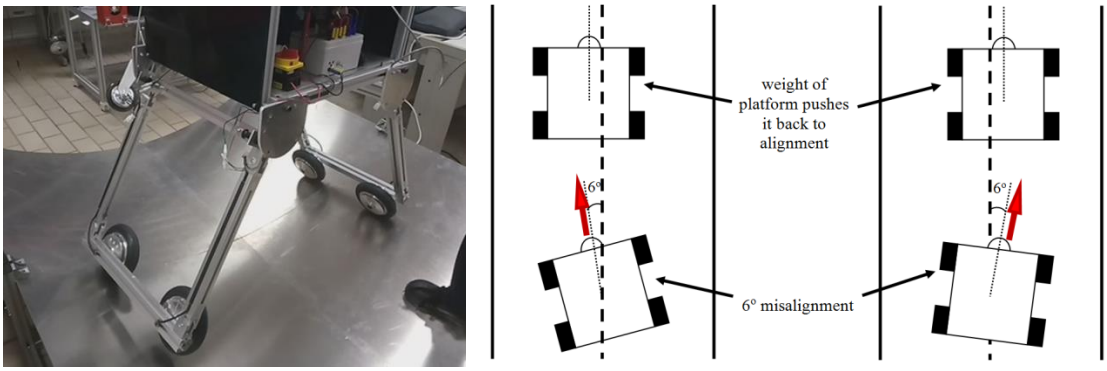

(a) (b)

Figure 5.17: Recovering from misalignment

During the test, the power supply to the motor and the average travelling speed were recorded accordingly, as shown in Table 5.5, to figure out the relationship between the power that is fed into the motors and the corresponding rotational speed of the wheels.

Power Supply (%)	Displacement (cm)	Travelling Time (s)	Average Speed (cm/s)
42	57	0.00	**0.00**
43	57	4.21	**13.53**
45	57	2.45	**23.30**
47	57	1.79	**31.77**
49	40	1.13	**35.27**

Table 5.5: Relationship between motor speed and power reduction

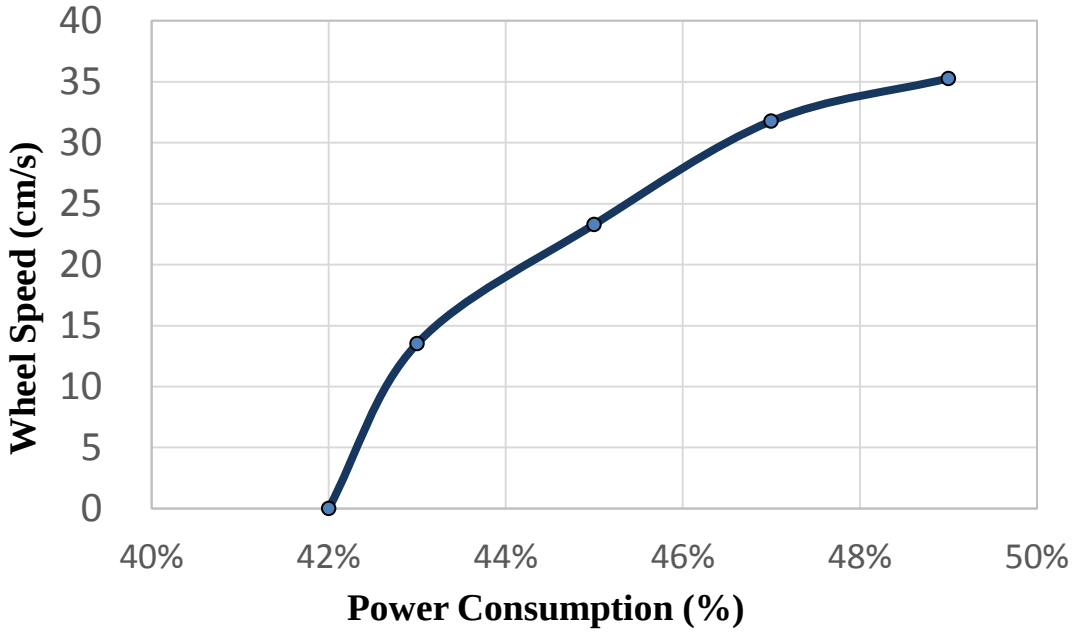

Figure 5.18: Speed vs Power plot for hub motor

In Figure 5.18, the wheels' speed is plotted against power consumpted by the four wheels. It was found that under load (self-weight of mockup) the wheels needed at least 43% of power supply to overcome static firctions and inertia to initiate driving. Additionally, from the relationship above we could observe that the speed increment became less significant at higher percentage of power consumption. This enables us to identify the required power issued to the motors when robot speed is determined.

CHAPTER 6: HOISTING AND INSPECTION SYSTEM

6.1 Literature Review

The tunnel robot has to coordinate with a hoisting and inspection system which has flexible, robust and reliable design to get into deep tunnel to perform inspection task. This chapter contrasts with scholarly materials about existing information of designs and control framework of hoisting and inspection system so that we can systematically examine all sources and justifies what we have done. There are four types of hoisting system designed for underground or underwater inspection, namely wireless system, tethered system, tethered system with TMS and tethered system with guide pulley.

6.1.1 Wireless System

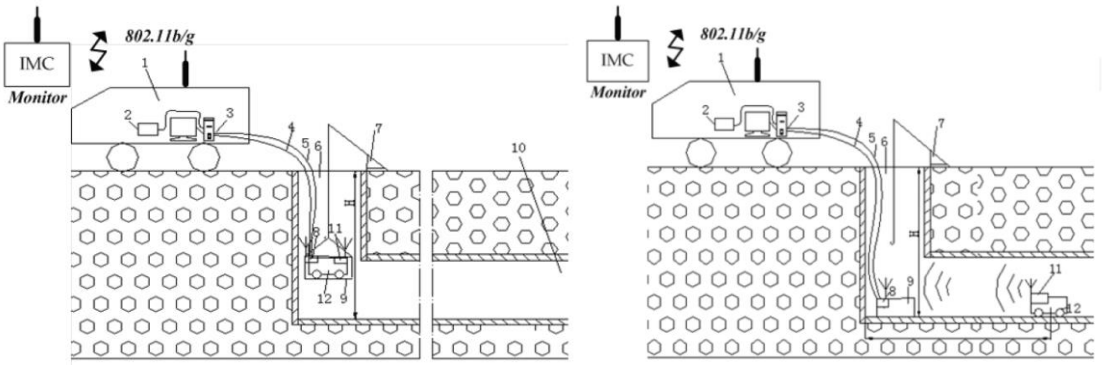

1- The engineering vehicle, 2- The tele-operator/monitor, 3- The UPS, 4- The power cable, 5- The signal cable, 6- The manhole, 7- The hoisting machine, 8- The Wireless transmitter/receiver on ground, 9- The overhead bin, 10- The cable tunnel, 11- The Wireless transmitter/receiver on the robot, 12- The robot

Figure 6.1: Operating procedure of the robot in a cable tunnel [20]

In the wireless system, a hoisting machine is adopted to deploy the robot into a cable tunnel by lowering an overhead bin. When the bin is located at the bottom of the manhole, the robot moves out of the bin and drives wirelessly into the cable tunnel. A portable tele-operator in the engineering vehicle is utilized to tele-operate the movement of the robot. An Intelligent Maintenance Center (IMC) is located far apart from the tele-operator. It serves as a monitor to receive the wireless sensing data from the robot via the wireless receiver and the tele-operator so that the environment of the cable-tunnel can be inspected from the real time online system. When the task is done, the robot will go back to the overhead bin. Subsequently, the bin is lifted to the ground by the hoisting machine.

6.1.2 Tethered System

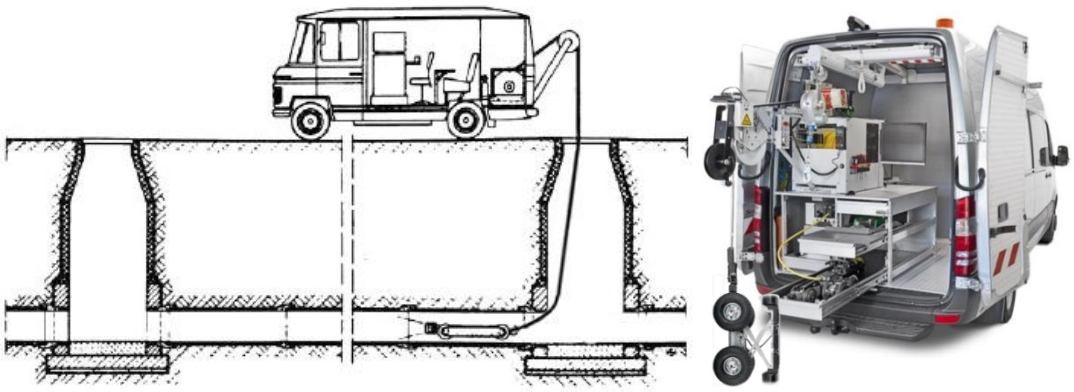

Figure 6.2: High-End System developed by IBAK [48]

This is a conventional configuration of an inspection robot system. IBAK [48] is a manufacturer and supplier of pipe inspection systems in Germany. A number of complete systems are provided by IBAK for inspection and repair, for instance, the High-End System, which consists of a steerable camera tractor for the inspection of sewers of DN150 and above, a fully automatic, motor-driven cable winch with capacity of 600m of camera cable, and an operating system for IBAK inspection equipment for fixed installation in an inspection vehicle. During the operation, the cable is coiled or uncoiled from the winch drum in accordance with the speed of the camera tractor. This prevents the camera tractor from running over the camera cable and ensures the camera tractor reverses at a consistent speed. The automatic cable guide on the winch ensures even winding of the camera cable onto the winch.

6.1.3 Tethered System with TMS

This system consists of control system, an umbilical winch, an A-frame, a TMS and a ROV. The umbilical winch with sufficient capacity accommodates the maximum length of TMS cable that system requires. A level wind mechanism is fitted onto the winch so that even spooling of the cable to the winch drum can be achieved. The winch is mounted on the chassis of the A-frame. The A-frame is utilized for TMS lifting without the need of any other external lifting devices. This helps to simplify the mobilization process. As shown in Figure 6.3, the A-frame designed by SAAB can be erected up to 2 meters, enabling the ROV and TMS to be deployed over a greater reach than a conventional A-frame. The TMS comprises a side entry garage to accommodate the ROV. The top section of the TMS contains tether controls and management mechanism and a bobbin where the tether is stored. During the operation, the garage is lowered to the working depth. At the working depth the ROV can then be safely moved out of the TMS with the maximum reach of its tether.

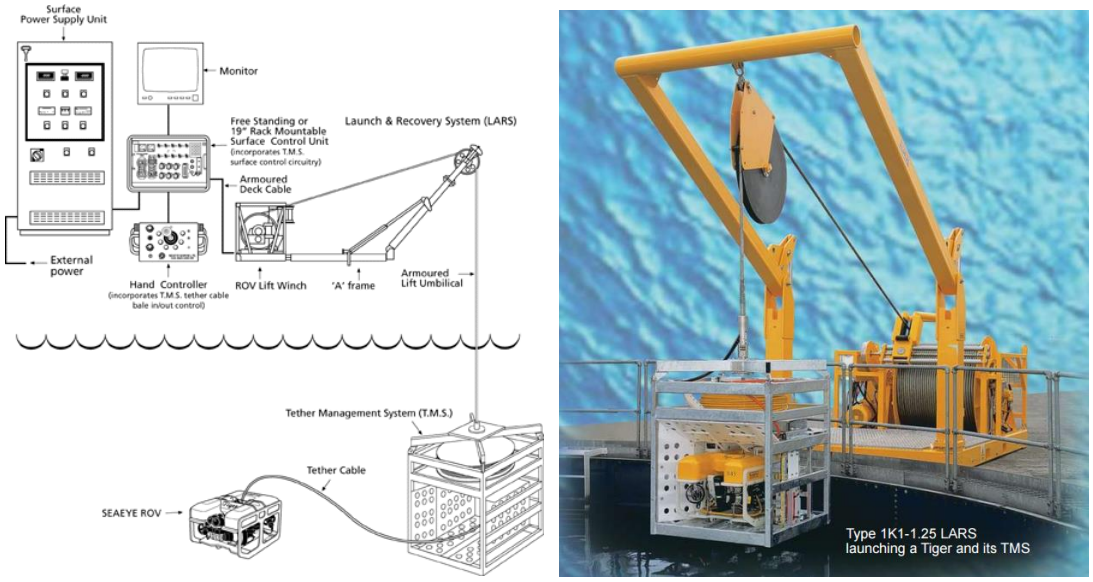

Figure 6.3: A ROV launch and recovery system developed by SAAB [49]

6.1.4 Tethered System with Guide Pulley

This method is performed using a cable-tethered robot with an onboard camera system. An operator controls the robot motion and the video system remotely. The cable is guided by a guide pulley at the junction of the tunnels to avoid rubbing against the sharp edge of the tunnel.

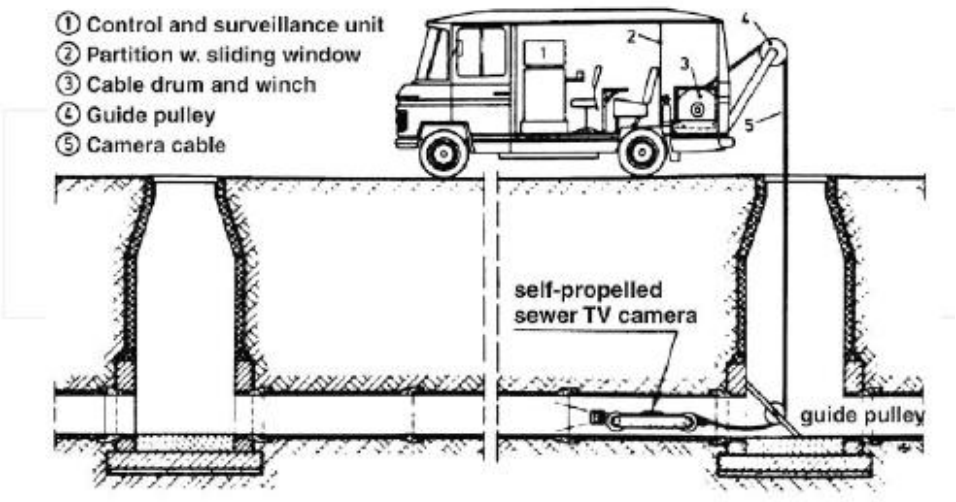

Figure 6.4: Diagram of visual inspection [16, 50]

6.1.5 System Design Evaluation

In the first system design, a wireless motion control is adopted. Due to the fact that no tethered cable for power supply and data communication, batteries, wireless devices and other electrical components have to be used and this lead to the increment of load on the robot. Robot can only stay inside the tunnel during malfunction as it cannot be pulled out of the tunnel without tether. This will cause the loss of robot, thus waste of money and effort.

For the tethered robot design, it can avoid the disadvantages mentioned above. Tethered robot is hardly to be washed away by rapid flow in the tunnel during rainy season. With the length of the cable unreeled from winch drum, we can measure the travel distance of the robot inside the tunnel. However, the movement of the robot might be constrained by the tether. Large traction force is needed for the locomotion because it needs to pull the cable along the travel distance.

After the evaluation of these four configurations, the tethered robot is selected. Due to the fact that the guide pulley in the fourth system design is inconvenient to be fixed onto the tunnel, a TMS is selected instead due to its flexibility. There are quite a number of related off-the-shelves inspection systems can be found, however, most of the systems cannot be directly integrated into our application due to the insufficient drum capacity, cable breaking strength and etc. Many existing robots have a lack of

function of either navigating by water or moving on the tunnel wall. Most of them are only applicable for small and medium pipelines. Thus, a special customized hoisting and inspection system is needed to satisfy the requirement of maintenance task for large-diameter tunnel.

6.2 Embodiment Design

Figure 6.5 shows an illustration of the inspection system from simulation software, showing the sectional view of the vertical shaft and the trunk sewer, and the hoisting system. The main purpose of this simulation is to enable us to address the main elements needed for the tunnel inspection. The A-frame and winch module can be installed on an inspection vehicle or placed directly on the ground for the deployment of the robotic platform and the TMS. The robot is tethered to the operating system via the TMS to achieve data transmission. The system described above depicts a typical system with full accessories. The configuration can be expected to vary from the final design. Additional lifting equipment can be expected to position a launch platform which does not encompass additional equipment to prepare the site for inspection.

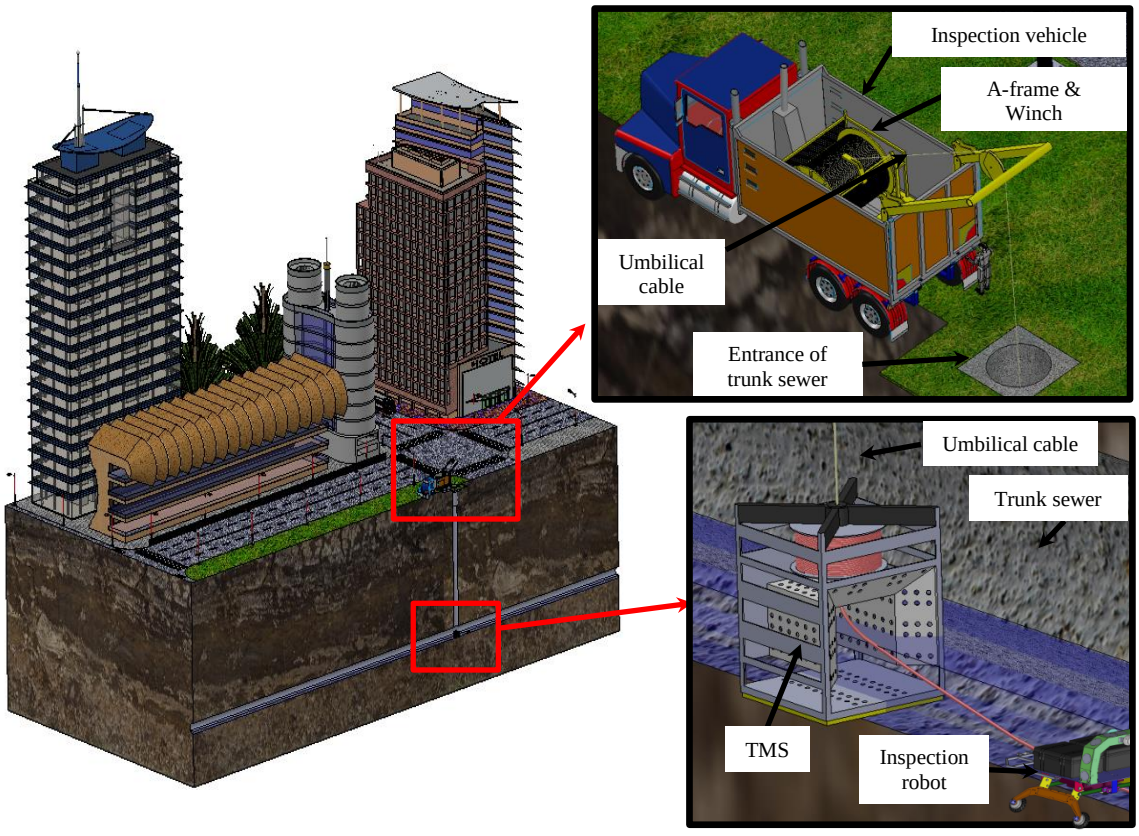

Figure 6.5: The 3D Simulation of the Hoisting System

6.3 Fluid flow analysis with different shape of TMS

Flow analysis is the observation of the simulated fluid passing through an object and investigates the impact to improve product performance. When the used water is blocked, the dreg or sludge will settle and accumulate at the TMS. It may affect the operation of the inspection process. In order to inspect whether the TMS will block the used water in the tunnel, the flow simulation is carried out to troubleshoot and optimize the TMS structure design. The first step in the analysis is to build up the 3D models of the TMS and the DTSS. Thus, a CAD model is established using the Solidworks software. Next, perform the calculations to simulate the interaction of water with TMS surfaces base on boundary conditions. The boundary constraints and the shape of TMS defined as an input in the calculation are as follows:

Conditions of the tunnel:

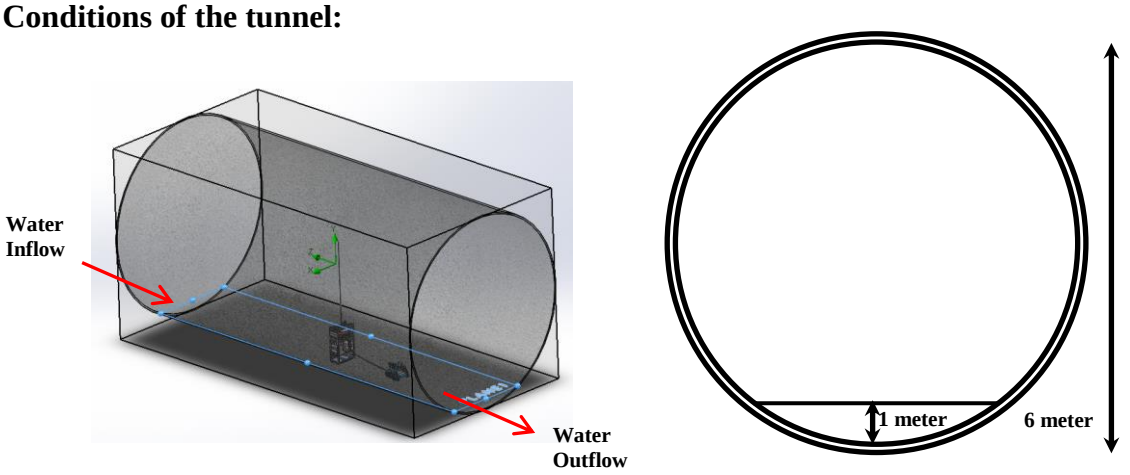

Input of Simulation: Shape of TMS

With defined constraints:

Liquid:	Water
Flow speed:	1m/s
Water level:	1m
Flow rate:	1.5484 m^3/s
Pressure:	101325 Pa
Temperature:	20 Celsius

Output of Simulation: Water flow speed

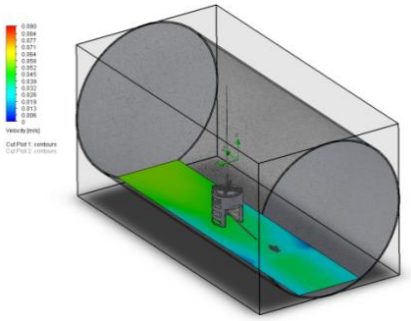

Figure 6.6: Constraints assumption of the simulation

We assume the water level in the tunnel is 1 meter with flow speed of 1 meter per second and is under atmospheric pressure with 20 Celsius. Based on the tunnel with diameter of 6 meters, the water flow rate can be derived by mathematical and

geometrical method, and thus we obtain the value of 1.5484m^3/s. The diameter of the manhole access is 1.8 meters, the size of the TMS is considered so that the TMS can be able to pass through the manhole opening and reach the deep tunnel. A total of five designs of TMS are analyzed in the simulation and the corresponding results are projected onto the cut plots accordingly. The top view of the simulation is shown in the figure below.

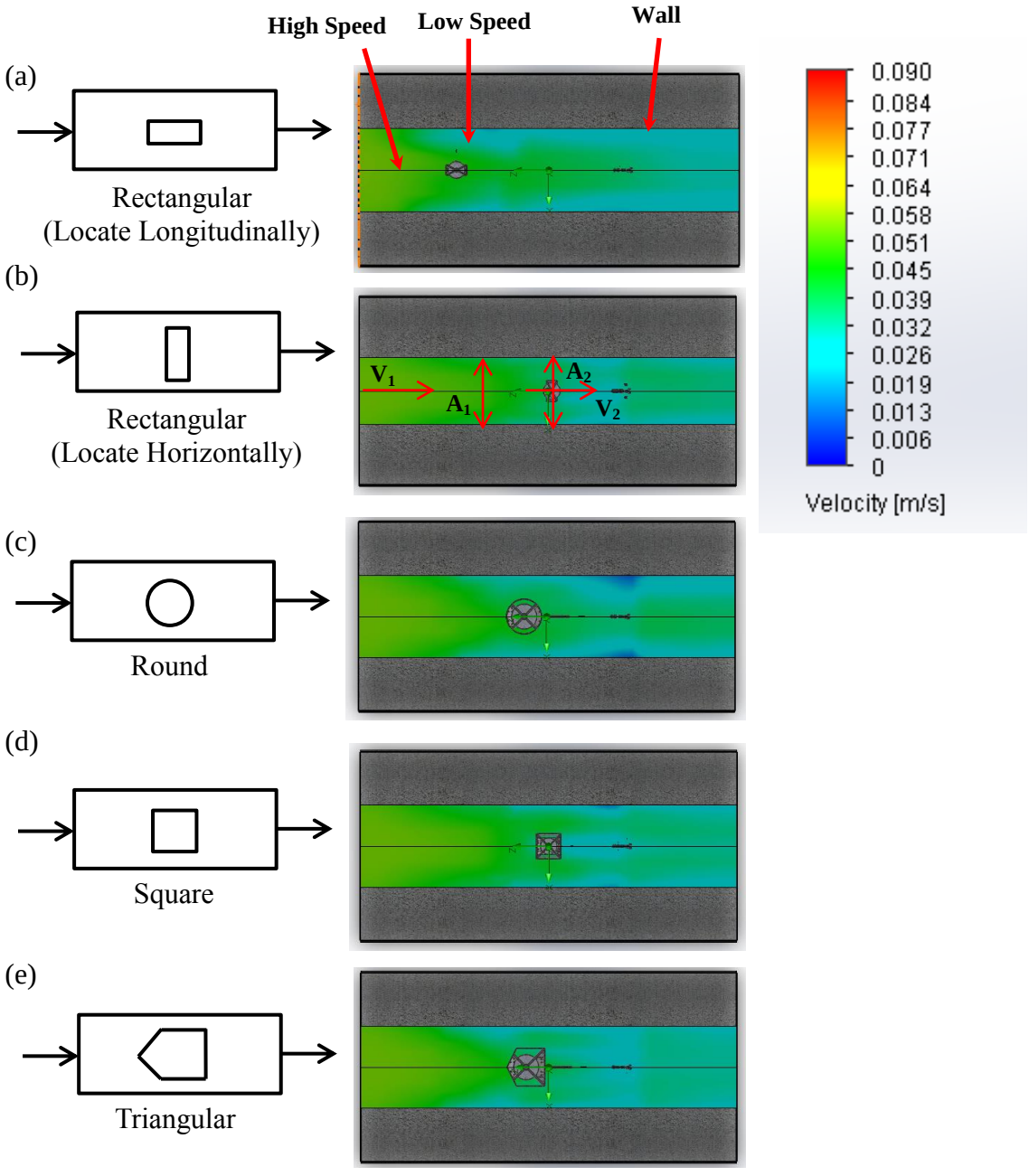

Figure 6.7: Fluid flow simulation results

From this simulation, the used water is flowing through the tunnel with different velocities. The water moves more quickly near to tunnel axis and more slowly near to tunnel wall due to the fluid viscosity. The viscosity is a property of collisions between neighboring particles in a fluid that move at different velocities. This concept can be proved by the Principle of Continuity. The volumetric flow rate can be defined by

$$Q=A_1.V_1=A_2.V_2$$

where A = cross-sectional vector area or surface
V = flow velocity of the substance elements

In this case, we assume the used water in the tunnel is a steady flow, where the quantity of water passing by a section does not change with time. In addition, no water is added or removed between any two sections. Therefore, the water flow rate Q is always a constant. Due to the fact that $A_1>A_2$, based on the equation we thus obtain $V_2>V_1$.

From result (b) to (e), the water flow speed in front of the TMS is relatively slow compare to (a) and it will most probably cause water blocking. The water flow speed in result (a) is distributed more uniform compared to other designs and it has less affect upon the blockage of water. Careful evaluation and consideration has been taken place and the design (a) is consequently selected because it has simple design, low fabrication cost, and the used water has more even flow speed when passing through the TMS.

6.4 Design of Hoisting and Inspection System

The setup of the inspection system consists of a number of subsystems, namely the auxiliary system and control station on the surface, the hoisting and winch system, and the robotic platform as shown in Figure 6.8.

On the surface, the auxiliary system provides electrical power to the winch and the robotic platform as well as hydraulic power to actuate the A-frame. The control station houses the control units for the robotic platform and monitors displaying images from cameras and measurements from sensors.

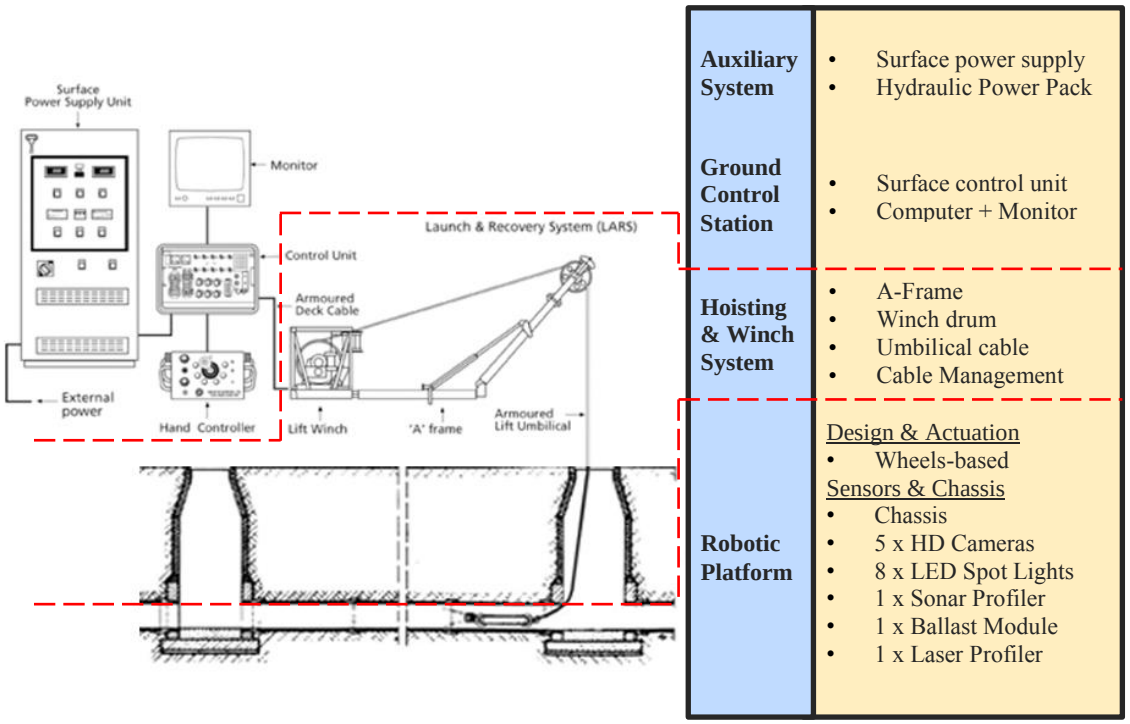

Figure 6.8: The hoisting and inspection system

The hoisting and winch system comprises an A-frame, a winch module and an umbilical cable. The A-frame is for lowering and lifting the robot along the access shaft without the needs of any other heavy-duty hoisting devices. The portable hydraulic A-frame system consists of hydraulic power pack and local control station. It equips with dual hydraulic cylinder, which helps to position the sheaves for proper guiding of cables and to gain fail-safe protection. The winch is mounted on the A-frame platform for easy transport and operation. An external 3-Phase 400VAC power generator will supply the power to the winch module and provides power supply for the tethered robotic platform. The electrical power is transmitted along multi-core umbilical cable which carrying a Kevlar core, data optic fiber and 4-core copper wires.

The robotic platform has its own actuation and houses various sensors needed for the inspection of the sewer tunnel. It will have lightings to illuminate the tunnel and cameras to capture the tunnel images. In particular, three cameras and four LED spot lights are integrated into the semi-circular frame and the coverage would overlap each other in order to provide seamless images and illumination for the sewers investigation. A sonar profiler and a laser profiler are utilized to scan the surface condition of the tunnel below and above the water surface respectively. A ballast control is used to vary

the weight of the robot by drawing in or discharging water in accordance to the internal condition of the sewer. For instance, high water level and high water flow rate may cause the robot floating and losing its mobility. The ballast system needs to draw in water to increase robot weight to maintain the maneuverability and stability of the robot.

6.5 Tripod Winch

The manhole openings across Singapore may locate at some places with constrained space. For instance, the entrance may locate at the side of highway or be surrounded by plants, etc. The setup of A-frame is not allowed at such ground condition and thus a tripod winch will be used instead to achieve the hoisting of the robotic platform. The space needed for the setup of tripod is minimal, and the use of tripod is common due to its ease of setup, convenience and low cost. In the first phase of this project is more focus on the testing of concept. Due to the tight project time frame, we will work on the detailed design of the A-frame system in the next phase of the project.

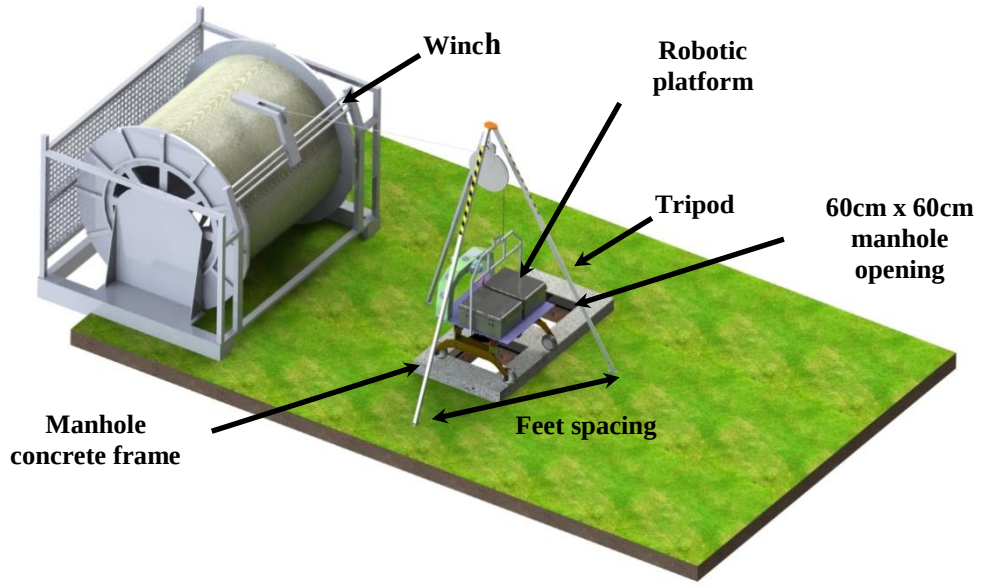

Figure 6.9: Simulation of robot launching

Figure 6.9 shows the terrain of the manhole opening modeled in Solidworks based on the drawing of sewer at Pasir Ris / Tampines area. This helps to simulate the environment of the manhole opening for robot launching. There are many off-the-shelf tripod winches available in the market but selecting the one that is suitable for our

application is crucial. The proposed tripod is simulated base on the dimension given by supplier. After the legs of the tripod are fully deployed, it provides large feet spacing and allows the robotic platform to have larger clearance away from the manhole concrete frame. However, it is seen that the size of the robotic platform is larger than the 600 mm × 600 mm manhole opening and a modular robot design is required. For the deployment of robotic platform, human intervention is required in the access shaft to guide the robotic platform away from the intermediate platform as well as to open up the wheel frames to the desired angle.

6.6 Testing of Robotic Platform Prototype

The robotic platform prototype will first be tested along a corridor with circular rooftop shelter as shown in Figure 6.10 for its functionality. The corridor is about 180m in length and the circular shelter has a diameter of 3.76m which is close to that of the tunnel of the trunk sewer.

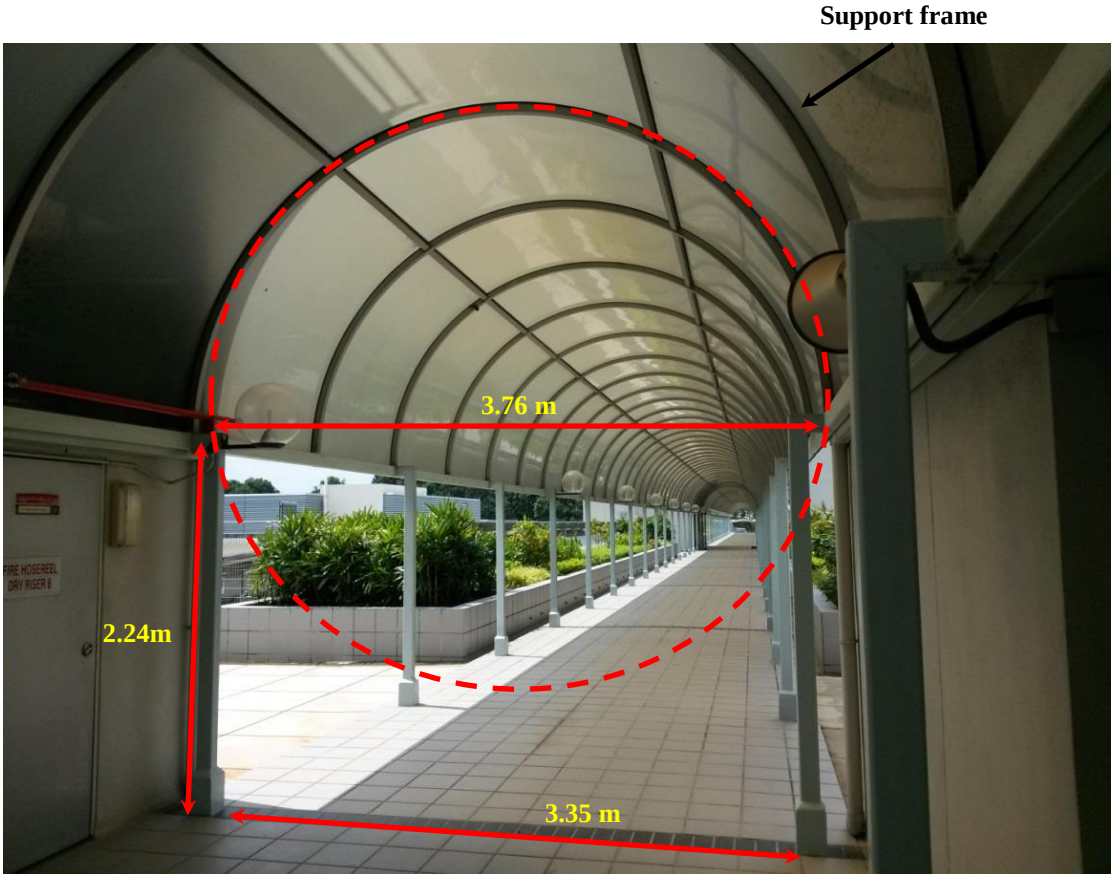

Figure 6.10: Corridor with circular rooftop shelter

The capability of the lighting system to illuminate the rooftop and of the camera to capture the image with required resolution can therefore be assessed as the robotic platform moves along the corridor at various speeds. In addition, the steering and control of the robotic platform to move in a straight line along the corridor can also be tested as the platform moves forward and backward. The location of the robotic platform along the corridor needs also to be computed based on the distance travelled. This may be done by counting the number of the lateral support frames of the shelter from the starting point as they are placed at regular interval. This is similar to the notion of counting the segment markings on the tunnel ceiling along the trunk sewer.

6.7 Control and Communication Architecture

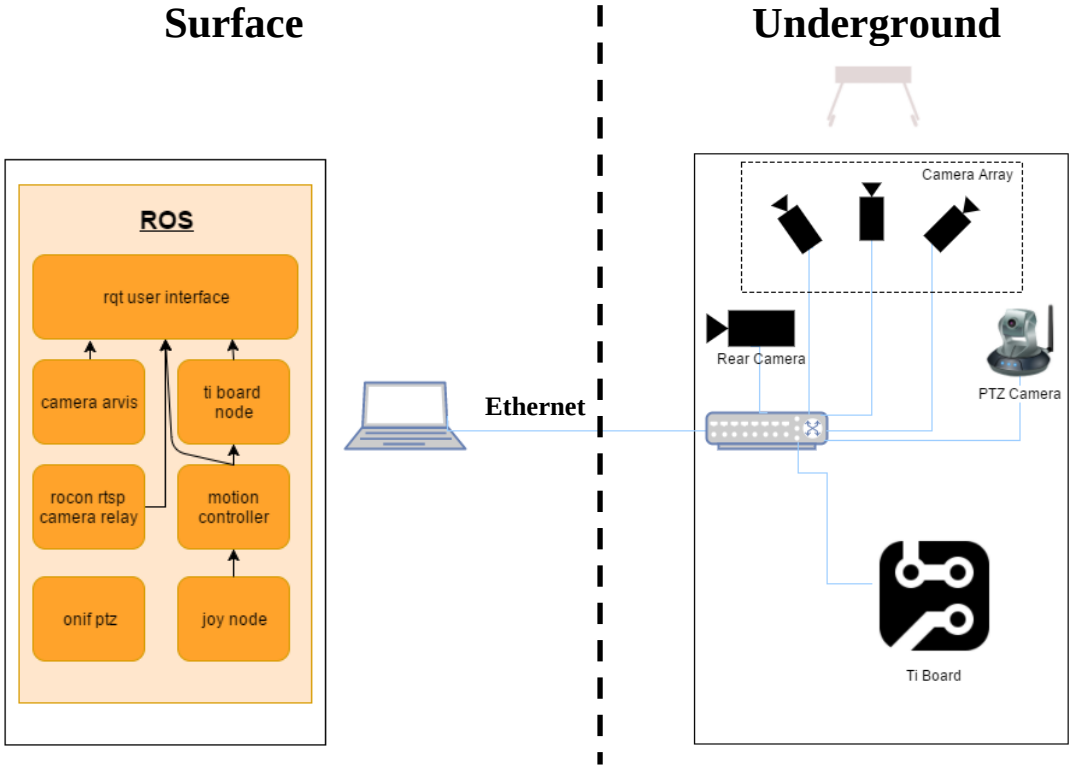

Figure 6.11: (a) Software Architecture and (b) Communication Architecture

The robotic platform runs on an Ethernet based communication system. This allows us to send all communicating data with just a single Ethernet cable from the robot up to the surface, reducing the total size of the communication cable required from the surface to the robot. The cable weight is thus lighter and less power is needed for robot to steer. However, one of the limitations of realizing the communication through

Ethernet cable is that the communicating data is vulnerable to the noise interference which can scramble the signal and long distance transmission may weaken the signal. Additionally, there are limits to the number of devices that can coexist in a single network. Contention and latency may occur if attach too many devices because each device needs to wait for a chance to transmit data.

As the communication network run via Ethernet, ROS was chosen as the middleware software stack to support the communication and operation of the robot. In this configuration, the laptop on the surface will host both the ROS system for the user interface and run all the required applications required to operate the various sub-systems on board.

ROS, or Robotic Operation System, is an open source robotic middleware framework developed to help to simplify the task for creating software to run complex robotics operations. It provides a TCP/UDP based inter-application communication framework which fits with the physical communication system defined above.

6.8 Sub-Systems

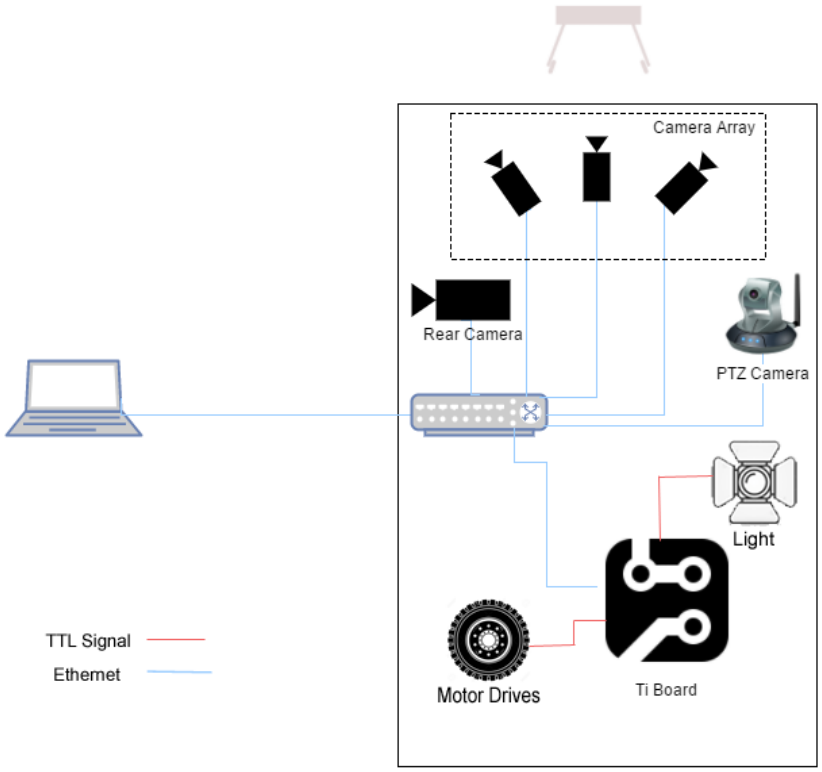

Figure 6.12: Sub-systems of signal communication

Within the robot, the sub systems can be categorized into two main types, based on how it communicates with the laptop. The first type via the Ethernet and the second type communicate via TTL signaling. We will look into each sub systems based on the categories.

6.8.1 Ethernet based Subsystems

- Laptop controller

  The laptop controller is the brain of the robot, running the core applications as well as providing the control interface to the pilot of the robot. It is located on the surface and connects to rest of the system via Ethernet network.

- Network Switch

  The device in charge of connecting all the Ethernet based subsystems together. It is located on the robot.

- Camera Array

  The Camera Array consists of three Ethernet Cameras each connected independently to the network and the controller. Its main purpose is to capture images of the ceiling of the tunnels.

- Rear Camera

  An Ethernet Camera located at the back of the robot. It provides the pilot with the back view from the robot to assist in reversing.

- PTZ Camera

  An Ethernet Camera located at the front of the robot. It provides the pilot with the front view from the robot to assist in moving forward. The PTZ camera come with pan, tilts and zoom capability which allow the pilot to have control on the perspective of the robot.

- Ti Board

  The Ti Board is an ARM microcontroller based Input/output (I/O) board which supports control via Ethernet. It helps to bridge the control and communications between the Laptop controller and TTL based subsystems.

6.8.2 TTL based Subsystems

- Light

  Illumination systems on the robot which help the cameras capture images in the trunk sewer.

- Motor drives

  The drivers used to control the speed and directions of the motors for propulsion of the robot.

- Laser profiler

  A laser profiler is used for inspecting the tunnel surface above water level.

- Sonar profiler

  A sonar profiler is utilized to scan the tunnel surfaces that are submerged underwater.

- Pressure sensor

  The pressure sensor is used to measure the pressure inside the enclosures. Pressure drop indicates water leakage in the enclosures.

6.9 User Interface

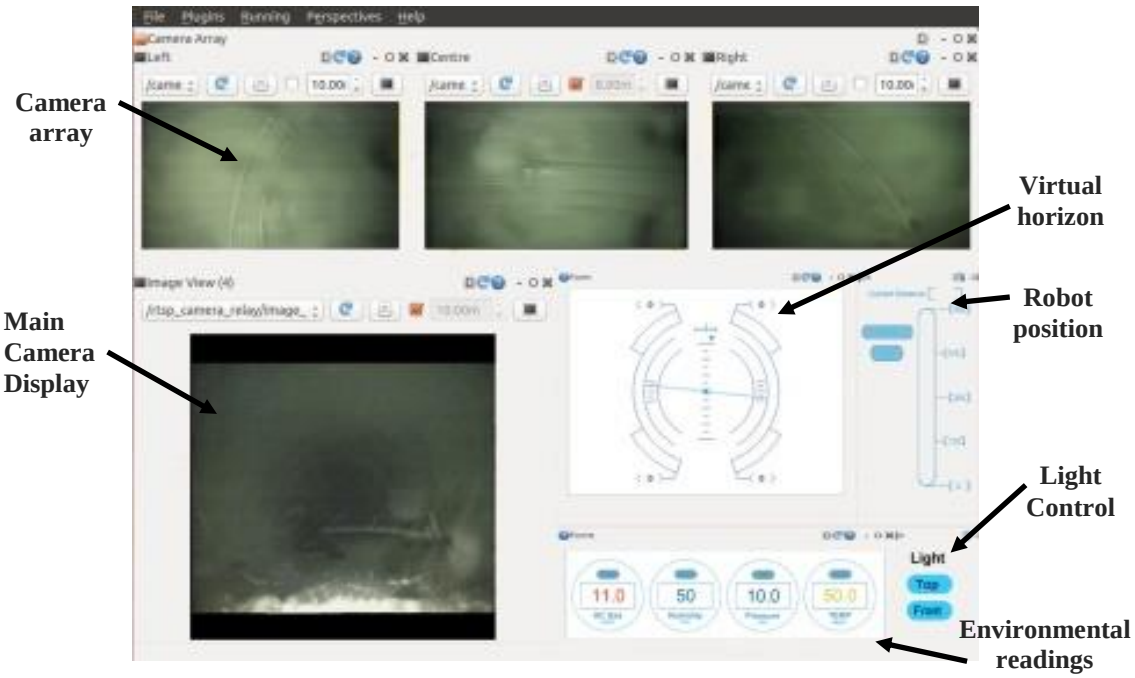

Figure 6.13: Mockup of RQT Interface

The user interface is running on ROS's RQT GUI framework. ROS's RQT is built upon an open source GUI frame work call QT. The advantage of RQT is that it runs on

a widget based concept, where users are allowed to add, move, remove and resize the existing RQT widgets and built their own customized layout of the interface. In Figure 6.13, the virtual horizon widget displays the pitch and roll values of the robotic platform as well as the power command being issued to the individual motors on the robotic platform. The environmental readings widget shows the level of explosive gases, humidity, pressure and temperature with status indicators (Green: Normal Range, Yellow: Caution Range, Red: Danger Range).

CHAPTER 7: CONCLUSION AND FUTURE WORK

7.1 Discussion and Conclusion

In order to prolong the service life of the wastewater superhighway based in Singapore, maintenance tasks have to be carried out periodically. There will always be a need to use pipeline and tunnel robots to do maintenances due to its ability to access underground spaces and its flexibility of performing tasks in constrained areas. In this report, the main objective is reviewed, that is to design a tunnel robot for inspections in large-diameter tunnel with a hoisting system. In particular the robot was designed to have the flexibility to stretch its width and get its wheels onto the sides of the tunnel wall, and elevated the whole platform higher away from the sediment and wastewater below the tunnel.

Basically the objective of this project has been met as the proposed robotic platform for larger diameter tunnel and the hoisting system have been designed. The major tasks completed in this project are summarized as follows:

7.1.1 Pipeline and Tunnel Robots

(i) Patent Search

To understand different types of locomotion mechanism used in the design of pipeline and tunnel robot and of preventing the infringement of copyright, literature review is conducted and summarized. From various patents reviewed, different types of locomotion for existing pipeline or tunnel robots were introduced and compared. Nine

robotic systems are classified, namely conventional PIG type, wheels type, crawler type, cylindrical type, legs or articulated foot type, inchworm type, helical type, snake type and variable velocity PIG type. After reviewing the available technologies for maintenance of deep large sewers, it is hard to identify any single robotic technology that can effectively combine all the desired functionalities such as inspection, cleaning and repairing into single unit. Also, most of the existing in-pipe robots are for small or medium pipelines while the existing large pipeline robots cannot access the 60cm x 60cm manhole opening. Therefore, this patent search points out the possible gaps that there is a need to develop a tunnel robot to perform the maintenances in large-diameter tunnel with small entrance.

(ii) Design of Tunnel Robot

The design of the robot is designed base on the environment of the trunk sewer because it has severer condition compared to the DTSS. If the challenges of trunk sewer inspection can be solved, the inspection task of DTSS will be relatively easier. The access conditions of the trunk sewer were raised in this project:

a) Possible presence of soft debris along the pipe bottom;
b) Manhole opening is square 600 mm × 600 mm into an interior shaft with a diameter of 1.8m;
c) Intermediate platforms in the trunk sewers;

The access conditions (b) and (c) are very serious constraints on the design of the robotic platform and are not comparable to that of DTSS. The priority will be to design the locomotion of the platform that can travel the required distance in the trunk sewer and capture images suitable for inspection. The access constraints will then be taken into consideration. A possible way around the problem is to design as modules and assemble at the bottom of the access shaft. However, this increases the complexity of the design and thus may compromise on the performance of the robot. Modular assembly would inherently necessitate man intervention in the tunnel. It is likely that the top concrete cover with the 600 mm × 600 mm may need to be removed. Hence, it

is desirable if a test site without the severe access constraints can be identified for testing.

Four conceptual designs of the tunnel robot are proposed and evaluated. After the design comparison, the design of wheeled robot is selected for further development and the detailed design of every component that made up this design was presented. The design calculation of the deformation and stress analysis on the robotic platform and the drawbar were done. The modular robot design has been proposed for further development.

A simple robotic platform was built with aluminum frames and equipped with hub motors, drivers and controllers for functionality test. The testing shows that the all-wheel drive with front cable fixing has the best performance, which yields valuable information on the tunnel robot design.

7.1.2 Hoisting and Inspection System

(i) Patent Search

A hoisting and inspection system is needed for the deployment of tunnel robot and the control of the inspection system on the robot. The information gathered from the patents has been analyzed and there are four types of system configuration designed for inspection and robot deployment, i.e. wireless system, tethered system, tethered system with TMS and with guide pulley. The configuration of tethered robot with TMS is selected because the tethered robot can be pulled out of the tunnel when malfunction occurred. This can help to prevent from losing the robot. With the length of the cable unreeled from the winch drum, we can measure the travel distance of the robot inside the tunnel. There are quite a number of related off-the-shelves hoisting system can be found, however, most of the systems cannot be directly integrated into our application because the challenges of maintenance of large-diameter tunnel are different from those of the conventional small and medium pipes. Thus, a customized hoisting and inspection system is needed to satisfy the requirement of maintenance of large-diameter tunnel.

(ii) Design of hoisting and inspection system

With the completion of steps mentioned in previous chapters, the conceptual design of the system is completed. In addition, fluid flow analysis has been conducted to simulate how the shape of TMS impacts on the behavior of water flow in the tunnel to ensure the proposed design is fit for operation. In other words, the design with less water blocking is optimum as the dreg or sludge will hardly accumulate at the TMS so that it will not affect the operation of the maintenance process. Some assumptions are made in the flow simulation and five different shapes of TMS are analyzed. The corresponding results are projected onto cut plots accordingly and it shows that the rectangular TMS located longitudinally in the tunnel has better result as the used water has more even flow speed when passing through the TMS and thus less water is blocked. Besides, it has simple design and therefore reduces the fabrication cost and eases the maintenance of machinery.

The subsystems which establish the hoisting and inspection system have been identified, namely the auxiliary system, the ground control station, the hoisting and winch system, and the robotic platform. In order for the robot to collect video images from the tunnel for visual inspection, various sensors are used, such as HD cameras, LED spot lights, sonar profiler and laser scanner. Pressure sensors measure the internal pressure of enclosures, water sensors identify the influx of underground water into the enclosures, and LED spot lights are used to illuminate the dark tunnel. A tripod winch will be used to replace the A-frame due to its ease of setup and transportation. An environment has been simulated for further testing on the performance of the locomotion and inspection system of the robotic platform on a curved surface.

7.2 Future Work

Although this report has established a comprehensive study on the design and development of tunnel robot and hoisting system, there are other related issues that are not addressed. First, this research has identified and shown several types of robotic system for in-pipe locomotion. However, an issue this work does not address is that how much traction force the robot needs to generate in such humid and slippery condition to obtain its locomotion. Further study on the wheels design and traction force calculation is required to determine this issue.

Second, it is important to have a proper hoisting system that can lower down and lift up the sewer robot safely. The design of mobile robot and hoisting system in this report is shown theoretically. It helps to illustrate the operational concept of the whole system. However, when building the actual robot and the inspection system, we may encounter some practical problems which have been overlooked.

Third, there are too many uncertainties in the tunnel because long-distance inspection work of the large-diameter tunnel had never been achieved before. The water level, water flow speed, level of sludge, etc. cannot be exactly determined. Robot may operate abnormally under certain conditions. Therefore, a basic understanding of the internal condition of the deep tunnel is required so that we can improve our robot base on the in-pipe information to reduce the chance of abnormal operation.

Forth, there is another future plan on integrating a tunnel robot with multifunction like inspection, cleaning and repair for maintenance of large-diameter tunnel. The platform design should be done in such a way that it could be able to house additional components in case of any additional functions for the creation of long term solution of sewage maintenance such as cleaning and repairing that may be desired in the near or far future. From the survey, the system design of SVM-RS [8] with inspection and cleaning function for medium tunnel seemed to be also suitable for large-diameter sewerage tunnel. Regarding to this robotics system, there are several aspects that need to be taking care of, for examples, robot kinematics in tunnel, control system and operator interface, cleaning system, repairing system as well as the supply of water, power and repair material

However, some of the aspects are not possible to include in this work due to the extensive evaluation and study required for the design of the additional functions. Thus, this area requires a separate research study and it is beyond the scope of this thesis.

REFERENCES

1. PUB. *About Deep Tunnel Sewerage System*. November 2014 [cited 2016 July 9]; Available from: https://www.pub.gov.sg/dtss/about.
2. Bischoff, R. and T. Guhl, *The strategic research agenda for robotics in Europe.* IEEE Robotics & Automation Magazine, 2010. **17**(1): p. 15-16.
3. Walter, C., et al., *Design Considerations of Robotic System for Cleaning and Inspection of Large-Diameter Sewers.* Journal of Field Robotics 2012. **29(1)**: p. 186-214.
4. Archila, J.F. and M. Becker, *Study of Robots to Pipelines, Mathematical Models and Simulation.* IEEE Latin American Robotics Symposium and Competition (LARS/LARC), 2013: p. 18-23.
5. Archila, J.F., et al., *Study of pipeline inspection robots and numeric simulation inside service pipes.* p. 1298-1306.
6. Marinho, C.A., et al., *Petrobras' developments in underwater inspection.* 8th World Conference on Nondestructive Testing, 2012.
7. FinancialPost. *Pipelines in Canada: Sophisticated arteries*. 2013 November 2014. [cited 2016 27 July]; Available from: http://business.financialpost.com/2013/03/02/pipelines-in-canada-sophisticated-arteries/?__lsa=cd4e-3b98/.
8. Saenz, J., et al., *Robotic systems for cleaning and inspection of large concrete pipes.* 1st International Conference on Applied Robotics for the Power Industry, 2010: p. 1 - 7
9. Ahrary, A., *Sewer Robotics*. Service Robot Applications. 2008: InTech. 400.
10. Șteopan, A., M. Steopan, and A. Nicu, *Competitive Design and Mockup of a Modular Pipe Cleaning Mobile Equipment.* IEEE International Conference on Automation Quality and Testing Robotics (AQTR), 2012: p. 396 - 399
11. Bedkowski, J., et al., *Improvement of the robotic system for disaster and hazardous threat management.* 14th IFAC International Conference on Methods and Models in Automation and Robotics, 2009: p. 19-21.
12. Mashimo, H. and T. Ishimura, *State of the art and future prospect of maintenance and operation of road tunnel.* ISARC2006: p. 299-302.
13. Balaguer, C., et al., *Towards Fully Automated Tunnel Inspection: A Survey and Future Trends.* The 31st International Symposium on Automation and Robotics in Construction and Mining (ISARC 2014), 2014.
14. Gavilán, M., et al., *Mobile Inspection System For High-Resolution Assessment of Tunnels.* The 6th International Conference on Structural Health Monitoring of Intelligent Infrastructure, Hong Kong, 2013.

15. Inuktun. *Crawler Vehicles*. October 2014 [cited 2016 July 23]; Available from: http://www.inuktun.com/crawler-vehicles/.

16. Truong-Thinh, N., N. Ngoc-Phuong, and T. Phuoc-Tho, *A study of pipe-cleaning and inspection robot.* 2011 IEEE International Conference on Robotics and Biomimetics (ROBIO), 2011: p. 2593-2598.

17. Erasteel. *Conventional High Speed Steels*. January 2015 [cited 2016 July 23]; Available from: http://www.erasteel.com/content/conventional-high-speed-steel/.

18. DrRobot. *Jaguar Platform*. October 2014 [cited July 23; Available from: http://www.drrobot.com/.

19. Questinspar. *Quest Inspar - Pipeline Rehabilitation Specialists*. January 2015 [cited 2016 July 23]; Available from: http://www.questinspar.com/.

20. Zhuang, F., et al., *A cable-tunnel inspecting robot for dangerous environment.* International Journal of Advanced Robotic Systems, 2008. **5**(3): p. 243-248.

21. Mateos, L.A. and M. Vincze, *DeWaLoP In-Pipe Robot Position from Visual Patterns.* MICAI 2012, Part I, LNAI 7629, 2012: p. 239–248.

22. Mateos, L.A., K. Zhou, and M. Vincze, *Towards Efficient Pipe Maintenance: DeWaLoP In-pipe Robot Stability Controller.* 2012 IEEE International Conference on Mechatronics and Automation, 2012: p. 1 - 6.

23. Mateos, L.A., M.R.y. Dominguez, and M. Vincze, *Automatic In-pipe Robot Centering from 3D to 2D Controller Simplification.* 2013 IEEE/RSJ International Conference on Intelligent Robots and Systems (IROS), 2013: p. 258-265.

24. Kim, Y.-G., et al., *Design and Implementation of an Optimal In-pipe Navigation Mechanism for a Steel Pipe Cleaning Robot.* 8th International Conference on Ubiquitous Robots and Ambient Intelligence (URAI 2), 2011. **Nov. 23-26**: p. 772 - 773

25. Gettyimages. *An Autonomous robot for inspection and maintenance of large-sized pipes*. [cited July 16 2016]; Available from: http://www.gettyimages.com/pictures/adrian-tomoiaga-of-romania-a-member-of-a-team-of-inventors-news-photo-521141382.

26. Jurasko, I. *Romanian invention, that received Geneva inventions award, to be produced in Romania*. 2016 [cited 2016 July 23]; Available from: https://positivenewsromania.com/2016/06/19/romanian-invention-that-received-geneva-inventions-award-to-be-produced-in-romania/.

27. Ye, C., et al., *Development of a Pipe Cleaning Robot for Air Conditioning System.* 2010 IEEE International Conference on Robotics and Biomimetics, 2010: p. 1525-1529.

28. Li, Z., et al., *A New Pipe Cleaning and Inspection Robot with Active Pipe-diameter Adaptability Based on ATmega64.* 9th International Conference on Electronic Measurement & Instruments, 2009. **2**: p. 616-619.

29. Mohamad, S.N.B., *Fully autonomous pipeline cleaning robot.* Thesis of the degree of Bachelor of Engineering (Electrical - Mechatronics), 2012.

30. Roh, S.-g. and H.R. Choi, *Differential-Drive In-Pipe Robot for Moving Inside Urban Gas Pipelines.* IEEE Transactions On Robotics, 2005. **21**(1): p. 1 - 17

31. Kwon, Y.-S., et al., *Design and Motion Planning of a Two-Moduled Indoor Pipeline Inspection Robot.* IEEE International Conference on Robotics and Automation, 2008: p. 3998-4004.

32. Feng, D., et al., *Research on Key Technology in Downhole Crawling Robot.* Reconfigurable Mechanisms and Robots, ASME/IFToMM International Conference, 2009: p. 536 - 539.

33. BostonDynamics. *BigDog - The Most Advanced Rough-Terrain Robot on Earth*. November 2014 [cited 2016 July 23]; Available from: http://www.bostondynamics.com/robot_bigdog.html.

34. Raibert, M., et al., *BigDog, the Rough-Terrain Quaduped Robot.* 13th IFAC International Conference on Methods and Models in Automation and Robotics, 2008.

35. Hu, Z. and E. Appleton, *Dynamic Characteristics of a Novel Self-Drive Pipeline Pig.* IEEE Transactions On Robotics, 2005. **VOL. 21**(NO. 5): p. 781-789.

36. Fang, H., et al., *Design and experimental gait analysis of a multi-segment in-pipe robot inspired by earthworm's peristaltic locomotion.* Proc. of SPIE, 2014. **Vol. 9055, 90550H**.

37. Horodinca, M., et al., *A simple architecture for in-pipe inspection robots.* Colloquium on Mobile and Autonomous Systems, 10 Years of the Fraunhofer IFF, 2002.

38. Ohno, H. and S. Hirose, *Design of Slim Slime Robot and its Gait of Locomotion.* IEEE/RSJ International Conference on Intelligent Robots and Systems, 2001. **2**: p. 707-715.

39. Ohno, H. and S. Hirose, *Study on Slime Robot (Proposal of Slime Robot and Design of Slim Slime Robot).* 2000 IEEE/RSJ International Conference on Intelligent Robots and Systems, 2000. **3**: p. 2218 - 2223.

40. AZOMaterials. *Aluminium Alloy 6061 - Composition, Properties, Temper and Applications of 6061 Aluminium*. 2006 March 24 [cited 2016 July 23]; Available from: http://www.azom.com/article.aspx?ArticleID=3328

41. eMachineShop. *Stainless Steel Properties*. [cited 2016 July 23]; Available from: http://www.emachineshop.com/machine-shop/Stainless-Steel-Properties/page54.html.

42. Aalco. *Stainless Steel - General Information - St St Introduction*. [cited 2016 July 23]; Available from: http://www.aalco.co.uk/datasheets/Stainless-Steel_St-St-Introduction_61.ashx.

43. eFunda. *General Properties of Steels*. [cited 2016 July 24]; Available from: http://www.efunda.com/Materials/alloys/alloy_home/steels_properties.cfm.

44. L.T., F., *FEA Applications in DOE and Design Optimization.* IEEE/CPMT Electronic Packaging Technology Conference, 1997: p. 177 - 182

45. Onta, S., S. Dag, and M. Gokler, *Structural Finite Element Analysis of Stiffened and Honeycomb Panels of the RASAT Satellite.* 3rd International Conference on Recent Advances in Space Technologies 2007: p. 171 - 175

46. Suhir, E., *Predicted Failure Criterion for Moisture-sensitive Plastic Packages.* 45th Electronic Components and Technology Conference, 1995: p. 266 - 284

47. CNE. *Deformation Analysis*. 2013 [cited 2013 March 14]; Available from: http://www.cne.go.cr/CEDO-CRID/CEDO-CRID%20V4/pdf/eng/doc2291/doc2291-4.pdf

48. IBAK. *High-End System*. July 2015 [cited 2016 July 16]; Available from: http://www.ibak.de/en/produkte/ibak_show/frontenddetail/product/high-end-system/.

49. SAAB. *Saab Seaeye Launch & Recovery Systems (LARS) - 'A' Frame Systems*. April 2015 [cited 2016 July 17]; Available from: http://www.seaeye.com/larsaframe.html.

50. Ahrary, A., *Sewer Robotics.* Service Robot Applications, Yoshihiko Takahashi (Ed.), ISBN: 978-953-7619-00-8, InTech, 2008.

APPENDIX A: SPECIFICATION OF ROBOT SYSTEM

There are numerous ready off-the-shelves toolsets which seemed suitable to build up the basic infrastructure presented in Chapter 2 to Chapter 6. In order to provide a basis, this appendix provides the specification of the existing tunnel robots, hoisting systems, umbilical cables and winches from different companies.

A1 IBAK High-End System

A1.1 Cable Drums and Cable Winches

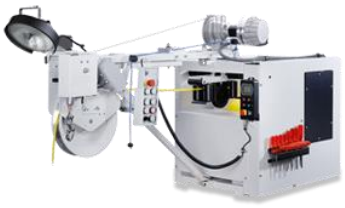

Product classification	Fully automatic, motor-driven
Max. cable length	500/600 m (in combination with the control system BS 5)
Width x height x depth	approx. 550 x 860 x 900 mm (without boom)
Weight (with 500 m cable)	approx. 170 kg
Protection class	IP 54
Length measurement	yes – display on the monitor and on the cable winch
Length display	yes – display on the monitor and on the cable winch
Motor-driven	yes
Even winding of cable	yes, automatic
Emergency-stop switch	yes
Steel rope winch for insertion of the camera system	yes

A1.2 Control Units

Product classification	Control system for IBAK inspection systems
Width x height x depth	BP 3.5:770 x 100 x 390 mmBE 7:483 x 266 x 358 (+200*) mm
Weight	BE 7:approx. 11 kg
Intercom loudspeaker, microphone	yes (gooseneck microphone, volume control in BP)
Camera cable length	500 m
Data display generator	yes (EDE 7), RS232 interface
Video input/output	yes, multiple
Keyboard	yes
Operating voltage	100-240 VAC, 50/60 Hz
Length measurement	yes
Length display	yes
Autostop function	yes
Safety device	secondary circuit in the camera cable limited to 120 V with insulation monitor
TV standard	NTSC / PAL

A1.3 Camera System

Product classification	Camera tractor
Inspection range	DN 150 and up
Weight	approx. 21 kg (with rim 93 and CB3)
Speed	continuously variable
Folding connector	bends horizontally and vertically
Protection class	IP 68
Pressure monitoring	2 integrated pressure sensors (LCD indicator and acoustic alarm in the control unit)
ATC (Automatic Tilt Compensation)	yes
Explosion protection	optional
Tilt measurement	yes
Height adjustment	electric, lift of up to 210 mm
Temperature measure-ment	yes, via temperature measurement module

A2 SAAB Underwater Inspection System

A2.1 Cable Drums and Cable Winches

Umbilical winch cable storage capacity	1600 m
Umbilical cable diameter	32 mm
Umbilical winch dynamic pull, at 1st layer of cable	5.89 Te
Umbilical winch mean recovery speed	0.5 m/s
Electrical supply type	3 ph
Voltage / frequency	50 Hz 380 or 415V
Electric motor power	37 kW
Maximum outboard reach	3500 mm
Nominal host vessel bulwark height transit capability	2000 mm
Overall length	4750 mm
Overall width, over mounting weldments	3100 mm
Transport width	2900 mm
Maximum height over A frame in operation	6808 mm
Transportation height	2375 mm
Gross weight including umbilical cable	13.2 Te

A2.2 Camera System

ROV model	Seaeye Tiger
Construction	Galvanised steel
Baling System	Polypropylene construction with hard anodized aluminium central boss. Seaeye SM4 motor drive with hard rubber universal coupling to bale arm gearbox
Electronics Pod	Hard anodized aluminium cylinder. Seaeye metal shell connectors
Tether capacity	140m of 17mm tether
Length	1200 mm
Width	1200 mm
Height to lift eye	1640 mm
Total Weight in air	Approx. 460 kg
Depth Rating	1000 meters

A3 Umbilical Cables

	TE connectivity	Nexans	DATALINE	Tyco Electronics	LEONI	NOVACAVI	Technip take it further.	Псков ГЕОКАБЕЛЬ	HYDROCABLE SYSTEMS
Diameter (mm)	30.48	20-80	36.32	NA	NA	22-41	NA	NA	NA
Breaking Strength (kN)	271	0-1500	449	NA	NA	100	NA	NA	NA
Weight in water (kg/km)	598	NA	2833	NA	NA	NA	NA	NA	NA
Power Cable	3	Customized	4	NA	Yes	Yes	NA	No	Yes
Fibers	3	Customized	6	1-60	Yes	Yes	NA	NA	Yes
Neutrally Buoyant	NA	NA	NA	Yes	NA	Yes	NA	Yes	Yes
Voltage (kV)	NA	4.5	3	2.4	NA	NA	NA	NA	NA
Power (kVA)	NA	2000	NA	NA	NA	NA	NA	NA	NA
Bend Radius (cm)	NA	NA	74	NA	NA	NA	NA	NA	NA

A4 Winches

	NICOLETTI				Ingersoll Rand	PLANETA	HADEF	ГЕОКАБЕЛЬ				KÖSTER	SEIK
	Winding Machine With Shaft		Reel Winding Machine With Mobile Arms		Electric Winches	Planetary Standard Build Winches SB-Series	Electric Wirerope Winch with planetary gear	Logging hoists with electrically driven winch	Mobile Winches	Stationary Geophisical Winches	Sea Hydrographic Hydraulic Logging Winches	Special cable winches	Electrical winches
													
Model	CD-15M3	CD-100M3 SE-1	CD-15M3/BM2 SE-1/MP-CD	CD-100M3/BM2/SE-1/TC-1-100/PLC	25000B25	SB 316-E H50095	47/05 E 1Bm/M3 40000daN 55kW	PKS-3.5E	LM 150/2100	-	LMG 150/2100	Type E 600	Traction power 20t
Height (mm)	1600	1700	1600	1700	NA	2100	1500	NA	NA	NA	NA	NA	NA
Length (mm)	2850	4100	2850	4200	NA	2650	3100	NA	NA	NA	NA	NA	NA
Width (mm)	2200	2600	2200	2600	NA	1600	1600	NA	NA	NA	NA	NA	NA
Weight (Kg)	540	980	740	2200	1614	2900	4000	NA	NA	NA	NA	NA	NA
Mov. Speed (km/h) (1st layer)	4	4	4	4	0.45	0.36	0.42	NA	1.5	3	1.5	14.4	14.4
Power (Kw)	2.2	8	3.7	10	18.65	45	55	37	NA	37	NA	NA	NA
Nominal current (A)	NA	NA	NA	NA	NA	NA	93	NA	NA	NA	NA	NA	NA
Max Turning Speed (rpm)	70	50	70	50	NA	NA		NA	NA	NA	NA	NA	NA
Pulling Force (1st layer)	421Nm	2400Nm	421Nm	2400Nm	NA	NA	400kN	NA	150kN	Max 3000kN	150kN	NA	Max 220kN
Carrying cap. (Kg) (1st layer)	3000	10000	3000	10000	11364	37000	NA	NA	NA	NA	NA	600	NA
Recommended Wire rope size (mm)	NA	NA	NA	NA	32	48	40	Max 12.5	NA	2-36	NA	12	37
Full Drum Capacity (m)	NA	NA	NA	NA	262	NA	1008	3500	$3.7m^3$	NA	$3.7m^3$	2000	1030
Drum Capacity (m) (1st | 5th layer)	NA	NA	NA	NA	NA	18|137	NA	NA	NA	NA	NA	NA	NA

A5 Tripod

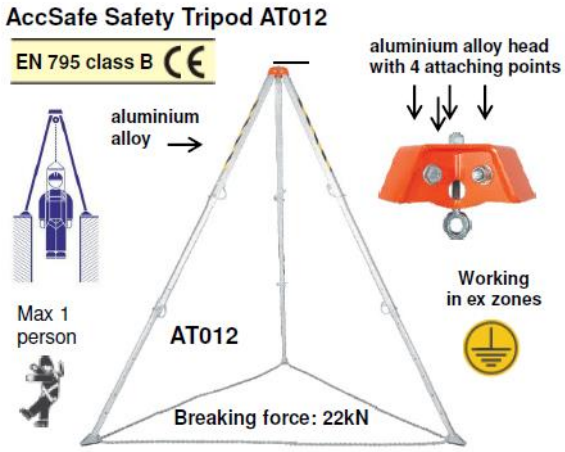

We provide both chain and webbing for legs fixing

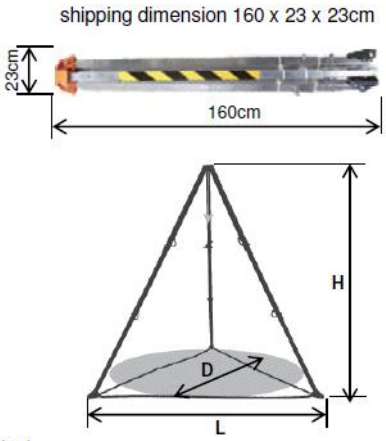

Table 1

Model	H (cm)	D (cm)	L (kg)	S (kg)	W (kg)
AT012	143 - 308	136 - 280	115 - 240	500	20

H: Height & extend D: Deployed leg diameter
L: Feet Spacing S: Safety load
W: Gross weight with chain

APPENDIX B: DRAWINGS FOR SYSTEM COMPONENTS

B1.1 Inspection Robot

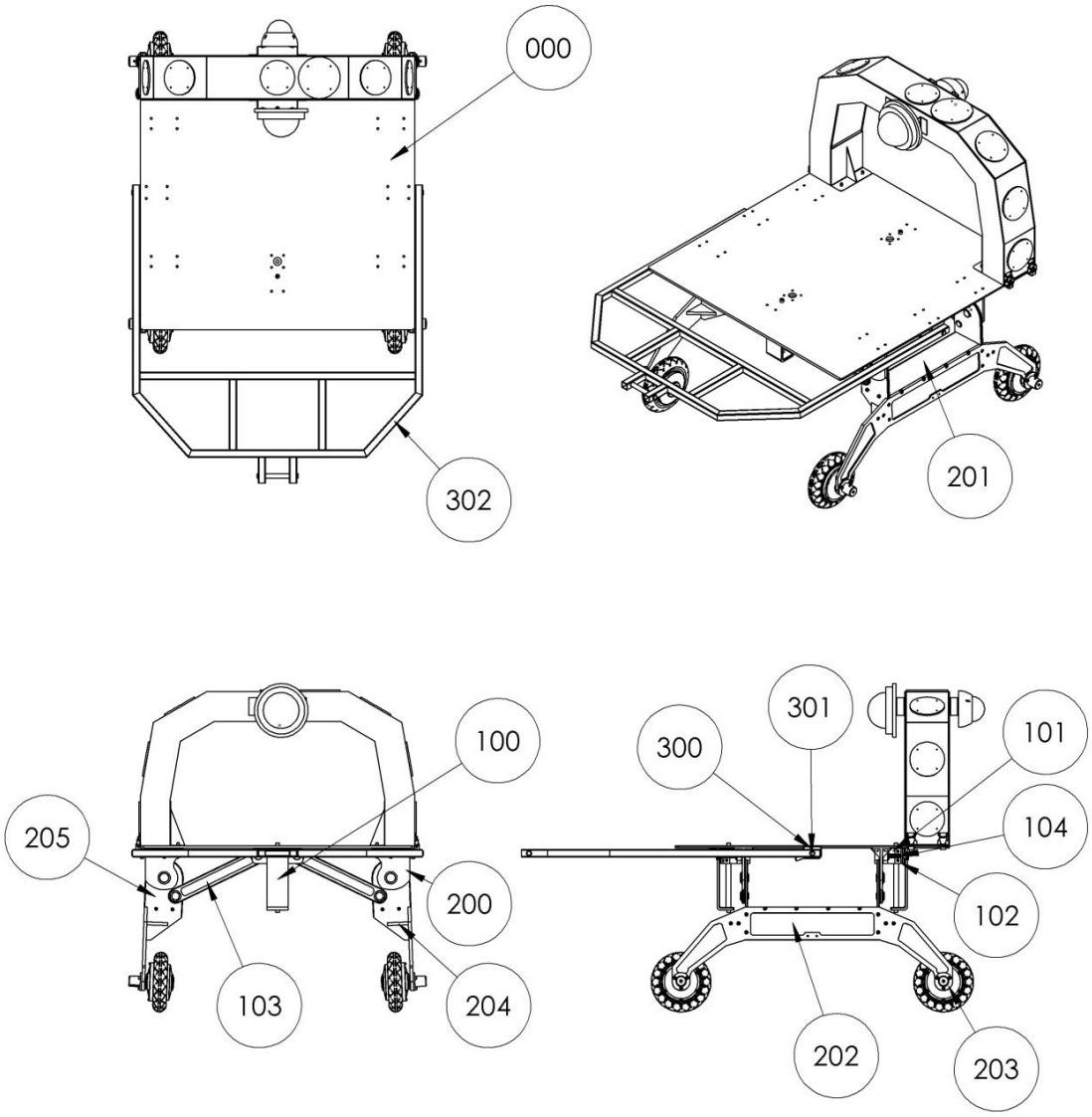

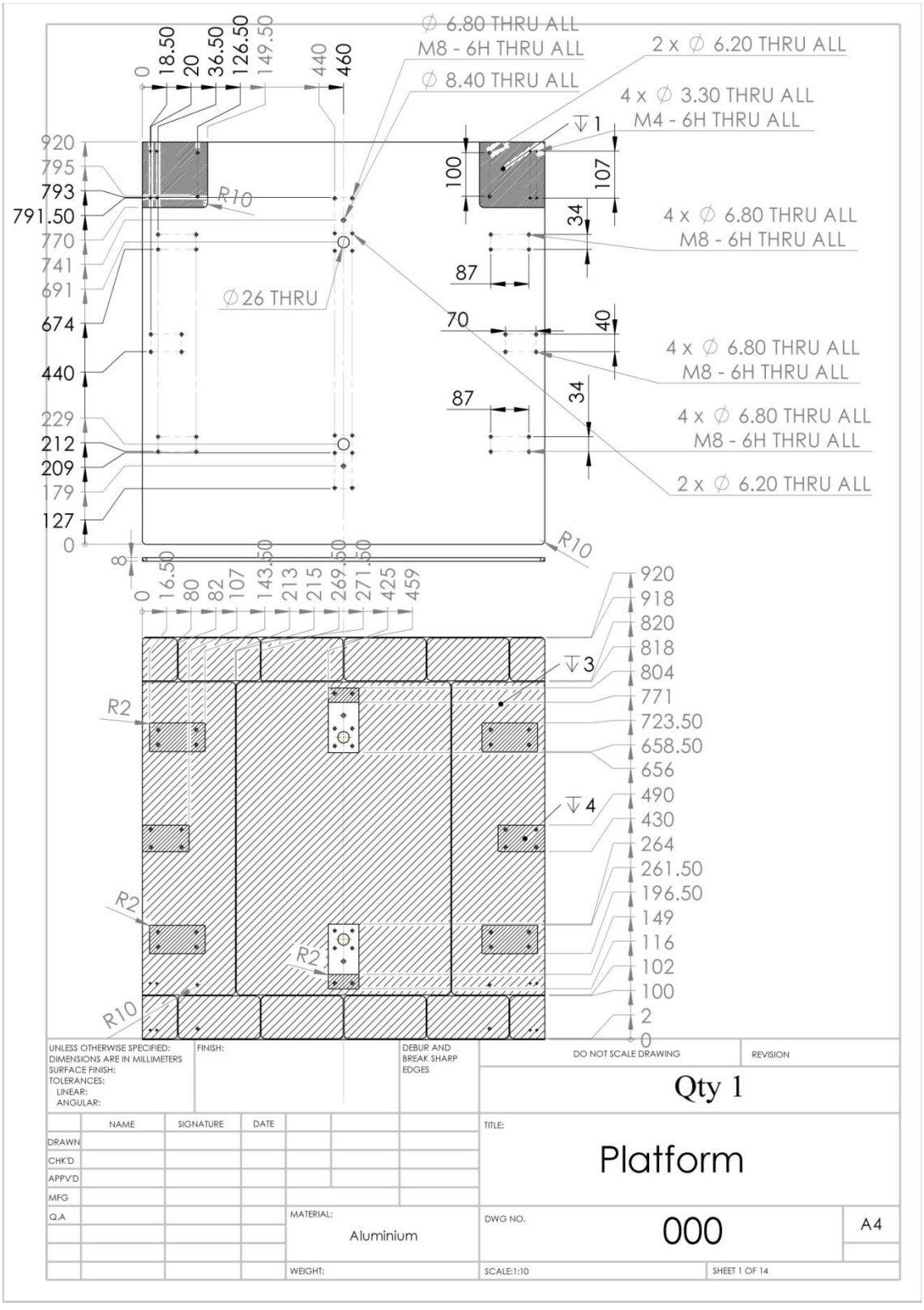
∅ 6.80 THRU ALL
M8 - 6H THRU ALL
∅ 8.40 THRU ALL
2 x ∅ 6.20 THRU ALL
4 x ∅ 3.30 THRU ALL
M4 - 6H THRU ALL
4 x ∅ 6.80 THRU ALL
M8 - 6H THRU ALL
4 x ∅ 6.80 THRU ALL
M8 - 6H THRU ALL
4 x ∅ 6.80 THRU ALL
M8 - 6H THRU ALL
2 x ∅ 6.20 THRU ALL
∅26 THRU
R10
R2
R10
UNLESS OTHERWISE SPECIFIED:
DIMENSIONS ARE IN MILLIMETERS
SURFACE FINISH:
TOLERANCES:
LINEAR:
ANGULAR:
FINISH:
DEBUR AND BREAK SHARP EDGES
DO NOT SCALE DRAWING
REVISION
Qty 1
NAME
SIGNATURE
DATE
DRAWN
CHK'D
APPV'D
MFG
Q.A
TITLE:
Platform
MATERIAL:
Aluminium
DWG NO.
000
A4
WEIGHT:
SCALE:1:10
SHEET 1 OF 14

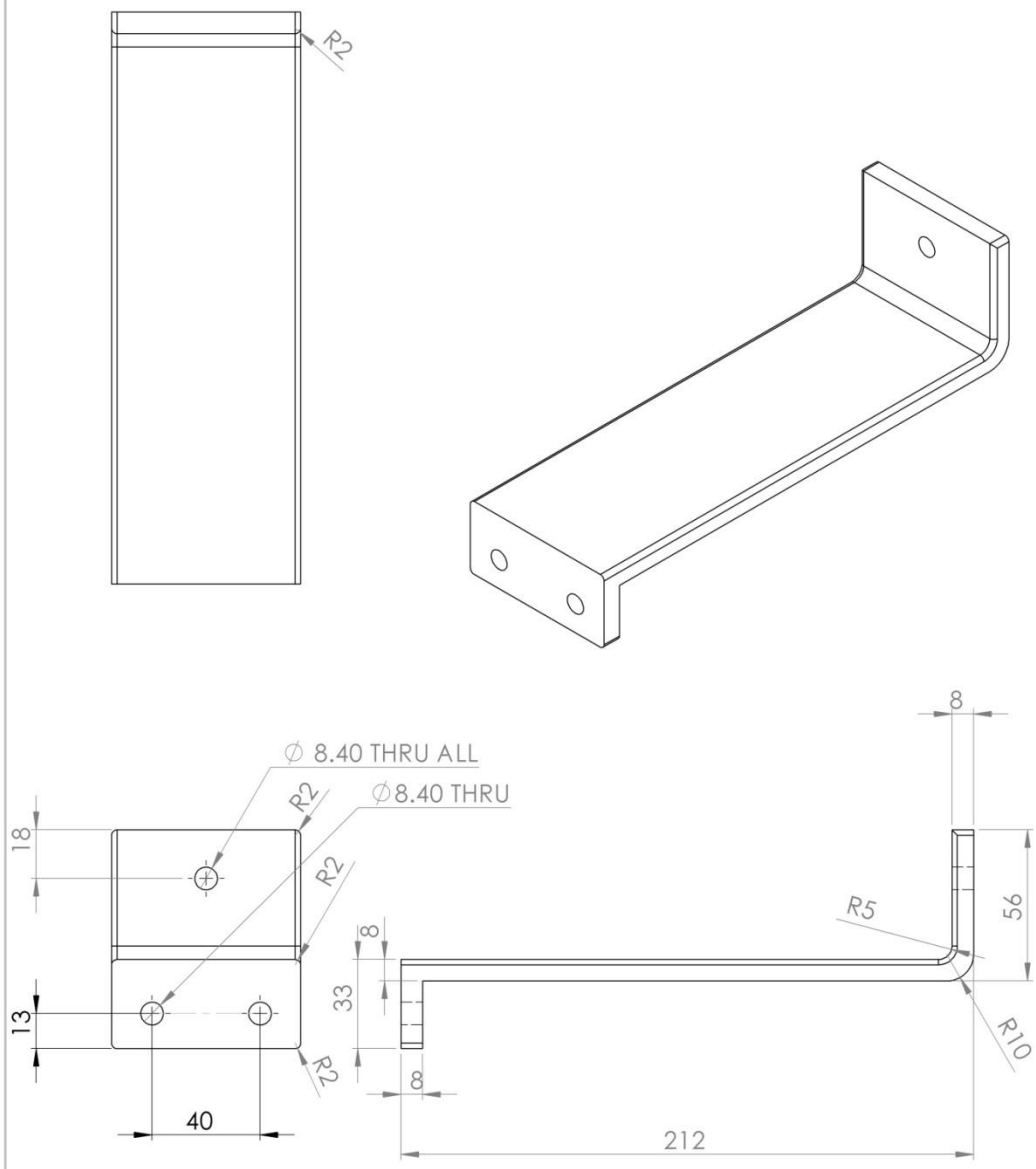

UNLESS OTHERWISE SPECIFIED: DIMENSIONS ARE IN MILLIMETERS SURFACE FINISH: TOLERANCES: LINEAR: ANGULAR:				FINISH:			DEBUR AND BREAK SHARP EDGES	DO NOT SCALE DRAWING / REVISION
								Qty 2
	NAME	SIGNATURE	DATE					TITLE:
DRAWN								Frame Platform Shaft Holder
CHK'D								
APPV'D								
MFG								
Q.A				MATERIAL:				DWG NO. / A4
				Aluminium				100
				WEIGHT:				SCALE:1:5 / SHEET 2 OF 14

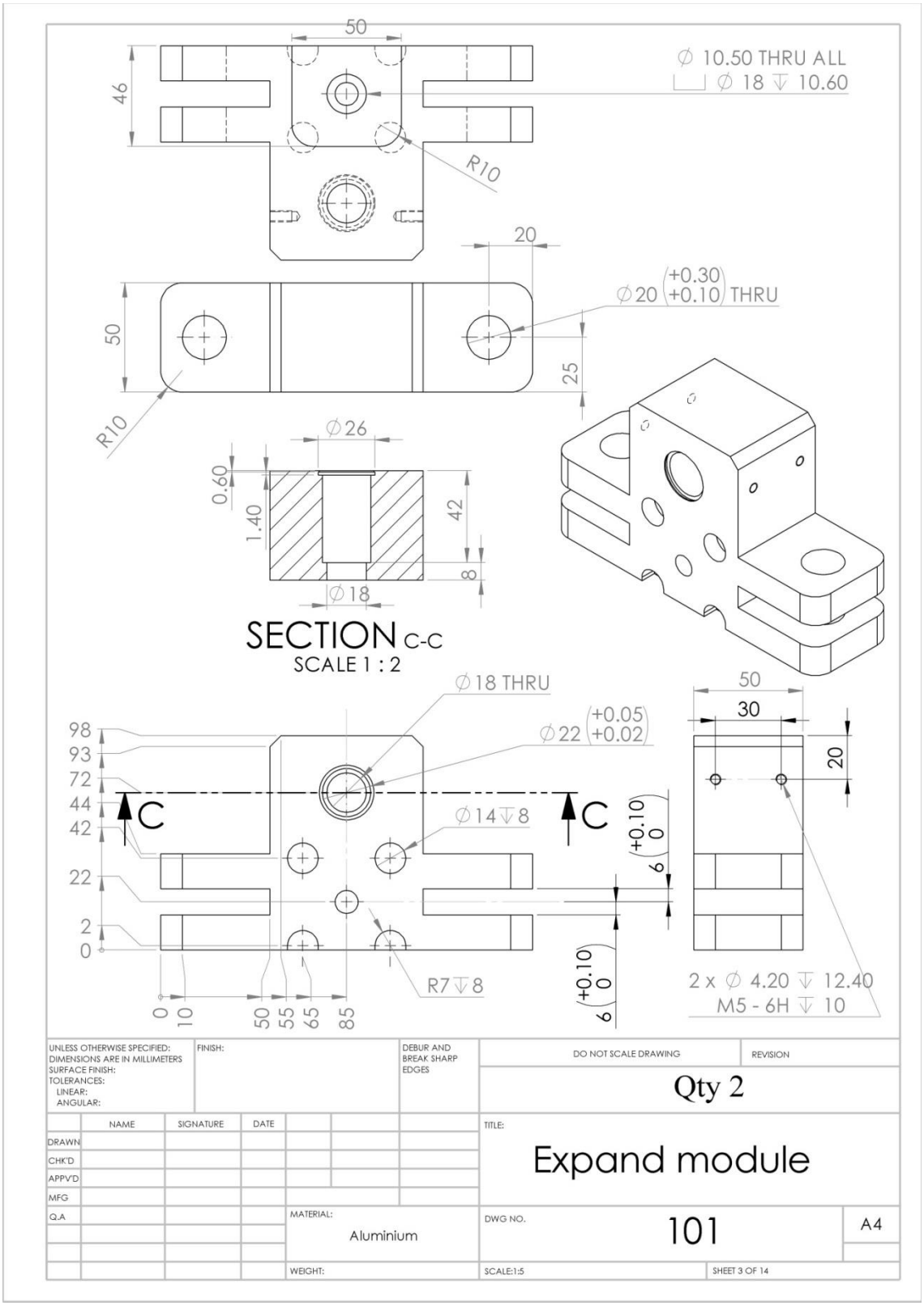
50
46
∅ 10.50 THRU ALL
⌴ ∅ 18 ↧ 10.60
R10
20
∅20 +0.30 +0.10 THRU
50
25
R10
∅26
0.60
1.40
42
8
∅18
SECTION C-C
SCALE 1 : 2
∅18 THRU
∅22 +0.05 +0.02
50
30
20
98
93
72
44
42
22
2
0
C
C
∅14↧8
+0.10 0
6
+0.10 0
6
R7↧8
0
10
50
55
65
85
2 x ∅ 4.20 ↧ 12.40
M5 - 6H ↧ 10
UNLESS OTHERWISE SPECIFIED:
DIMENSIONS ARE IN MILLIMETERS
SURFACE FINISH:
TOLERANCES:
LINEAR:
ANGULAR:
FINISH:
DEBUR AND BREAK SHARP EDGES
DO NOT SCALE DRAWING
REVISION
Qty 2
NAME
SIGNATURE
DATE
DRAWN
CHK'D
APPV'D
MFG
Q.A
TITLE:
Expand module
MATERIAL:
Aluminium
DWG NO.
101
A4
WEIGHT:
SCALE:1:5
SHEET 3 OF 14

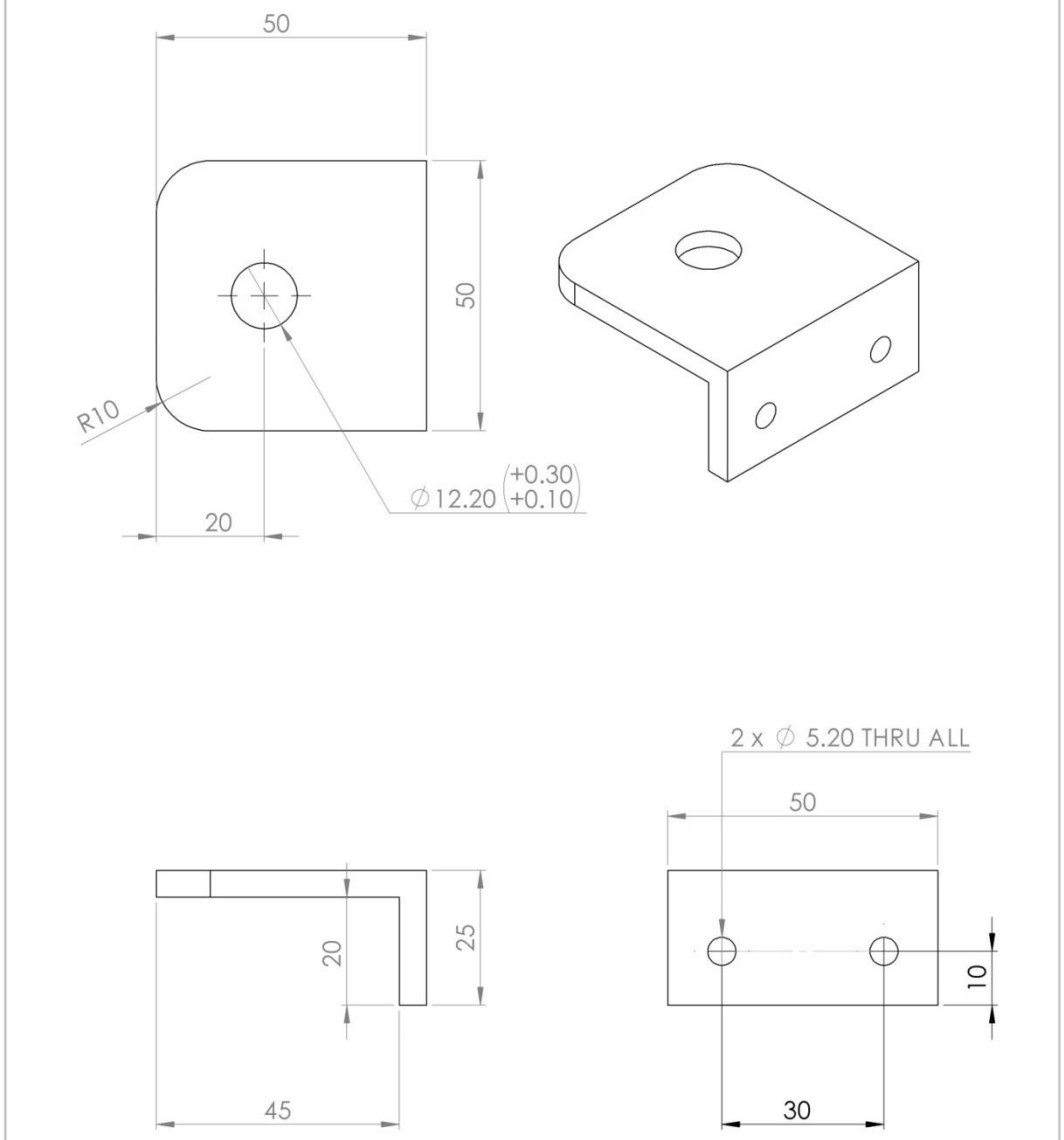

UNLESS OTHERWISE SPECIFIED: DIMENSIONS ARE IN MILLIMETERS SURFACE FINISH: TOLERANCES: LINEAR: ANGULAR:				FINISH:			DEBUR AND BREAK SHARP EDGES	DO NOT SCALE DRAWING / REVISION
								Qty 4
	NAME	SIGNATURE	DATE					TITLE:
DRAWN								Expand module 2
CHK'D								
APPV'D								
MFG								
Q.A				MATERIAL:				DWG NO. 102 / A4
				Aluminium				
				WEIGHT:				SCALE:1:1 / SHEET 4 OF 14

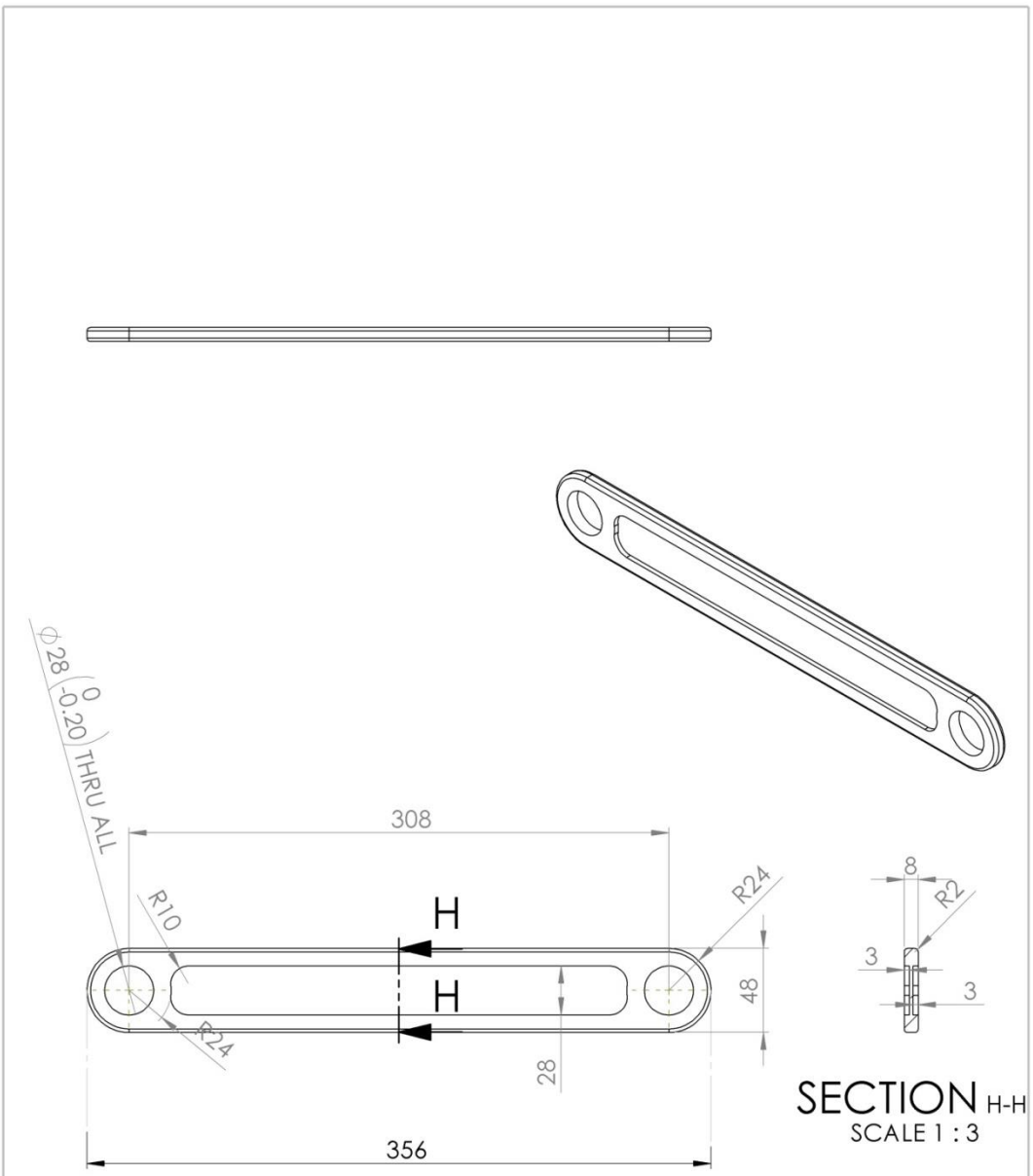

UNLESS OTHERWISE SPECIFIED: DIMENSIONS ARE IN MILLIMETERS SURFACE FINISH: TOLERANCES: LINEAR: ANGULAR:	FINISH:		DEBUR AND BREAK SHARP EDGES	DO NOT SCALE DRAWING	REVISION
				Qty 4	

	NAME	SIGNATURE	DATE	TITLE:
DRAWN				Bar linkage
CHK'D				
APPV'D				
MFG				
Q.A				

MATERIAL: Aluminium	DWG NO. 103	A4	
WEIGHT:	SCALE:1:10	SHEET 1 OF 6	

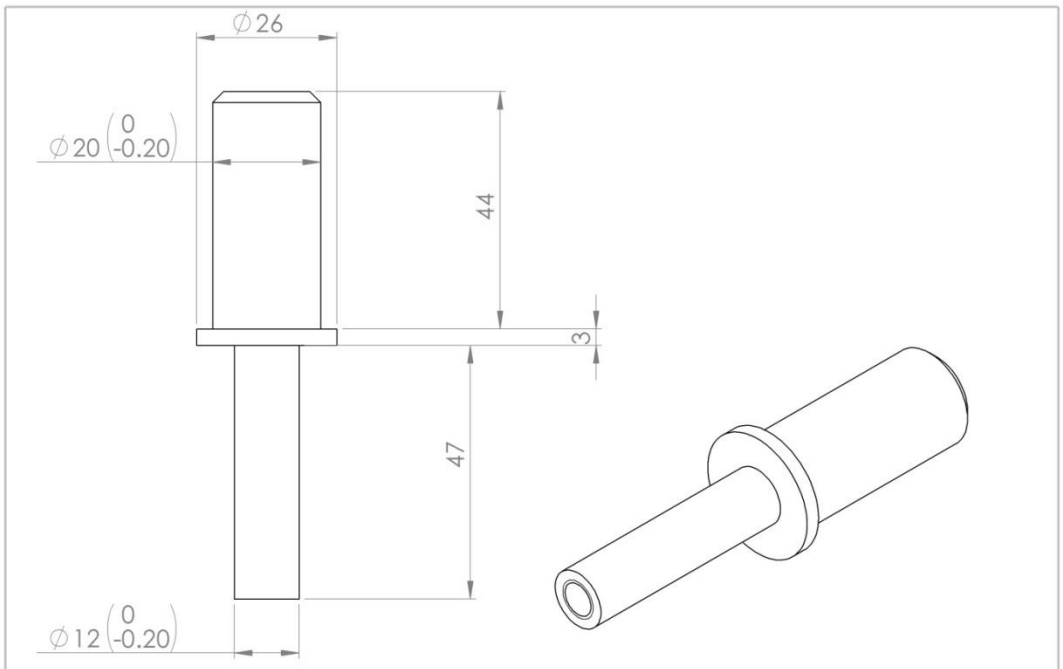

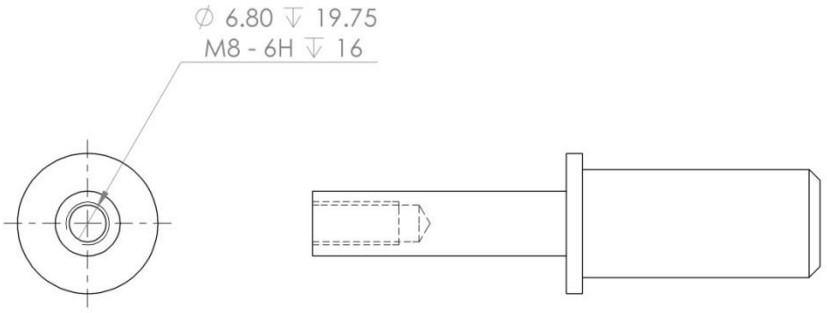

UNLESS OTHERWISE SPECIFIED: DIMENSIONS ARE IN MILLIMETERS SURFACE FINISH: TOLERANCES: LINEAR: ANGULAR:		FINISH:				DEBUR AND BREAK SHARP EDGES	DO NOT SCALE DRAWING	REVISION
							Qty 4	
	NAME	SIGNATURE	DATE				TITLE: Slider-crank pin	
DRAWN								
CHK'D								
APPV'D								
MFG								
Q.A				MATERIAL: Aluminium			DWG NO. 104	A4
				WEIGHT:			SCALE:1:2	SHEET 6 OF 14

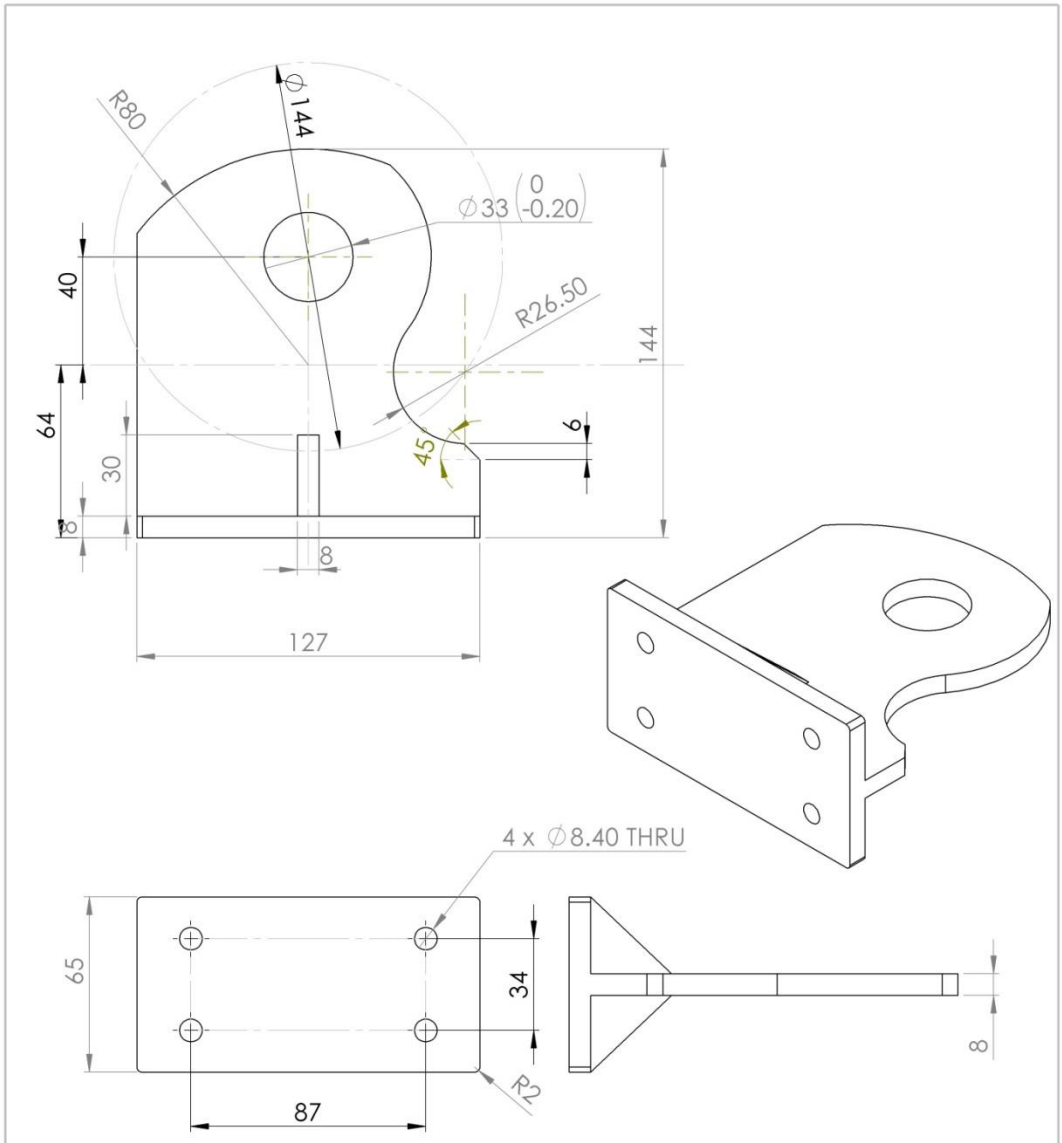

UNLESS OTHERWISE SPECIFIED: DIMENSIONS ARE IN MILLIMETERS SURFACE FINISH: TOLERANCES: LINEAR: ANGULAR:		FINISH:			DEBUR AND BREAK SHARP EDGES		DO NOT SCALE DRAWING	REVISION
							Qty 4	
	NAME	SIGNATURE	DATE				TITLE:	
DRAWN							Leg holder	
CHK'D								
APPV'D								
MFG								
Q.A				MATERIAL:			DWG NO.	A4
				Aluminium			200	
				WEIGHT:			SCALE:1:5	SHEET 7 OF 14

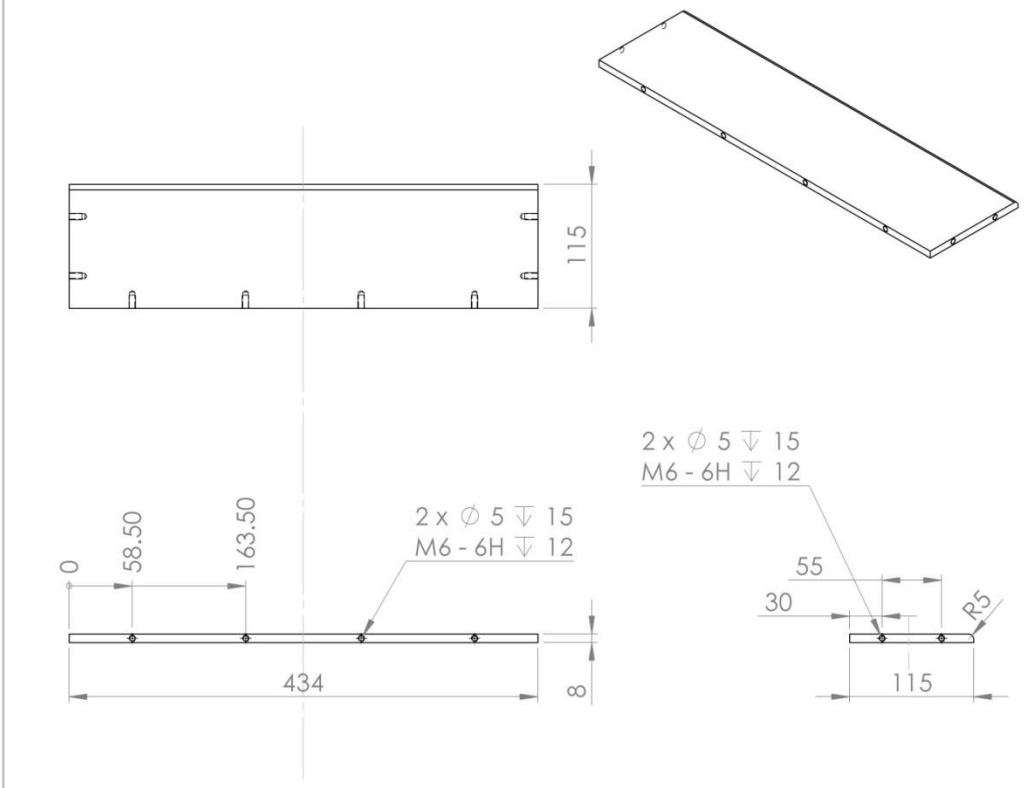

UNLESS OTHERWISE SPECIFIED: DIMENSIONS ARE IN MILLIMETERS SURFACE FINISH: TOLERANCES: LINEAR: ANGULAR:			FINISH:			DEBUR AND BREAK SHARP EDGES	DO NOT SCALE DRAWING / REVISION
							Qty 2
	NAME	SIGNATURE	DATE				TITLE:
DRAWN							Leg new 1-a
CHK'D							
APPV'D							
MFG							
Q.A				MATERIAL:			DWG NO. / A4
				Aluminium			201
				WEIGHT:			SCALE:1:10 / SHEET 8 OF 14

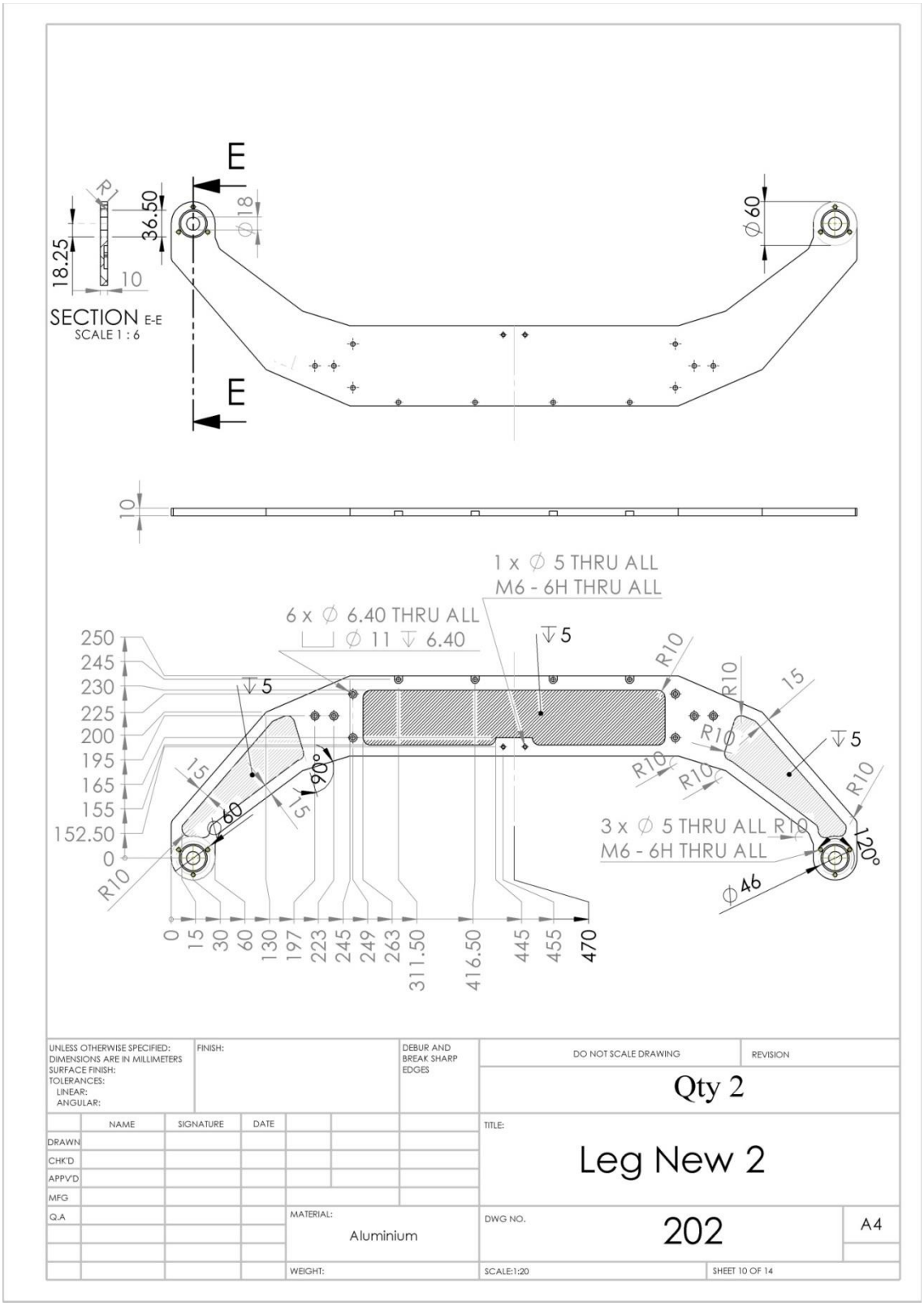
SECTION E-E
SCALE 1 : 6
18.25
36.50
10
R
E
E
Ø18
Ø60
10
1 x Ø 5 THRU ALL
M6 - 6H THRU ALL
6 x Ø 6.40 THRU ALL
⌴ Ø 11 ↧ 6.40
↧5
R10
15
60°
Ø60
3 x Ø 5 THRU ALL R10
M6 - 6H THRU ALL
120°
Ø46
250
245
230
225
200
195
165
155
152.50
0
0
15
30
60
130
197
223
245
249
263
311.50
416.50
445
455
470
UNLESS OTHERWISE SPECIFIED:
DIMENSIONS ARE IN MILLIMETERS
SURFACE FINISH:
TOLERANCES:
LINEAR:
ANGULAR:
FINISH:
DEBUR AND BREAK SHARP EDGES
DO NOT SCALE DRAWING
REVISION
Qty 2
NAME
SIGNATURE
DATE
DRAWN
CHK'D
APPV'D
MFG
Q.A
TITLE:
Leg New 2
MATERIAL:
Aluminium
DWG NO.
202
A4
WEIGHT:
SCALE:1:20
SHEET 10 OF 14

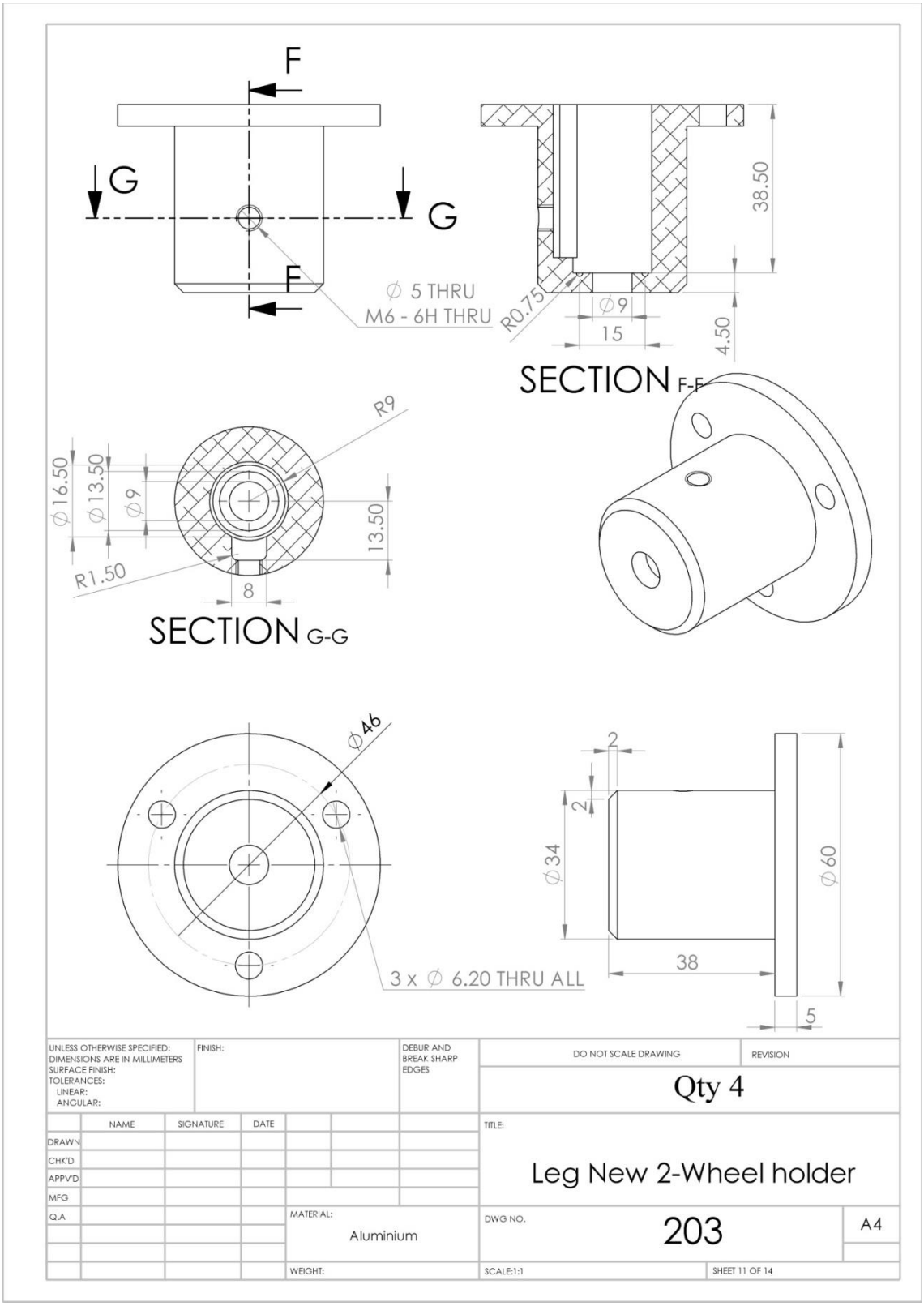
F
G
G
F
∅ 5 THRU
M6 - 6H THRU
R0.75
∅9
15
38.50
4.50
SECTION F-F
R9
∅16.50
∅13.50
∅9
13.50
R1.50
8
SECTION G-G
∅46
3 x ∅ 6.20 THRU ALL
2
2
∅34
∅60
38
5
UNLESS OTHERWISE SPECIFIED:
DIMENSIONS ARE IN MILLIMETERS
SURFACE FINISH:
TOLERANCES:
LINEAR:
ANGULAR:
FINISH:
DEBUR AND BREAK SHARP EDGES
DO NOT SCALE DRAWING
REVISION
Qty 4
NAME
SIGNATURE
DATE
DRAWN
CHK'D
APPV'D
MFG
Q.A
TITLE:
Leg New 2-Wheel holder
MATERIAL:
Aluminium
DWG NO.
203
A4
WEIGHT:
SCALE:1:1
SHEET 11 OF 14

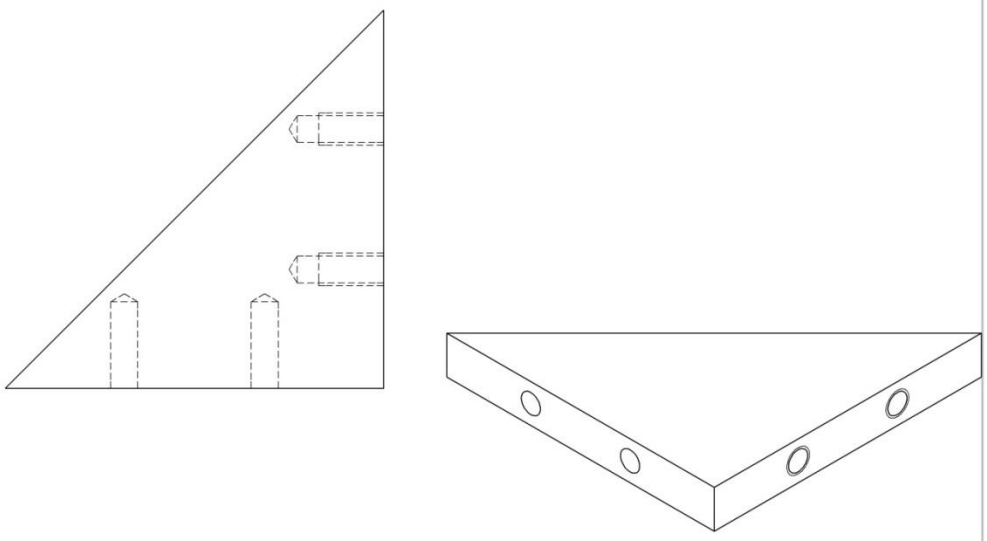

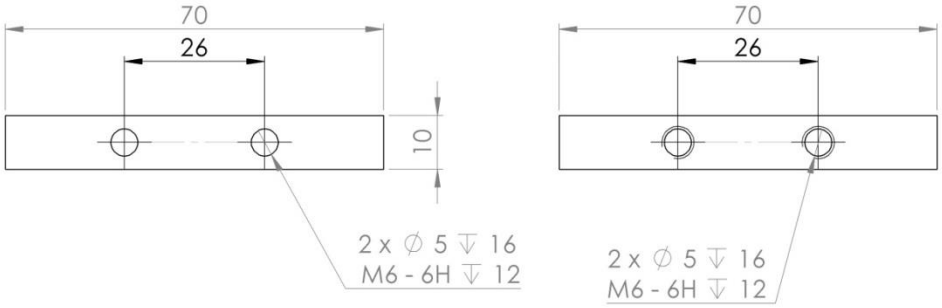

UNLESS OTHERWISE SPECIFIED: DIMENSIONS ARE IN MILLIMETERS SURFACE FINISH: TOLERANCES: LINEAR: ANGULAR:		FINISH:			DEBUR AND BREAK SHARP EDGES	DO NOT SCALE DRAWING	REVISION
						Qty 4	
	NAME	SIGNATURE	DATE			TITLE:	
DRAWN						Leg Rib	
CHK'D							
APPV'D							
MFG							
Q.A				MATERIAL:		DWG NO.	A4
				Aluminium		204	
				WEIGHT:		SCALE:1:2	SHEET 12 OF 14

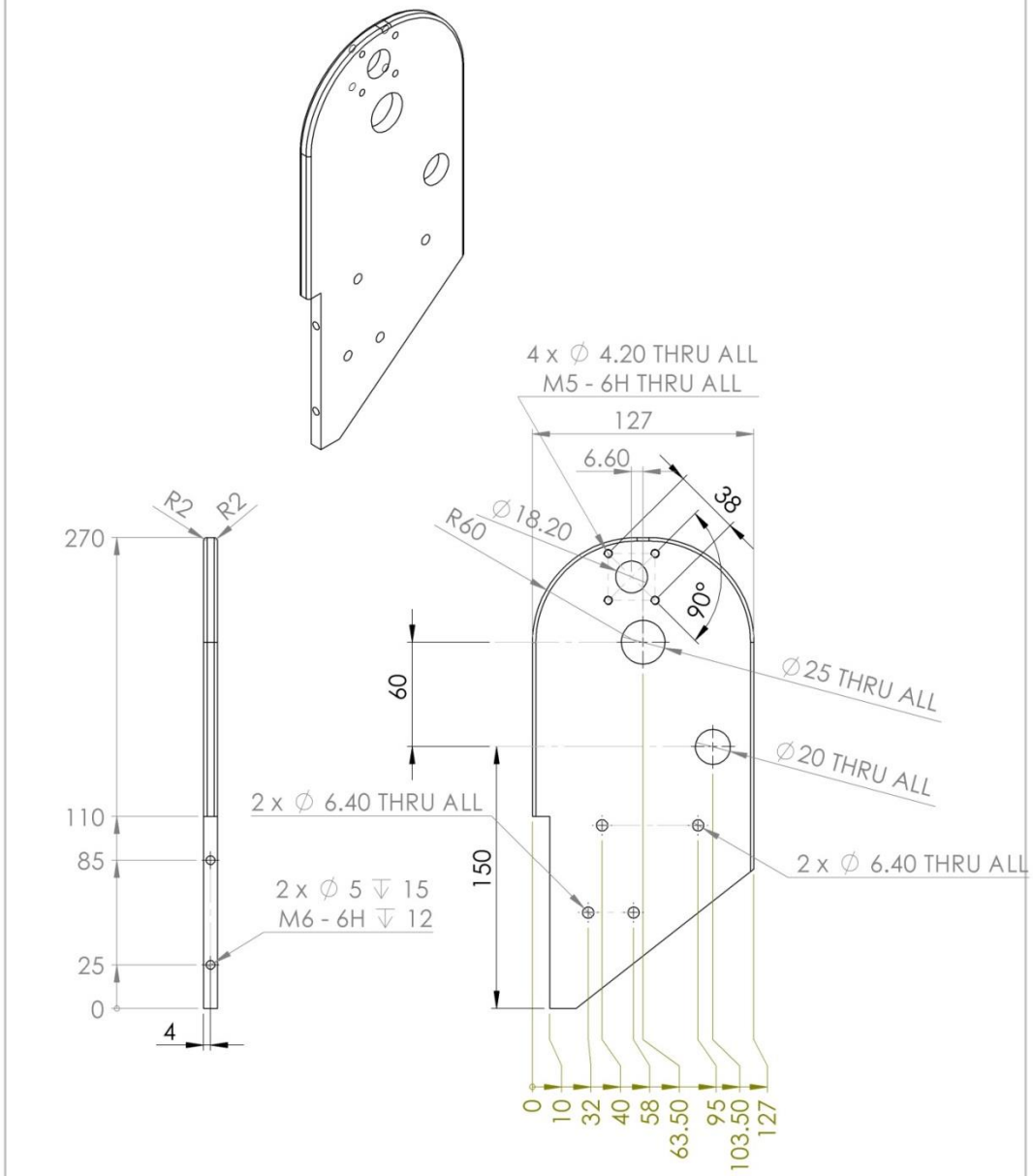

UNLESS OTHERWISE SPECIFIED: DIMENSIONS ARE IN MILLIMETERS SURFACE FINISH: TOLERANCES: LINEAR: ANGULAR:		FINISH:			DEBUR AND BREAK SHARP EDGES		DO NOT SCALE DRAWING	REVISION
							Qty 4	
	NAME	SIGNATURE	DATE				TITLE:	
DRAWN							Leg new 1-b	
CHK'D								
APPV'D								
MFG								
Q.A					MATERIAL:		DWG NO.	A4
					Aluminium		205	
					WEIGHT:		SCALE:1:5	SHEET 3 OF 6

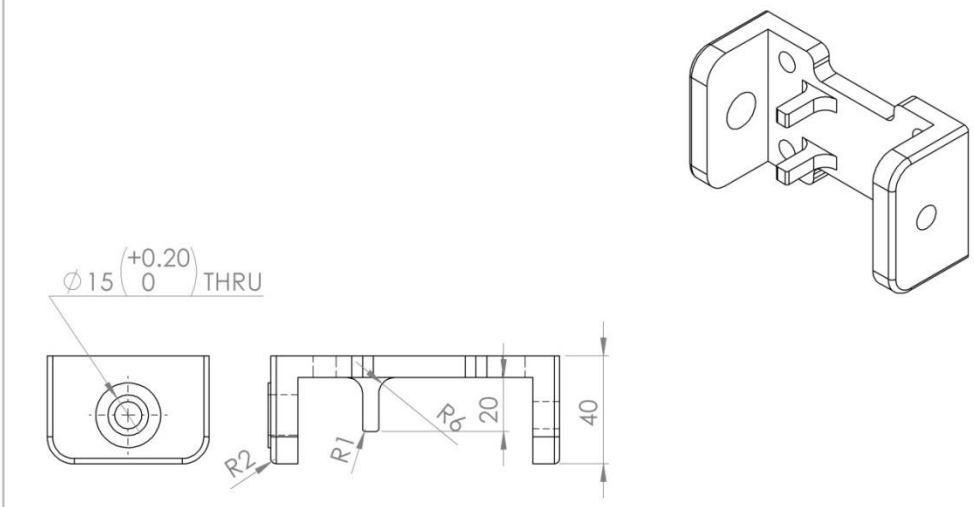

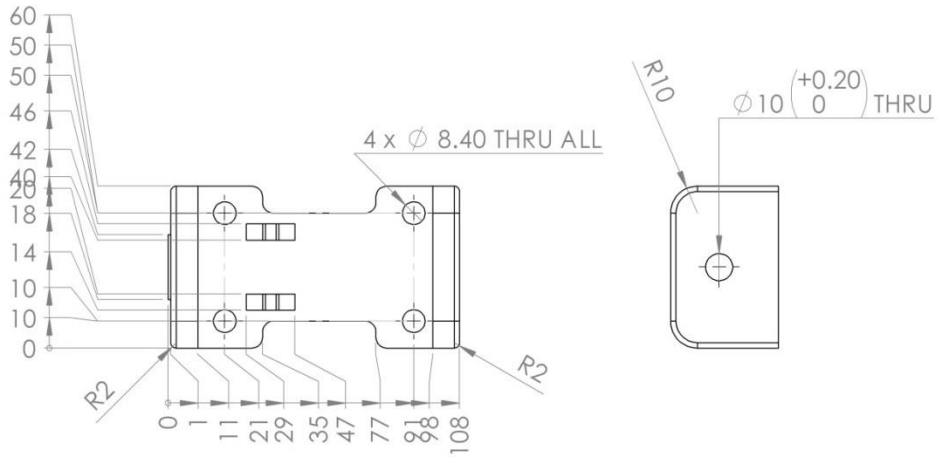

UNLESS OTHERWISE SPECIFIED: DIMENSIONS ARE IN MILLIMETERS SURFACE FINISH: TOLERANCES: LINEAR: ANGULAR:	FINISH:		DEBUR AND BREAK SHARP EDGES		DO NOT SCALE DRAWING	REVISION	
					Qty 2		
	NAME	SIGNATURE	DATE		TITLE:		
DRAWN					Drawbar shaft holder		
CHK'D							
APPV'D							
MFG							
Q.A				MATERIAL: Aluminium	DWG NO. 300		A4
				WEIGHT:	SCALE:1:2	SHEET 13 OF 14	

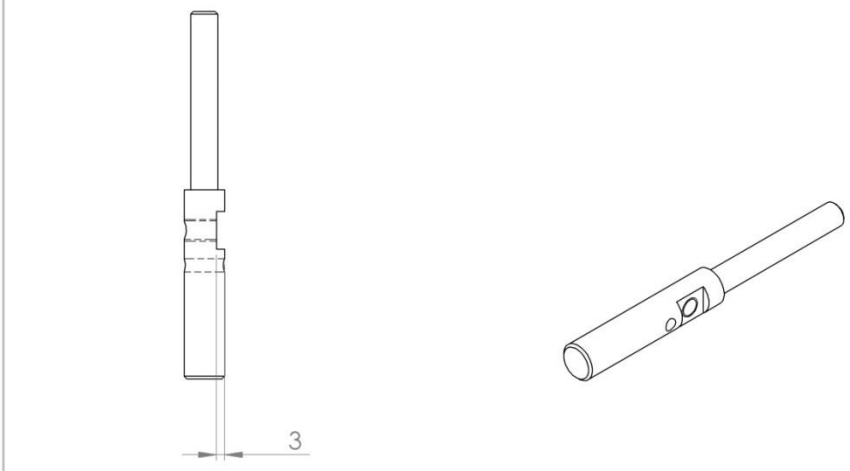

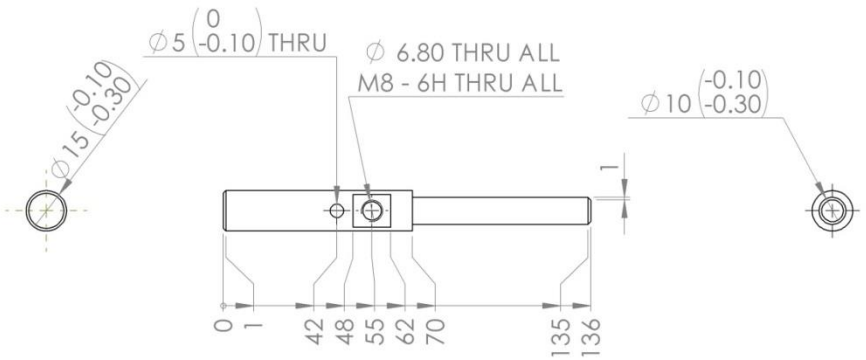

UNLESS OTHERWISE SPECIFIED: DIMENSIONS ARE IN MILLIMETERS SURFACE FINISH: TOLERANCES: LINEAR: ANGULAR:	FINISH:		DEBUR AND BREAK SHARP EDGES			DO NOT SCALE DRAWING	REVISION
						Qty 2	
	NAME	SIGNATURE	DATE			TITLE:	
DRAWN						Drawbar shaft	
CHK'D							
APPV'D							
MFG							
Q.A				MATERIAL:		DWG NO.	A4
				Stainless Steel		301	
				WEIGHT:		SCALE:1:5	SHEET 14 OF 14

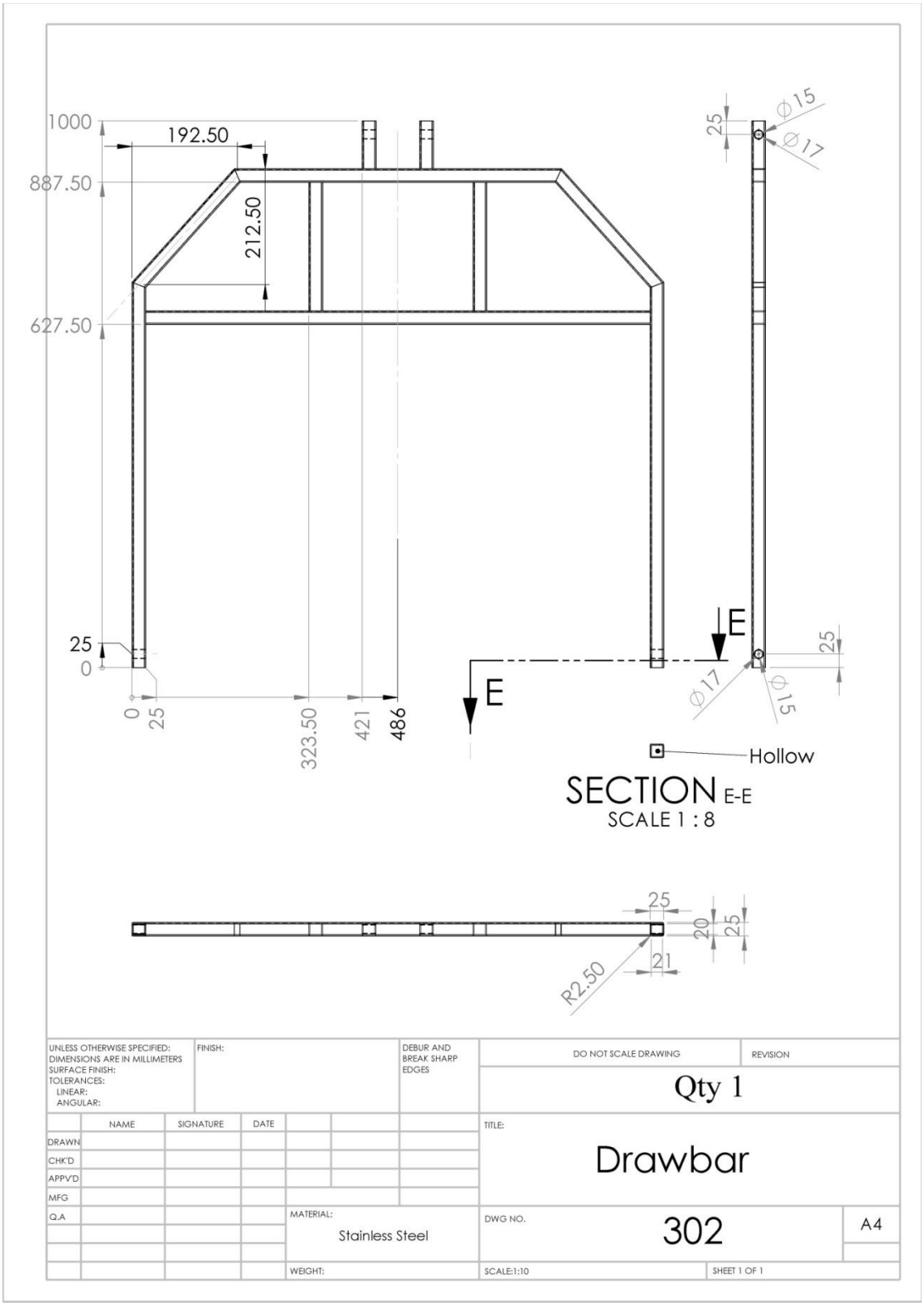
1000
887.50
627.50
192.50
212.50
25
0
0
25
323.50
421
486
E
E
25
Ø15
Ø17
Ø17
Ø15
25
Hollow
SECTION E-E
SCALE 1 : 8
25
20
25
21
R2.50
UNLESS OTHERWISE SPECIFIED:
DIMENSIONS ARE IN MILLIMETERS
SURFACE FINISH:
TOLERANCES:
LINEAR:
ANGULAR:
FINISH:
DEBUR AND BREAK SHARP EDGES
DO NOT SCALE DRAWING
REVISION
Qty 1
NAME
SIGNATURE
DATE
DRAWN
CHK'D
APPV'D
MFG
Q.A
TITLE:
Drawbar
MATERIAL:
Stainless Steel
DWG NO.
302
A4
WEIGHT:
SCALE:1:10
SHEET 1 OF 1

B1.2 TMS

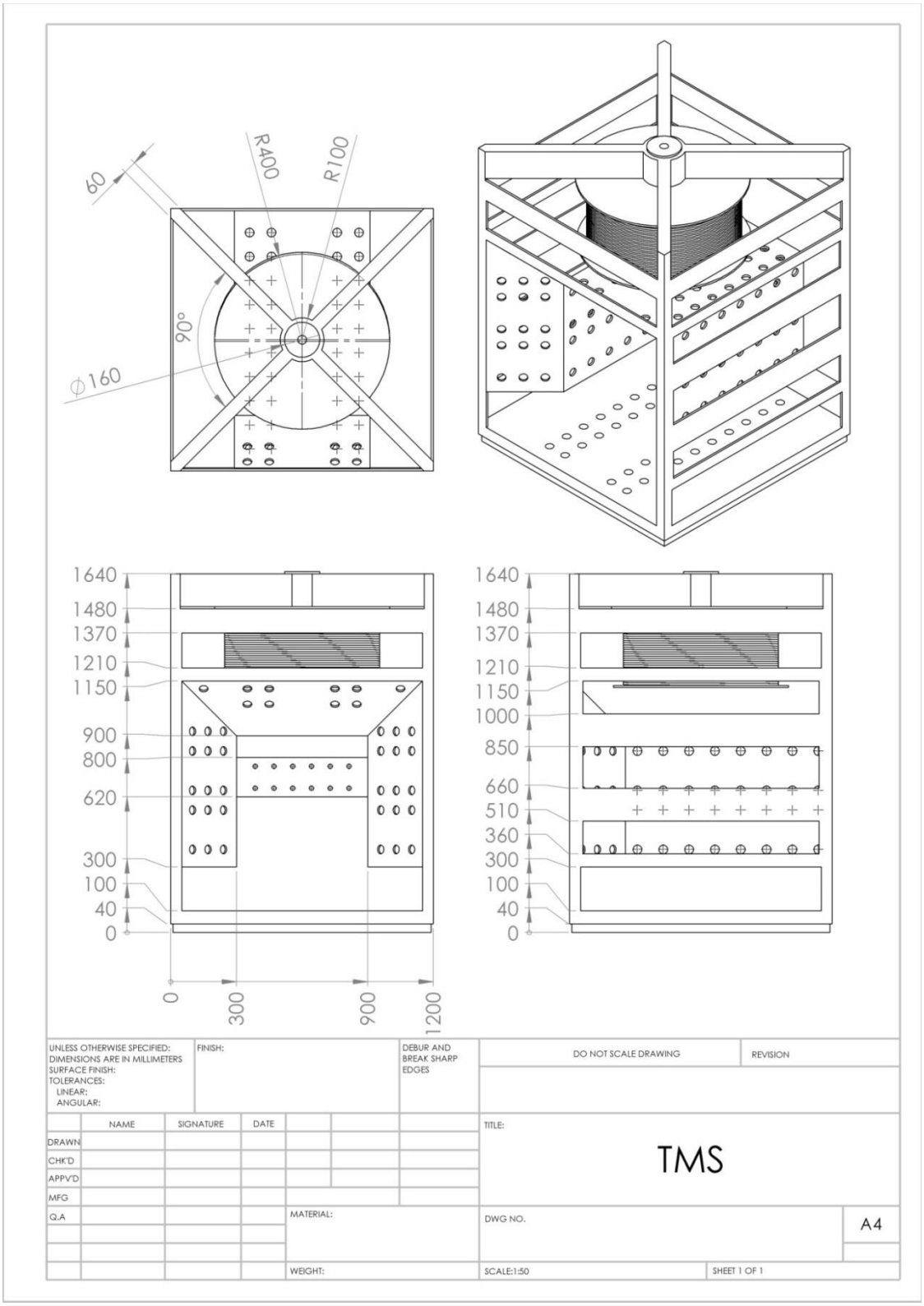
60
R400
R100
90°
ϕ160
1640
1480
1370
1210
1150
900
800
620
300
100
40
0
0
300
900
1200
1640
1480
1370
1210
1150
1000
850
660
510
360
300
100
40
0
UNLESS OTHERWISE SPECIFIED:
DIMENSIONS ARE IN MILLIMETERS
SURFACE FINISH:
TOLERANCES:
LINEAR:
ANGULAR:
FINISH:
DEBUR AND BREAK SHARP EDGES
DO NOT SCALE DRAWING
REVISION
NAME
SIGNATURE
DATE
DRAWN
CHK'D
APPV'D
MFG
Q.A
TITLE:
TMS
MATERIAL:
DWG NO.
A4
WEIGHT:
SCALE:1:50
SHEET 1 OF 1

B1.3 Inspection Vehicle and Winch

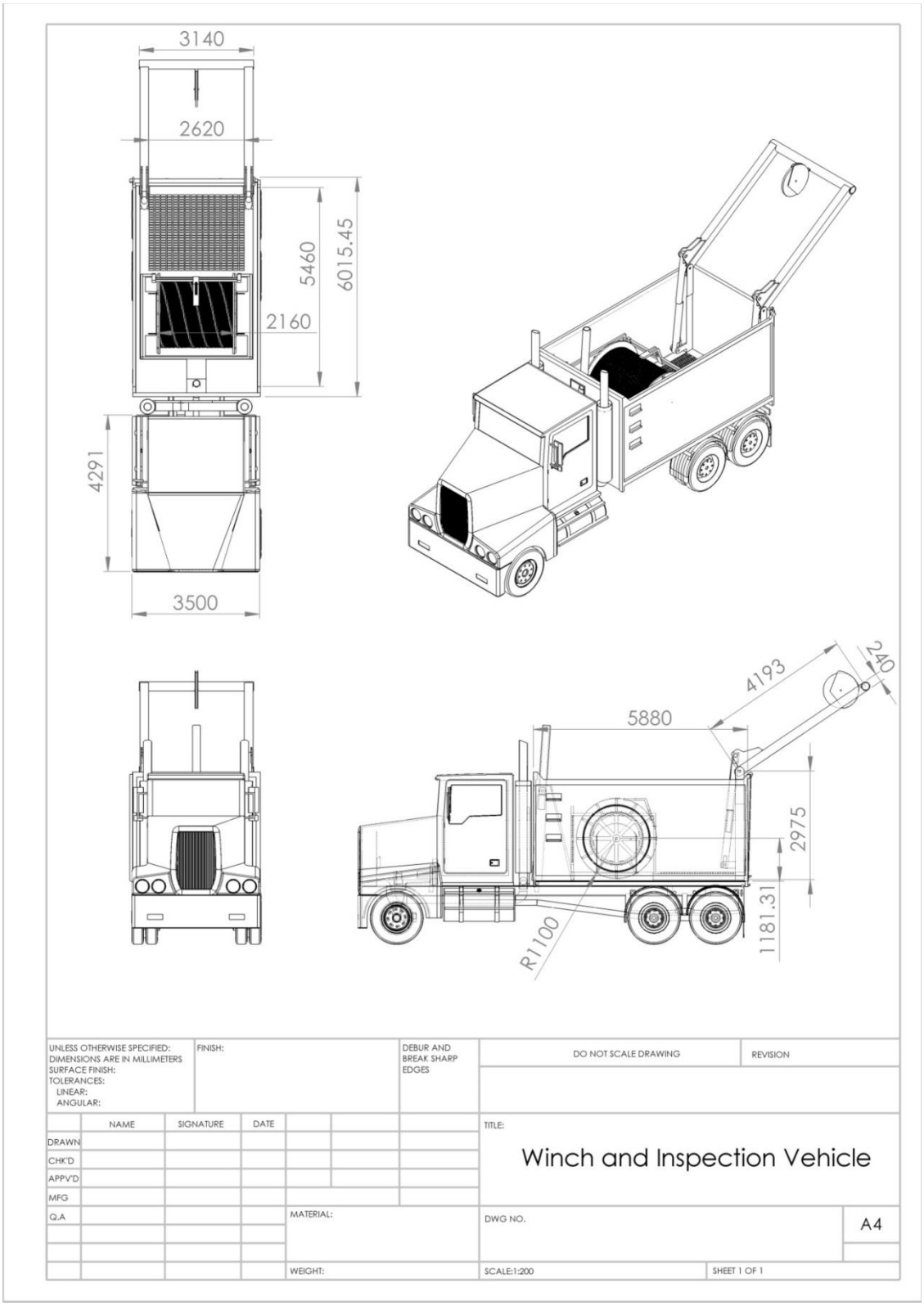

B1.4 A-frame Dimensions

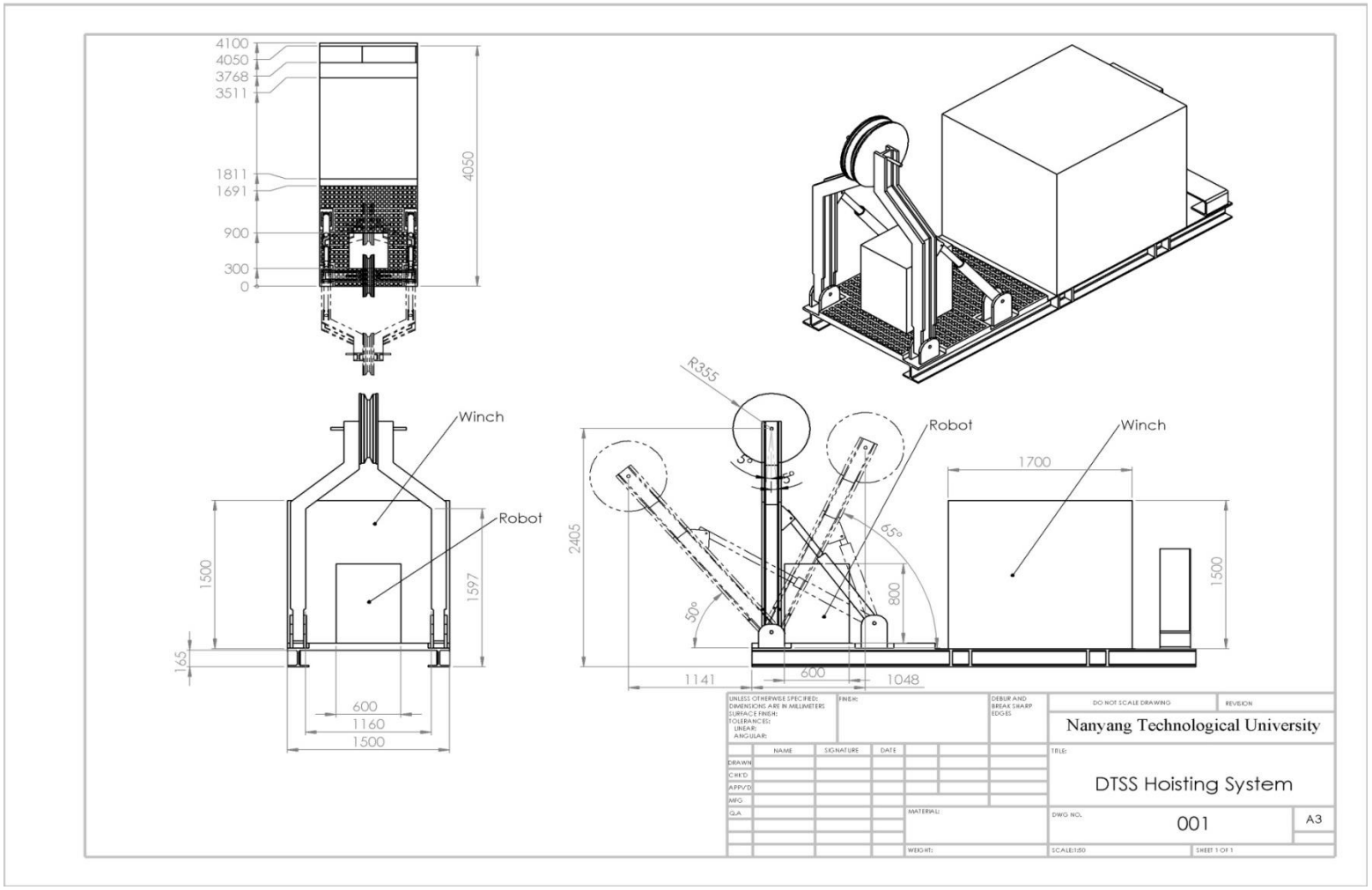

APPENDIX C: DESIGN OF ROBOT SYSTEM

C1.1 Wiring Diagram of Motor Controller

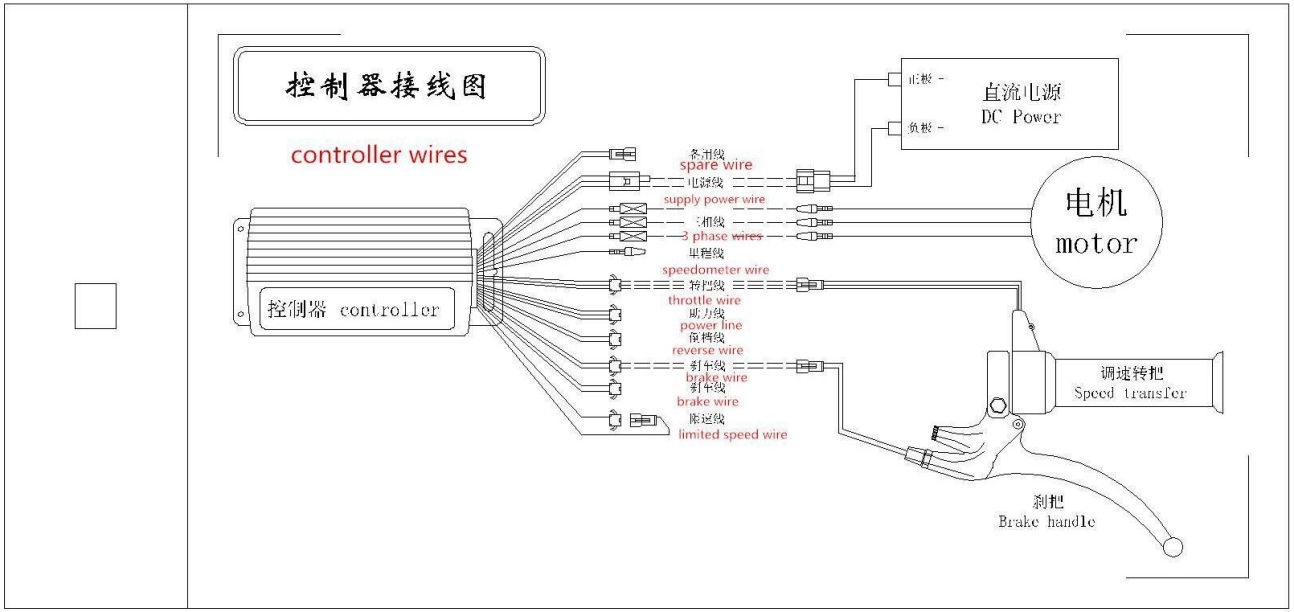

wire of controller and classify from up to down																					
spare wire		supply power wire			3 phase wire			speedometer wire	throttle wire			power line			reverse wire		brake wire		brake wire		limited speed wire
black	red	red thin	heavy red	black	yellow	green	blue	green	red	green	black	orange	blue	black	grey	grey	black	yellow	black	yellow	blue